Proceedings of Geoscience Colloquium

Geoscience Laboratory, Geological Survey of Pakistan
Islamabad

Volume 9
November, 1994

Geoscience Laboratory Project
A Technical Cooperation between
Geological Survey of Pakistan (GSP) and
Japan International Cooperation Agency (JICA)

Proceedings of Geoscience Colloquium-Volume 9 (November, 1994)

Proceedings of Geoscience Colloquium
Geoscience Laboratory, Geological Survey of Pakistan, Islamabad
Volume 9
November 30, 1994

Project Director: S.Hasan Gauhar (GSP)
Chief Advisor: Yoshiya Ikeda (JICA)

Geoscience Laboratory, Geological Survey of Pakistan
Chak Shahzad, P.O.Box 1461, Islamabad
Tel: +92-51-240423 Fax: +92-51-240223 Telex: 54663 GSL ID PK

Publication sponsored by Japan International Cooperation Agency (JICA)

CONTENTS

巻頭のことば

パキスタン地質科学研究所では、１９９２年３月より月１回程度のペースで所内コロキウム（研究談話会；Geoscience Colloquium）を開催してきている。これは、現在実施中のＪＩＣＡプロジェクト技術協力事業のイニシアチブで取り組み始めた企画であり、日パ双方の専門家や科学者が、日パの合同調査や共同研究、技術協力事業の成果発表を行い、また各々の最新の研究発表や普及講演などを行い、よって技術移転事業の推進と、研究所活動の活性化をはかる事を目的としている。本論文集(Proceedings of Geoscience Colloquium)は、上記の性格を有するコロキウムで発表された報告，講演及び関連するトピックスを論文としてまとめたものであり、これによりプロジェクト内部における技術移転と情報交換を一層促進することを目指している。

本第９巻では、マラカンド地域とチラス地域の共同研究成果のまとめ、新たな分析・測定技術の紹介、日本におけるカウンターパート・トレーニングの報告等を中心に６篇のレポートを収録している。

なお，以上の刊行目的から明らかなように本論文集は公開の学術雑誌を目指すものではなく、プロジェクトにおける内部情報誌として位置づけられる。掲載された論文には、オリジナルな内容が含まれる場合があるが、あくまで暫定的なものである。これらは今後の研究を待って改訂され別途学術雑誌に公表されるべき性格のものであるので、引用を希望される場合には事前に著者または編集者と連絡をとり適切な典拠にあたることを推奨する。

日パ双方の専門家と科学者が本誌を活用して活発に業務を展開し、パキスタン地質科学研究所が名実ともにパキスタンの地質科学研究の拠点となることを祈ってやまない。

１９９４年１１月

パキスタン地質科学研究所プロジェクト

チーフアドバイザー　池田嘉弥

EDITOR'S NOTE

This is the 9th volume of the Geoscience Colloquium Proceedings. The papers included in this volume were presented in the 26th (4th April, 1994) to 33rd (17th November, 1994) Geoscience Colloquia of the Geoscience Laboratory. The two papers on the Muslimbagh and Chilas are on the technical activities as parts of main Geoscience regular projects. The paper on the determination of As & Sb is part of the research programme for developing methods for different elements on AAS and other instruments. The paper on the rock magnetism is of a lecture from a practical training programme.

The authors would like to request the readers to send their suggestions and comments on these issues which could help in improving the standard of this publication. As has been previously mentioned the Proceedings of Geoscience Colloquium are characterized as internal circulars essentially for the information of the personnel associated with the GSP-JICA Technical Cooperation Project and is not aiming to be any academic periodical. Most of the papers are based on the preliminary and tentative results of the field and laboratory research work being done on various projects. Besides, some short notes and the lectures given from time to time under various in-house training programmes are also included. These reports and papers may be updated and revised following further research studies for subsequent publication in suitable research journals in and outside Pakistan.

Readers who intend to refer to any part of these papers are advised to contact the authors or the editors.

30th November, 1994

Editors

PART I. ARTICLES

Proceedings of Geoscience Colloquium, Geoscience Lab ,GSP, 9, 5-16

Geology and Petrography of the Landi Raud Chromite Deposits: A Part of the Malakand Ultramafic Complex, N.W.F.P., Pakistan

Said Rahim Khan and Sakae Sano***

** Geoscience Laboratory, Geological Survey of Pakistan, Islamabad*
*** JICA expert (Faculty of Education, Ehime University, Japan)*

ABSTRACT

The Malakand ultramafic complex lies close to the northern margin of the Indo-Pak continental plate in Pakistan (Fig. 1). It is mainly composed of harzburgite and designated as harzburgite-subtype. The chromite is restricted to the harzburgite-dunite rock association. The dunite is irregularly shaped, discordant and has a gradational contact with the adjacent orthopyroxene poor harzburgite. Modal analysis indicate that the rocks of the Malakand ultramafic complex have undergone high degree of partial melting. The chromite found in the Landi Raud area is massive, porphyritic-nodular and disseminated. Silicate minerals like olivine, pyroxene, amphibole, and mica are frequently observed as inclusions in the chromite.

INTRODUCTION

This report describes the petrographic studies of a part of the Malakand ultramafic complex at Landi Raud. The present investigation was undertaken as a GSP-JICA joint collaborative project. The main purpose was to study the economic potential of the chromite deposits and Platinum - Group elements. The ultramafic body striking east-west, is about 25 km long, with an average width of 3 km. The stream sediment samples collected for the study of platinum-group elements have been sent to Chemex Labs., Canada for analysis and the results are still awaited. The Malakand ultramafic complex is a klippe and its contacts with the overlying and underlying metasediments (most probably Paleozoic in age) of the Indo-Pak continental plate are faulted.

Previous work

The Malakand ultramafics have been previously named as Harichand ultramafic complex (Uppal, 1972), the Sakhakot-Qila complex (Ahmed, 1978), the Dargai ultramafic complex (Mehdi, 1979) and Chromite bearing mafic-ultramafic complex (Rossman et al., 1982). Ahmed (1984, 82 and 78) carried out detailed petrological and geochemical studies

of the peridotite and chromite without classifying the rocks. Tahirkheli, et al. (1979), described this ultramafic complex as a "klippe". Malinconico (1982) carried out gravity and magnetic survey across this ultramafic complex and described it as a rootless body. Rossman et al., (1982) conducted geological mapping of the complex and classified the rocks into a lower ultramafic tectonite and upper mafic-ultramafic cumulate units. Hussain et al., (1984) reported an ophiolitic melange in the Prang Ghar area just west of the present study area. Rafiq, (1984) presented the geology of the Utman Khel area and compared with the Malakand ultramafic complex. In the present report the term, "Malakand ultramafic complex" is retained.

General Geology

The ophiolites in Pakistan occur along the suture zone between the Indo-Pak and Asian plates (Tahirkheli et al., 1979). The Malakand ultramafic complex is the only locality which lies within the Indo-Pak plate apart from the suture zone. On the basis of the present work the rocks can be divided into two groups, 1) the harzburgite-dunite unit to the south and 2) dunite-wehrlite-metagabbro to the north (Fig. 2). The two zones are separated from one another by a serpentinized zone. The latter are more serpentinized. The chromite bodies occur in the harzburgite-dunite unit and particularly in the dunite part. The chromite has been mineralized as pods, lenses and stringers. The gravity and magnetic surveys carried out by Malinconico (1982) indicate that it is a rootless body, having a depth of about 1.5 km in its western part and becoming shallower towards its eastern extension. This was also described as an offshoot of the mafic-ultramafic rocks associated with the Main Mantle Thrust (MMT). This thrust marks a suture zone between the Indo-Pak plate and the Kohistan island arc (Tahirkheli et al., 1979). Previously only the northern contact was reported as a faulted contact (Tahirkheli et al., 1979 and Ahmed, 1978). But the present work succeeded in recognition of the southern contact with the metasediments as faulted too and is well exposed just north of Qila village.

Local Geology

1) Harzburgite-dunite unit

The Landi Raud chromite bearing area lying in the central part of the Malakand ultramafic complex, is composed predominantly of harzburgite with minor dunite intercalations. These rocks are fresh and less metamorphosed. The chromite bearing dunite is an irregular shaped and discordant with the enclosing orthopyroxene poor harzburgite

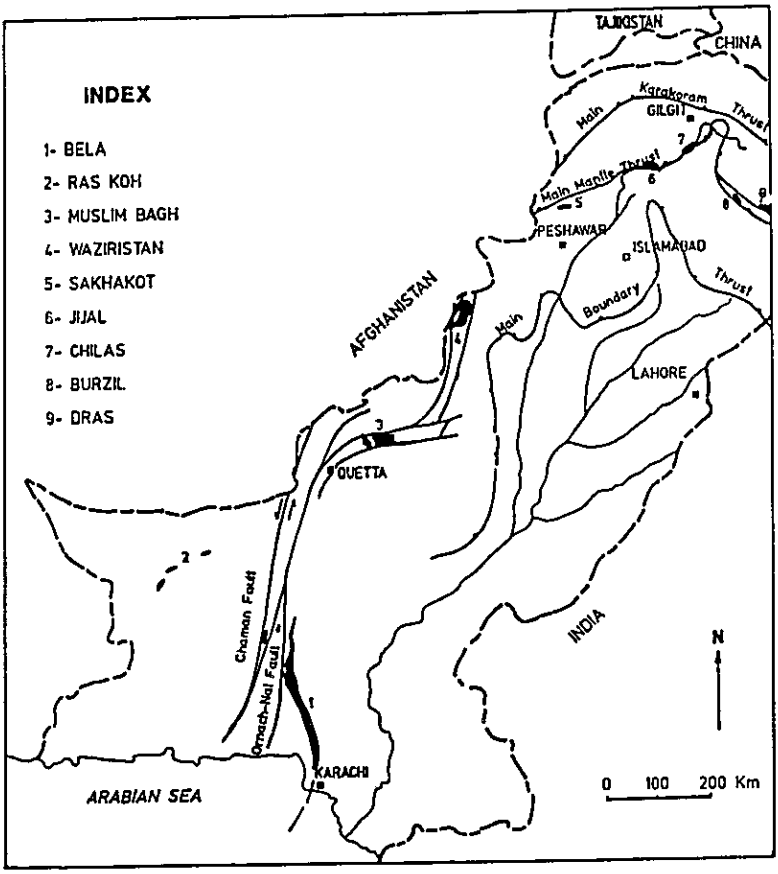

Figure 1. Map Showing Location of Major Ophiolite Occurrences in Pakistan

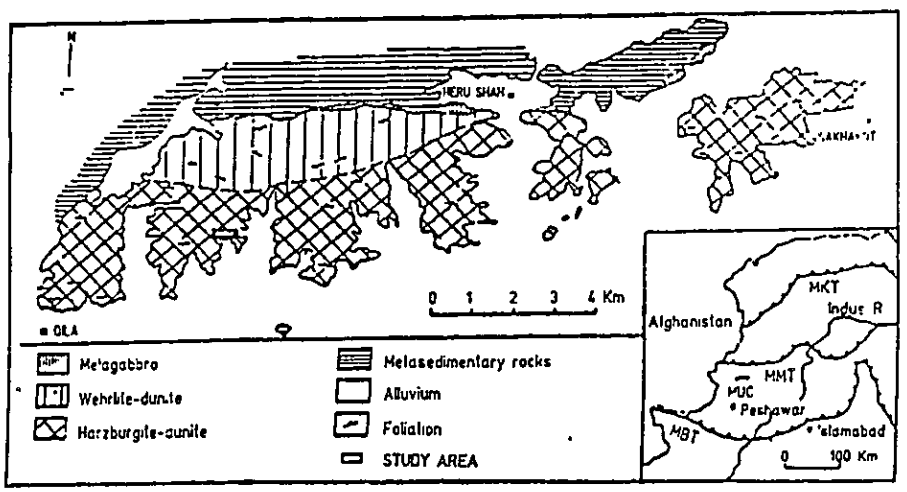

Figure 2. Geological map of the Malakand Ultramafic complex, NWFP, Pakistan (modified after Ahmed, 1982)

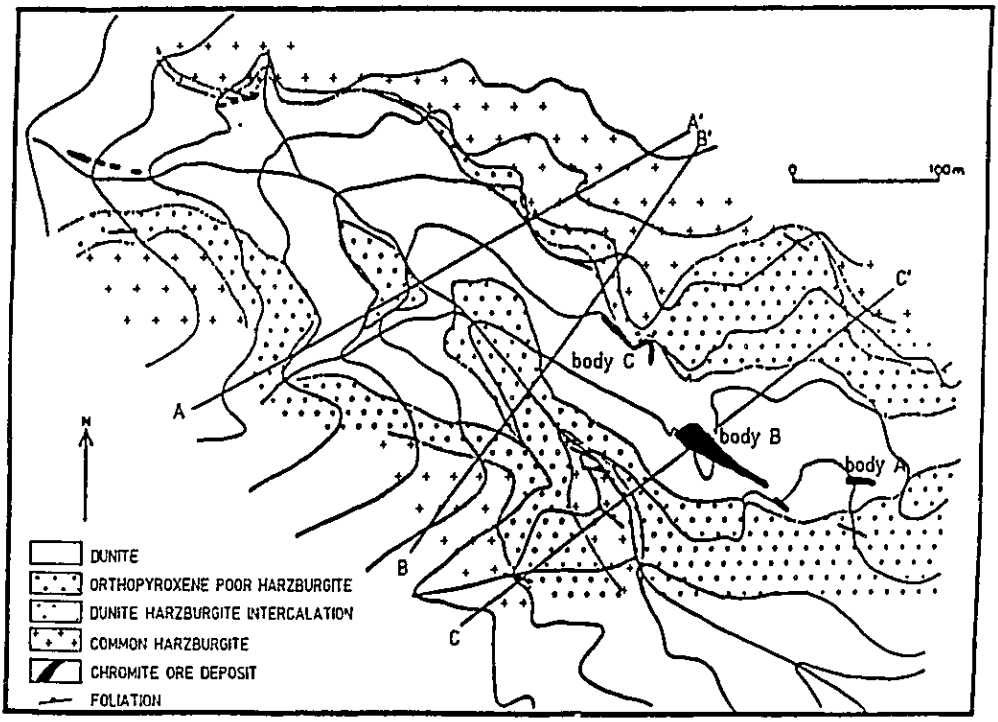

Figure 3. Geological map around Landi Raud chromite mine, Malakand, Pakistan.

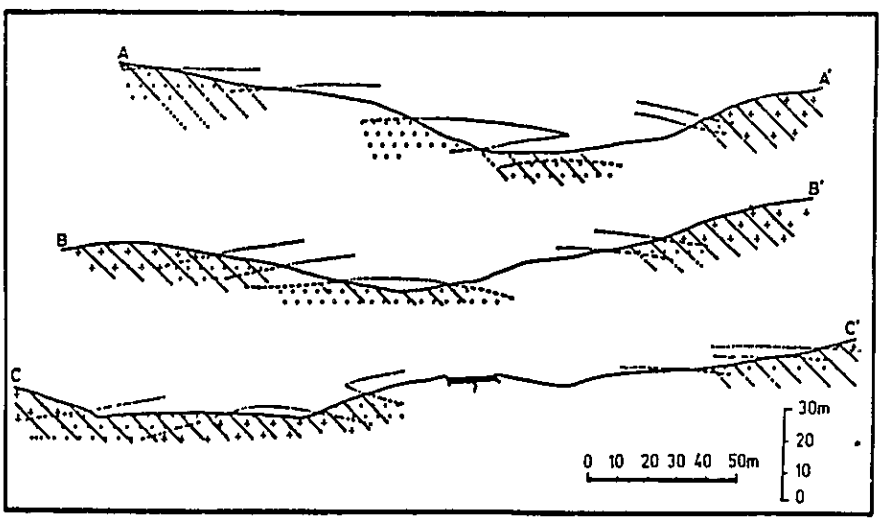

Figure 4. Cross section showing that the dunite is cross-cutting the foliation of harzburgite and the dunite is decreasing sothward.

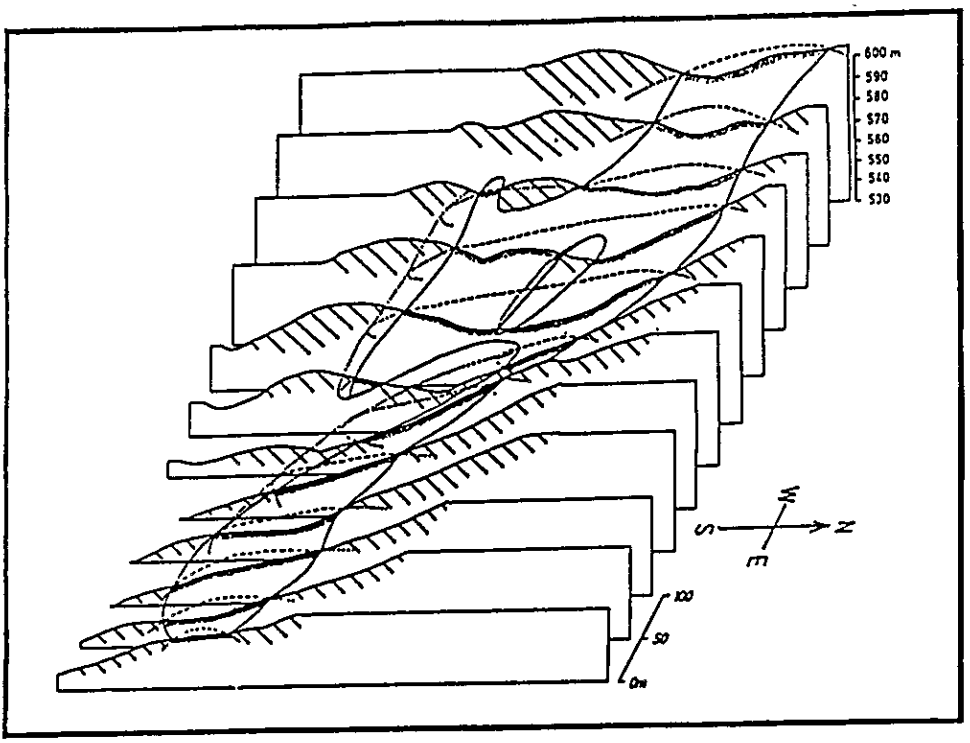

Figure 5. Cartoon section showing three dimensional internal structure of dunite.

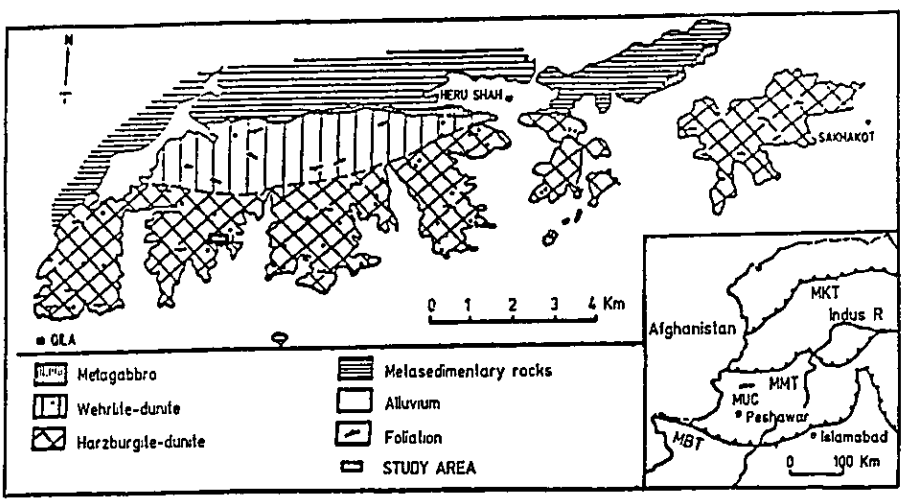

Figure 6 Map showing the location of chromite ore bodies, Malakand, Pakistan (after Ahmed, 1982).

followed by common harzburgite (Fig. 3). The dunite occurs as dyke and some times cross-cutting the foliation of harzburgite (Fig. 4 A-A' & B-B'). The bulk of dunite is decreasing towards south (Fig. 4 C-C'). Figure 5 shows three-dimensional internal structure of dunite. In the field the dunite can be distinguished from harzburgite due to smooth surface touch in the former. This dunite is the host rock of chromite. The chromite is found in the form of pods, lenses and stringers and crystallized as massive, porphyritic-nodular or disseminated. The massive and porphyritic-nodular chromites have sharp contacts with the host rock dunite, while the disseminated chromite has a gradational contact. In the Landi Raud chromite mine area, younger pyroxenite and dunite dykes are found in the dunite which are cross-cutting the foliations present in the dunite.

2) Chromite ore deposits

About 62 chromite bodies (Fig. 6) have been reported from the Malakand ultramafic complex (Ahmed, 1982). Among these, 60 bodies are located in the harzburgite-dunite unit, while only two small bodies occur in the dunite-wehrlite-metagabbro unit. The chromite bodies are found in the form of pods, lenses and stringers. The Landi Raud chromite mine area contains three chromite ore bodies (Fig. 3). They are of cone shape, opening upward and closing downward (Fig. 7) based on our field survey. The massive and porphyritic-nodular chromite have sharp contacts with the host rock dunite while the disseminated chromite has a gradational contact and grades gradually into massive chromite.

Petrography

1) Harzburgite-dunite unit

Modal analyses on 20 rock samples of the Malakand ultramafic complex have been conducted (Fig. 8) These rocks are found as peridotites. An important observation is that the peridotites are far poorer in pyroxenes, particularly clinopyroxene. They contain olivine (88-92%), orthopyroxene (8-11%) and clinopyroxene (<5%). There is a systematic variation in modal mineralogy from peridotite to dunite with both the pyroxenes decreasing as olivine increases.

Euhedral to subhedral chromite grains are commonly observed in this unit. Besides these, wormy intergrowths of chrome-spinel are also present in the dunite part, which give rise to large chromite crystals. These wormy intergrowths of chrome-spinel (Fig. 9) are associated with pyroxene, especially clinopyroxene. The chromite grains are altered to serpentine and chlorite on their peripheries. Porphyroclastic texture is also commonly noted in the harzburgite. Inclusions of silicate minerals such as pyroxene, amphibole and mica are commonly observed in the chromite grains.

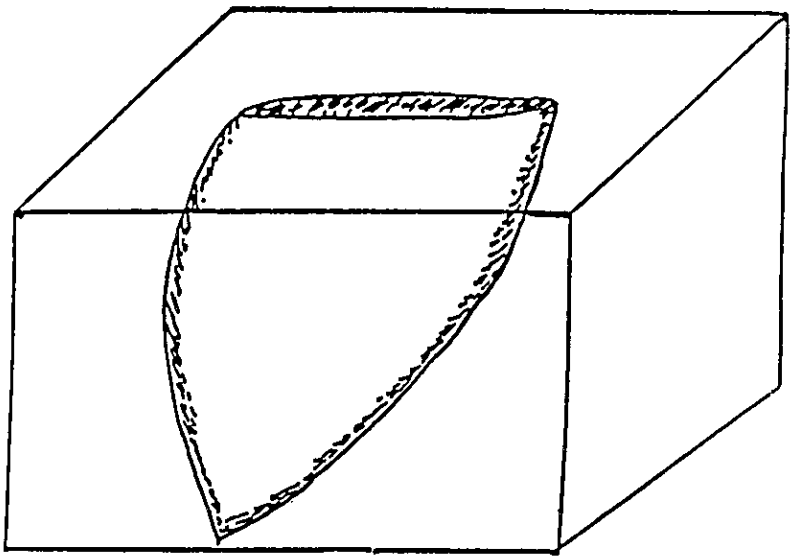

Figure 7. Cartoon cross section showing the cone-shaped structure of the he Landi Raud Landi Raud chromite body.

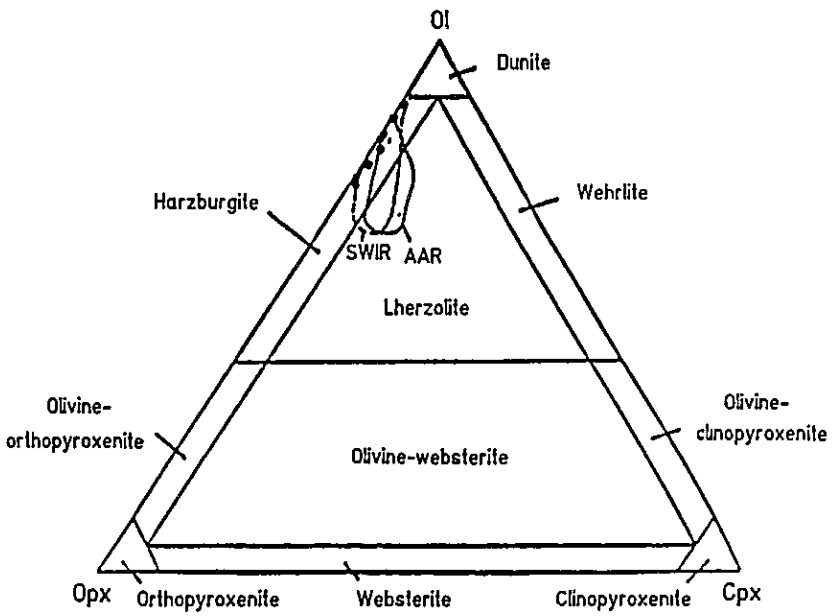

Figure 8. Ol-Opx-Cpx ternary diagram showing the position of the Malakand ultramafics marked as black spots. (AAR=American Atlantic Ridge and SWIR=South West Indian Ridge) (after Dick and Fisher, 1984).

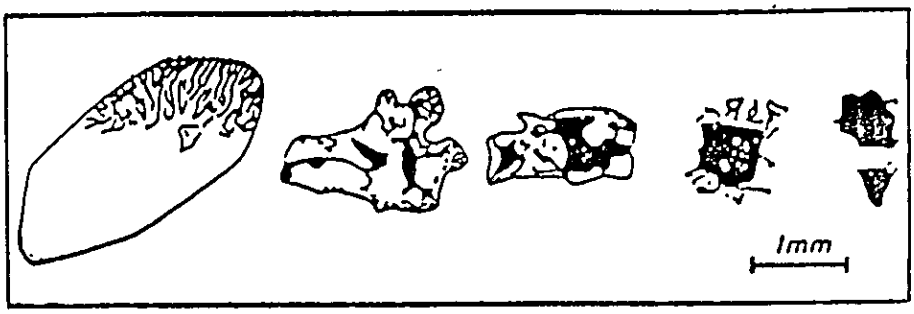

Figure 9. Resorption of orthopyroxene and recrystallization of spinel in chrome across a transitional zone from harzburgite (left) to dunite (right) (Leblanc, et al. 1979)

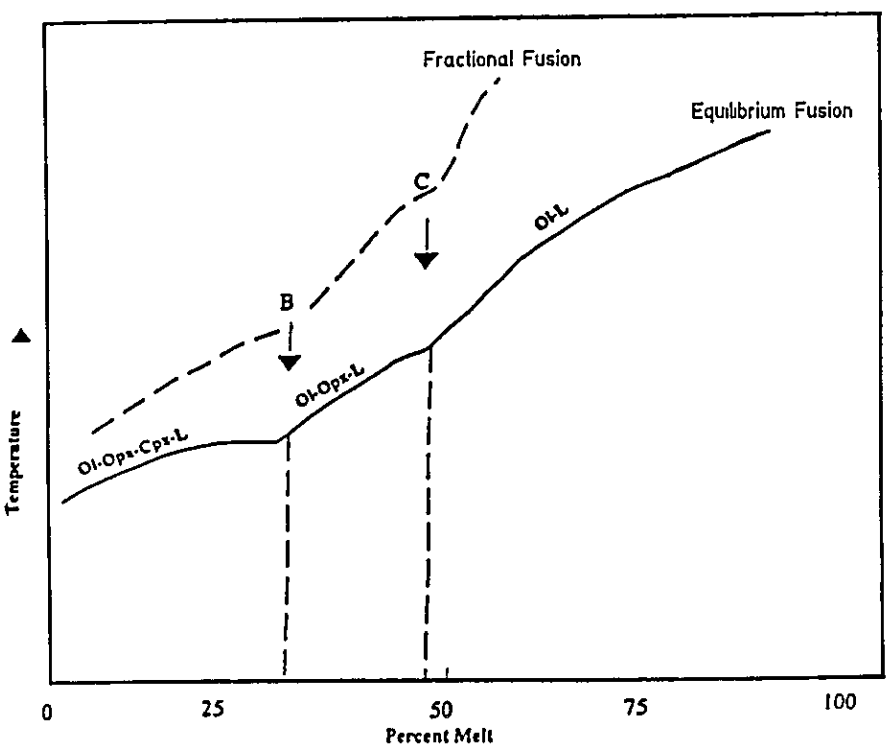

Figure 10. Temprature-partial melting diagram showing the position of the Malakand ultramafics (after Mysen and Kushiro, 1977).

2) Texture of chromite

The following textures have been recognized in the Landi Raud chromite ore deposits.

2-1 Disseminated: It is a most common texture in the chromite ores. This texture is characterized by fine grained chromite grains scattered in the olivine matrix and gradually grades into a massive texture.

2-2 Massive: It is found only in the chromitite. The chromite is coarse grained, completely interlocked and some grains depict small silicate minerals in their interspaces. These silicate minerals (olivine, ortho & clinopyroxene) are altered to chlorite and serpentine (Ahmed and Hall, 1984).

2-3 Porphyritic-nodular: It is the characteristic texture of the Alpine type deposits and never found in the stratiform type deposits. The nodules are rounded to subrounded which provide strong evidence to be of podiform nature (Thayer, 1960; Dickey, 1975). The nodules also show pull-apart texture which are filled mostly by olivine and is presently altered to serpentine. Silicate inclusions, like olivine, pyroxene, amphibole and mica are frequently observed in the chromite. They are spherical, oval as well as hexagonal in shape.

DISCUSSION

The rocks of the Malakand ultramafic complex are divided into two units and separated by a serpentinized zone. This may be the "Moho", which separates the upper mantle residual rocks from the lower crustal rock (Clague and Straley, 1977).

Modal analysis indicate that the Malakand ultramafics are depleted in ortho-and clinopyroxenes (particularly clinopyroxene) and rich in olivine, indicating that they have undergone high degree of partial melting. The variations plotted in the ternary diagram Ol-Opx-Cpx defines trend similar to the paths predicted for the residues of partial melting (Dick and Fisher, 1984). The mineral assemblage of the peridotites show that they have undergone 30-45 percent partial melting (Fig. 10). Similarly the porphyroclastic texture and the wormy intergrowths of the chrome-spinel are characteristic of the upper mantle residual rocks.

The dunite is of irregular shape, discordant and crosscutting the foliation found in the surrounding harzburgite (Fig. 3). The progressive disappearance of orthopyroxene around the dunite can be attributed to a process of local partial melting (Leblanc, 1987). It also indicates that the dunite crosscutting the foliation was formed later than the harzburgite.

The hydrous minerals like mica and amphibole, found in the chrome-spinel may be the trapped melts suggesting an-hydrous environment for the chromite formation.

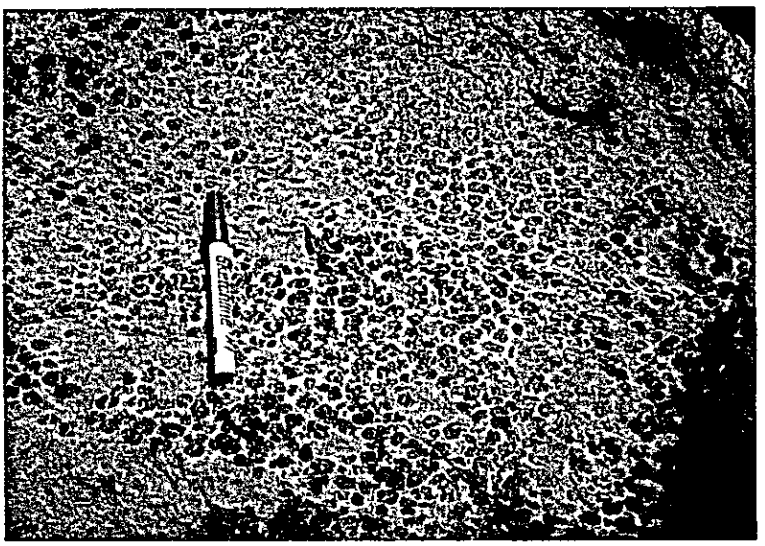

Plate 1: Photograph of nodular chromite, Landi Raud chromite deposit, Malakand

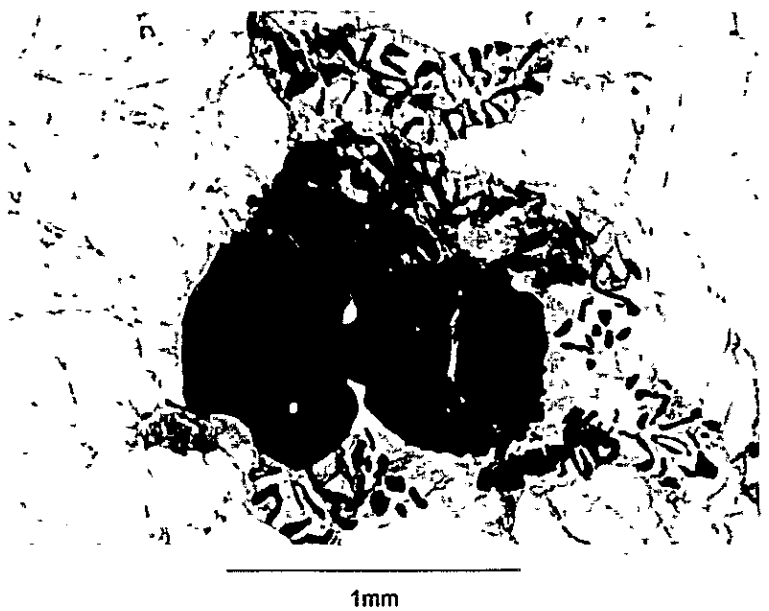

Plate 2: Photomicrograph showing resorption of Opx (yellowish) and recrystallization of spinel into chromite.

CONCLUSIONS

1) The rocks of the Malakand ultramafic complex are depleted in ortho-and clinopyroxenes and rich in olivine, indicate that they have undergone high degree of partial melting and represent upper mantle residual rocks. The boundary separating the harzburgite-dunite unit from dunite-wehrlite-metagabbro unit may represent the "Moho".

2) The chromite host rock dunite is of irregular shape, discordant and crosscutting the foliation found in the harzburgite and is younger than the harzburgite.

3) The wormy intergrowths of chrome-spinel, formed by the exsolution of the pyroxene and the porphyroclastic texture are characteristics of the upper mantle residual rocks.

4) The hydrous mineral inclusions in the chrome-spinel are indicative of anhydrous environment for the chromite formation.

References

Ahmed, Z., 1978, Chromite from Sakhakot-Qila area, Malakand Agency, Pakistan. Short communication, Mineral. Mag , Vol. 42, 155-157.

Ahmed, Z., 1982, Porphyritic-nodular, and orbicular chrome ores from the Sakhakot-Qila complex, Pakistan: their chemical variation. Mineral Mag., vol. 45, 67-178.

Ahmed, Z., 1984, Stratigraphic and Structural variation in the chromite composition of the Sakhakot-Qila ophiolitic complex, Pakistan. Econ. Geol. Vol. 79, 1334-1359.

Ahmed, Z., and Hall, A., 1984, Petrology and mineralization of the Sakhakot-Qila ophiolite, Pakistan. Ophiolite and Oceanic Lithosphere: (Gass, Lippard and Shelton, eds). Black-well Sc. Assoc. London, 241-252.

Asrarullah, Ahmad, Z., and Abbas, S. G., 1979, Ophiolites in Pakistan: An introduction. In A. Farah and K. A. DeJong, (Editors), Geodynomic of Pakistan . Geol. Surv. Pakistan, Quetta, 181-192.

Basu, A. R., and MacGregor, I. D., 1975, Chromite spinel from ultramafic xenoliths: Geochem. Cosmochim. Acta, Vol. 39, No. 6/7, 937-945.

Clague, D A., and Straley, P. F., 1977, Petrologic Nature of the Moho. Geology, 5, 133-136.

Dick, H J. B., and Bullen, T., 1975, Chromian spinel as a petrological indicator in abyssal and alpine-type peridotites and spatially associated lavas. Contrib. Mineral. Petrol., vol. 86, 54-76.

Dick, H. J. B , and Fisher, R.R., 1984, Mineralogic studies of the residues of mantle melting: abyssal and alpine type peridotites. Kimberlite 11: The Mantle and Crust-Mantle relationships. (Kimprobst, J. ed)). Elsevier, 295-308.

Dickey, J. S., 1975, A hypothesis of origin for podiform chromite deposits. Geochim. Cosmochim. Acta, 39, 1061-1074.

Greenbaum, D., 1977, The chromitiferous rocks from the Troodos ophiolite complex, Cyprus. Econ. Geol., Vol. 72, 1175-1193.

Hussain, S. S., Khan, T., Dawood, H. and Khan, I., 1984, A note on the Kot-Prang Ghar melange and associated mineral occurrences. Geol. Bull. Univ. Peshawar, vol. 17, 61-66.

Leblanc, M., 1987, Chromite in oceanic arc environment. New Caledonia. In: Evolution of Chromium Fields (Stowe, ed). Van Nostrand Reinhold Co. N. York, 265-296.

Leblanc, M., Dupuy, C., Cassard, D., Maulle, J., Nicolas, A., Prinzhofer, A., Rabinovitch, M. and Routhier, P., 1980, Essei sur la genese des corps podiformes de chromite dans les peridotites ophiolitiques: Etude des chromites de Nouvelle Caledonie et comparison avec celles de Mediterranee orientale. In: Ophiolite Symp. Geol. Surv. Dept. Cyprus, 691-701.

Malinconico, Jr., L. L., 1982, Structure of the Himalayan suture zone of Pakistan: Interpreted from gravity and magnetic data. Unpublished Ph.D. Thesis, Dartmouth college, Hanover, N. H.

Mehdi, S. S., 1979, Geology and economic aspects of Malakand chromite deposits. Pak. Mineral Development Corporation, Peshawar, 130.

Mercier, J. C. C., and Nicolas, A., 1975, Textures and fabrics of upper mantle peridotite as illustrated by xenoliths from basalts. Jour. Petrol., No. 16, 454-486.

Mysen, B. O., and Kushiro, I., 1977, Compositional variation of coexisting phases with degree of melting of peridotite in upper mantle. Amer. mineral., 62, 843-865.

Rafiq, M., 1984, Extension of Sakhakot-Qila ultramafic complex in Utman Khel, Mohmand Agency, NWFP, Pakistan. Geol. Bull. Univ. Peshawar, Vol. 17, 53-59.

Rossman, D. L., Abbas, S. G., and Hussain, S., 1982, An ultramafic chromite-bearing rock complex near Dargai, Peshawar Division, Pakistan. PK-Report 59, 35.

Ryan, M. P., 1988, The mechanics of three-dimensional internal structure of active systems: Kilauea volcano, Hawaii. J. Geophys. Res., 93, 4213-4248.

Tahirkheli, R. A. K., Mathauer, M., Proust, F. and Tapponnier, P., 1979, The Indian-Eurasian suture zone in northern Pakistan: synthesis and interpretation of recent data at plate scale. In Geodynomic of Pakistan (A. Farah & K. R. DeJong, eds). Geol. Surv. Pakistan, Quetta, 125-130.

Thayer, T. P., 1960, Some critical difference between alpine type and stratiform peridotite-gabbro complexes. 21st Int. Geol. Congr., Copenhagen, X111, 147-259.

Uppal, I. H., 1972, Preliminary account of Harichand ultramafic complex, Malakand Agency, NEWF., Pakistan. Geol. Bull. Punjab Univ., Vol. 9, 55-63.

Proceedings of Geoscience Colloquium, Geoscience Lab ,GSP, 9, 17-50

Petrology And Mineral Chemistry Of Muslimbagh Ophiolite Complex And Its Tectonic Implications

*Rehanul Haq Siddiqui,*Abdul Aziz*, Jan Muhammad Mengal,** Kenichi Hoshino***,Yoshihiro Sawada****and Ghulam Nabi******

GSP Geoscience Laboratory, Islamabad; GSP, Quetta;*** Hiroshima University, Japan;**** Shimane University, Japan *****Balochistan University, Quetta*

ABSTRACT

The Muslimbagh Ophiolite Complex is harzburgite type ophiolite, which occurs in an area of about 800 km^2 and is represented by 17.5 km thick slab of oceanic lithosphere of southern Neo-Tethys. The upper mantle segment is represented by 11 km thick sequence of tectonized (foliated) harzburgite (Opx En_{90} 76-91.96, Ol Fo 91.27-92.73,) and dunite (Fo 92.50-94.36) The upper mantle is followed by 6.5 km thick crustal sequence, which is represented in the lower part by a 4 km thick intercalations of layered dunite ($Fo_{89.73-91.83}$) and wehrlite with minor harzburgite and is followed by 200-1500 meter thick cyclic repetition of layered dunite, wehrlite (Cpx En 44.27-49.88, Ol Fo 72.85-88.99), pyroxenite (Cpx En 47.32-48.35), and gabbro (An 58-70). This cyclic sequence is followed by a 600 meter thick sequence of mafic cumulates represented by layered (lower part) and foliated (upper part) gabbro (An 52-68). This mafic sequence is overlain by about 1000 meter thick sheeted dyke complex, which is represented by foliated, layered and massive metadolerites (An 30-54) The middle part of sheeted dyke complex is invaded by numerous small bodies of plagiogranites (An 8-30) The pillow basalts are not found on top of the sheeted dyke complex but do occur in the adjacent melange zone Whole of the Ophiolite sequence is transected by a NW trending diabase dyke swarm

The present microprobe data on orthopyroxene and olivine from ultramafic tectonite hold higher Mg # (91-94) and higher NiO (0 37-0 47) contents which suggest their residual upper mantle origin The chromian spinel in dunite and harzburgite generally have higher Cr # (> 0 56) relative to abyssal peridotites The clinopyroxene in wehrlite and pyroxinite from ultramafic cumulates have higher Mg # (82-93). These features are consistent with a higher degree of partial melting (30-45%) of a depleted mantle source and high pressure crystal fractionation ($\geq$ 10 kbar) in the magma chamber.

The petrochemical study of metadolerites from sheeted dyke complex and pillow basalts from melange zone show that they belong to low-K quartz tholeiite series In trace elements chemistry they are enriched in LILE and depleted in HFSE relative to N-MORB, and their average Nb/Y, Zr/Nb, K/Rb,

67°08 31°00' 68°15' 31°00'

FIGURE 1 A

GEOLOGICAL MAP OF MUSLIMBAGH AREA

(Modified after H S C 1960, Ahmed & Abbas 1979 Mengal & Siddiqui 1993)

0 10 20 Km

EXPLANATIONS

- Subrecent Recent (deposits)
- Oligocene-Pleistocene — Siwalik Group
- L1 Locene — Kirther Limestone
- Late Paleocene Early Locene (Age of Emplacement) Muslimbagh Ophiolite Complex
  - Sheeted dykes
  - Mafic cumulates
  - Ultramafic & mafic-cumulates
  - Ultramafic cumulates
  - Ultramafic tectonites
  - Bagh Complex (Melange)
- Eocene — Ghazij Formation
- Paleocene — Dungan Formation
- Late Cretaceous — Bibai Formation
- Early-Late Cretaceous — Parh Group
- Jurassic — Loralai Limestone
- Triassic — Wulgai Formation
- Anticline, Syncline, Attitude of beds
- Fault, Thrust Fault, Dyke

AFGHANISTAN PAKISTAN IRAN INDIA ARABIAN SEA

Muslimbagh

Chinjan

Khanozai

Kuchlak

Quetta

30°23' 67°08 Digitized by Aliya Habib GeoLab (1995) 30°23' 68°15'

Ba/Zr, Ce/Ba, La/Sm, La/Ce and La/Nd ratios are more consistent with back-arc basin basalt relative to N-MORB or island arc basalts (IAB) Their LILE enriched N-MORB normalized patterns and moderately LREE enriched Chondrite normalized REE patterns are also consistent with back-arc basin basalts The pillow basalts (tholeiitic) and gabbro found towards southeastern side of the melange zone show island arc like signatures exhibited by the lower K/Rb,Ti/V and Zr/Yratios relative to N-MORB A new modal is proposed for the origin and tectonic evolution of Muslimbagh Ophiolite Complex, which is based on the aforementioned data

INTRODUCTION

In Pakistan the northwestern margin of Indian continent is marked by the Waziristan-Muslimbagh-Bela Ophiolite suture zone In the regional geotectonic context the ophiolites included in this suture belong to Late Cretaceous Tethyan Ophiolite Belt (Pearce 1980) which also include Semail, Troodos and Vorinous ophiolites in the southwest and west, Waziristan, Malakand, Dargai and other ophiolites associated with Indus-Yarlung-Zangbo (Searle et al ,1987) suture zone in the north and northeast of Muslimbagh The Muslimbagh Ophiolite (Figure 1A) is one of the best exposed ophiolite of Pakistan which shows a continuous and complete sequence from ultramafic tectonite to sheeted dykes The Muslimbagh Ophiolite is harzburgite type ophiolite and considered to have formed during 82 to 67 m y (Sawada et al , 1993) in the southern Neo-Tethys

Ophiolite Sequence

The Muslimbagh Ophiolite Complex occurs in an area of about 800 km^2 and is represented by 17.5 km thick slab of oceanic lithosphere (Figure 1B) of the southern Neo-Tethys

Ultramafic Tectonites

The exposed thickness of this section in Muslimbagh area is about 11 km and which represents the upper mantle segment of oceanic lithosphere This sequence is mainly represented by tectonized (foliated) harzburgite and dunite with minor lherzolites In the lower ultramafic tectonite sequence harzburgite dunite ratio is 7 3 but in the upper part it is reversed These rocks are strongly sheared and occasionally foliated, and show partial to complete serpentinization. The extent to which they are serpentinized varies from 30% to 100%.

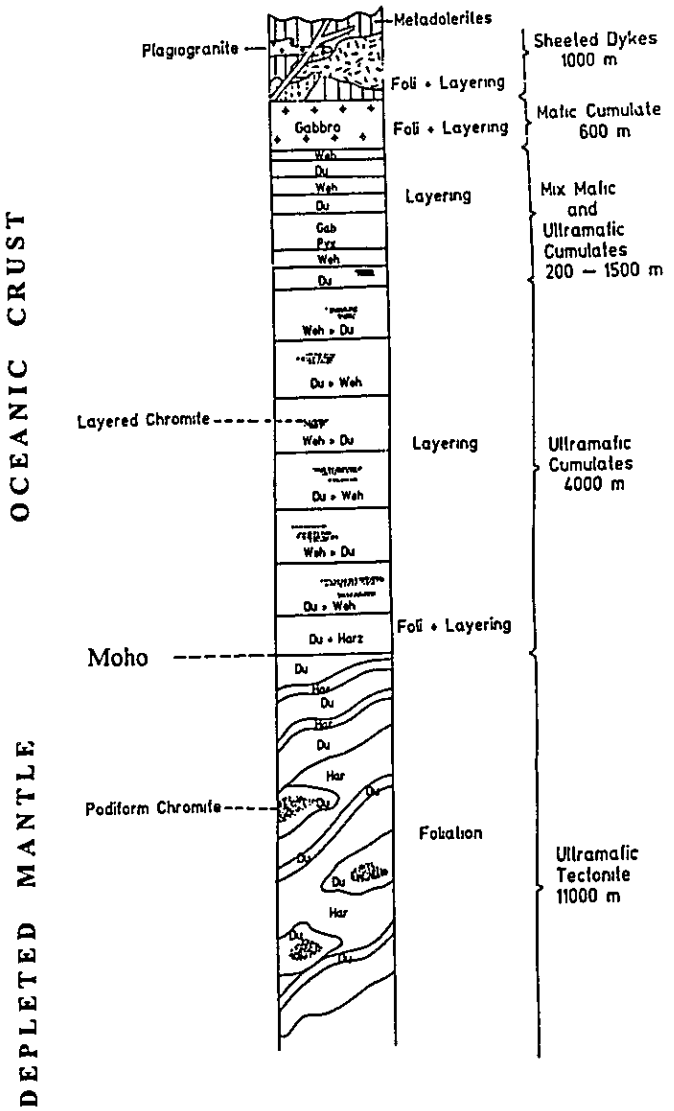

Figure 1 B. Schematic columnar section of Muslimbagh Ophiolite Complex

Ultramafic Cumulates

The upper mantle sequence is followed by a 6.5 km thick crustal sequence. This sequence is recognised in the field by the absence of foliation and the presence of cumulus layering and is represented in the lower part by a 4 km thick intercalation of layered dunite and wehrlite with minor harzburgite and lherzolite. The thickness of layering ranges from less than one centimeter to several hundred meter thick beds. This is followed by 200-1500 m thick cyclic repetition of layered dunite, wehrlite, pyroxenite and gabbro.

Mafic Cumulate

The above mix mafic and ultramafic cyclic sequence is followed by mafic cumulates. This is about 600 m thick and is represented by layered (lower part) and foliated (upper part) gabbro. Two compositional varities are found, the pyroxene gabbro occurs in the lower part which grades into hornblende gabbro in the upper part.

Sheeted Dyke Complex

The mafic sequence is overlain by about 1000 meter thick sheeted dyke complex Originally these rocks were dolerites (contain 48-53% SiO_2) but during emplacement metamorphosed into amphibolites and are represented by foliated and layered and non layered varities. This complex is represented by at least four phases of metadolerites, the earlier phase shows compositional banding of hornblende and plagioclase. The second phase of metadolerite which cut the earlier phase neither shows foliation nor compositional banding. The third phase which cuts the above two phases has foliation and is relatively more mafic in nature. The final phase is represented by dykes which not only cut the above three phases but also to the plagiogranites. This sequence is identified as sheeted dyke complex by earlier workers (Rossman et al., 1971, Ahmed and Abbas 1979). During the present investigation no clear evidence of asymmetrical chilling is observed which is characteristic of such dykes, rather compositional banding and foliation are well developed at many places.

Plagiogranites

The middle part of sheeted dyke complex is invaded by numerous small bodies of plagiogranites, which occur as small pockets, dykes and xenoliths Several varities are identified which include fine, coarse, foliated and mylonitized.

Plate 1

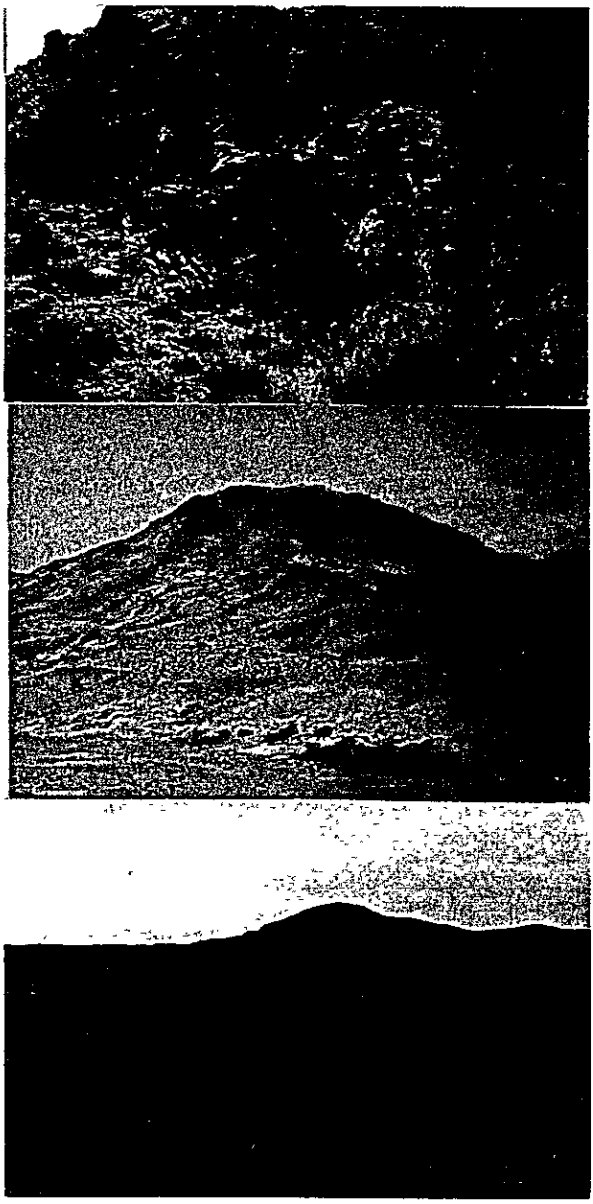

Plate 1. Field photographs of Muslimbagh Ophiolite Complex exposed towards south and southeast of Nisai village. (A) Strongly sheared harzburgite with boudinage of diabase dyke in the upper ultramafic tectonite sequence. (B and C) Layered intercalations of dunite (light Brown) and Harzburgite (dark brown to black) in the lower part of the ultramafic cumulates

Plate 2

(A)

(B)

(C)

Plate 2. Field exposures of Muslimbagh Ophiolite Complex towards southeast of Nisai village showing layering. (A) In wehrlite exhibited by dark (clinopyroxene) and light coloured (olivine) bands in the upper part of the ultramafic cumulate sequence, (B) in cumulate gabbro with dark (clinopyroxene) and light (plagioclase) bands in mafic cumulates (C) Layered metadolerite cut by non layered variety of the same rock in the sheeted dyke complex.

Plate 3

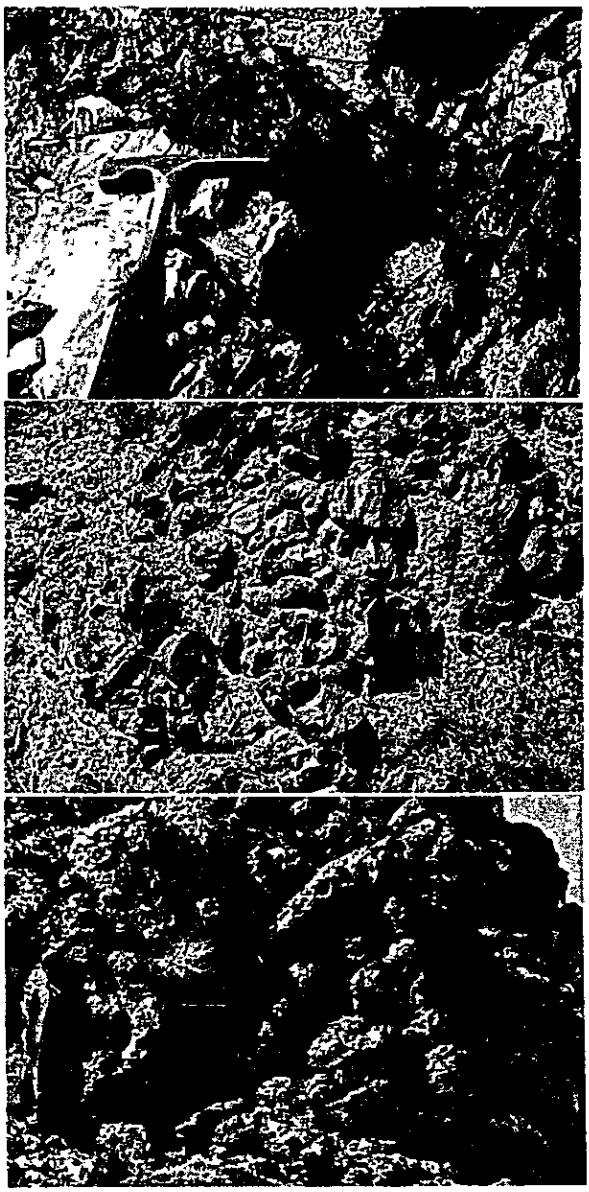

(A)

(B)

(C)

Plate 3 Photographs exhibiting, (A) the last phase of metadolerite dyke transecting the plagiogranite in the sheeted dyke complex, (B) the basaltic pillow lava exposed in the northwestern side of the melange zone, (C) another view of the basaltic pillow lava exposed towards southeastern side of the melange zone.

Pillow Lavas

The pillow basalts are not found on top of the sheeted dyke complex but do occur in the adjacent melange zone (Bagh Complex) These pillow lavas occur towards southern periphery of the Muslimbagh Ophiolite Complex and are 25 meter to 4000 meter thick At places pillows are intercalated with radiolarian chert, pelagic limestone and volcanic breccia. The pillows are ten centimeter to one meter in diameter, porphyritic and amygdaloidal in nature. Several varities of pillow basalts are found which include tholeiitic and alkaline (Sawada et al , 1993) An Early Cretaceous age is assigned to these pillow lavas by Kojima et al , (1993)

Other mafic and ultramafic rocks found in the melange zone include diabase, gabbro norite, dunite, wehrlite and pyroxenite Whole of the ophiolite sequence is transected by a NW trending diabase dyke swarm

PETROGRAPHY

Ultramafic Tectonites

i) Harzburgite: It is generally coarse grained and shows autoclastic, hypidiomorphic granular texture in relatively fresh varieties whereas granoblastic texture predominates in altered varities. Main primary minerals identified include enstatite (bronzite) and olivine Diopside is occasionally found (about 2%) The enstatite (En $_{90-92}$) is euhedral to subhedral. The olivine is subhedral to anhedral and is represented by forsterite (Fo $_{91-93}$) The clinopyroxene is mainly represented by diopside (En $_{47-49}$) The olivine is generally partially to completely replaced by antigorite and iddingsite and orthopyroxene is generally replaced by antigorite and chlorite The microveinlets of chrysotile are common and generally transect the ground mass Small euhedral to subeuhedral crystals of chromian spinel or occasionally magnetite are scattered throughout the groundmass Estimated mineral composition is as follows -

Enstatite	25 - 30 %
Olivine	5 - 10 %
Serpentine	55 - 60 %
Chromian spinel	3 - 5 %

ii) Dunite: It is medium to coarse grained and shows granoblastic texture represented by anhedral grains of olivines embeded in a medium to fine grained mesh of serpentine Minor diopside and enstatite are also observed in some varieties The olivine is represented by forsterite (Fo $_{92-94}$) and is partially to completely replaced by antigorite or occasionally

Plate 4

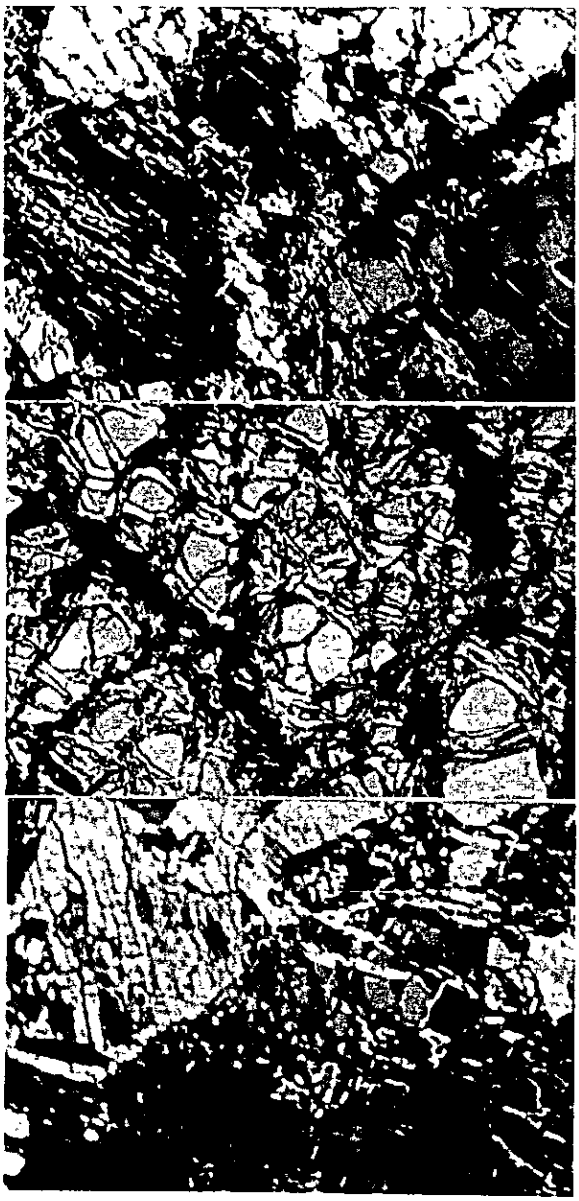

(A)

(B)

(C)

Plate 4 Photomicrographs displaying salient petrographic features of Muslimbagh Ophiolite Complex. (A) Harzburgite showing partial serpentinization of enstatite (white) and olivine (brown). (B) Dunite showing granoblasts of olivine within the serpentine mesh (C) Wehrlite exhibiting partial to complete serpentinization of olivine (pinkish yellow) and diopside (light yellow).

Plate 5

(A)

(B)

(C)

Plate 5. Photomicrographs. (A) Troctolite containing plagioclase (white to gray), olivine (yellow) and minor diopside (orange to purple) arranged in subporphyritic manner. (B) Foliated metadolerite showing alternate bands of hornblende (yellowish brown) and plagioclase (white). (C) Plagiogranite containing large phenocrysts of quartz (white) and smaller euhedral twined crystals of plagioclase.

altered into iddingsite. The chrysotile veinlets genrally transect the groundmass. Small subhedral to anhedral grains of chromian spinel are scattered throughout the groundmass. The estimated mineral composition is as follows:-

Olivine	10 - 15%
Serpentine	75 - 80 %
Diopside	2 - 3 %
Enstatite	1 - 2 %
Chromian spinel	2 - 3 %

Ultramafic Cumulates

i) *Dunite:* The dunite from ultramafic cumulates is relatively less serpentinized and shows granoblastic texture. The olivine generally range in composition from Fo_{89} to Fo_{92}. Diopside is also occasionally found in dunite. Chromian spinel is found as accessory mineral Other characterestics are similar as found in dunites from ultramafic tectonites Estimated mineral composition is as follows -

Olivine	15 - 20%
Serpentine	65 - 70 %,
Diopside	3 - 5 %
Chromian spinel	2 -3 %

ii) *Wehrlite:* It is medium to coarse grain and shows porphyritic and hypidiomorphic granular texture Granoblastic texture is also developed in some varities. Large subhedral to euhedral grains of diopside (En_{43-48}) and anhedral granoblasts of olivine are embedded in partially to completely serpentinized groundmass The olivine is found as small anhedral crystals embedded in an antigorite mesh The olivine is represented by forsterite which range in composition from Fo_{73} to Fo_{89}. Occasionally substantial quantity of enstatite is also found in some varities (< 2%) Olivine is usually altered to antigorite whereas chrysotile occurs in veinlets transecting the groundmass Estimated mineral composition is as follows:-

Olivine	10 - 15%
Serpentine	50 - 55%
Diopside	20 - 30%
Chromian spinel	2 - 3 %
Magnetite	1 - 2 %

iii) Pyroxenite: It is coarse to medium grained and subpoikolitic in texture. Large euhedral to subhedral grains of diopside (En_{47-48}) and small anhedral crystals of olivine are arranged in subpoikolitic manner. Euhedral to sub euhedral enstatite is also

occasionally found as phenocrysts. Olivine is partially serpentinized. Small euhedral to subhedral crystals of magnetite with minor chromian spinel occur as accessories. Estimated mineral composition is as follows.

Diopside	60 - 70 %
Olivine	15 - 20 %
Enstatite	2 - 3 %
Serpentine	5 - 7 %
Opaque	2 - 3%

iv) Troctolite: It is melonocratic holocrystalline, mdium to coarse grained and sub-poikolitic in texture Euhedral to subhedral crystals of plagioclase subhedral to euhedral olivine (Fo_{73-75}) and minor subhedral diopside (En_{43-44}) occur in subpoikolitic manner. Plagioclase show polysynthetic twining according to albite law. Anorthitic contents in plagioclase ranges from An_{58} to An_{70} which fall in labradorite range. Rock shows minor alteration. Antigorite is developed after olivine, sericite after plagioclase and chlorite after diopside. Apatite found as small accicular crystals enclosed in the plagioclase. Chromian spinel and minor magnetite are scattered throughout the groundmass. Estimated mineral composition is as follows

Plagioclase	55 - 60%
Olivine	30 - 35%
Diopside	5 - 10%
Opaque	2 - 3 %

Mafic cumulate

The mix mafic and ultramafic cumulates grade into mafic cumulates which are represented by following rock types:

i) *Pyroxene Gabbro*: It is melanocratic holocrystalline medium to coarse grain and subpoikolitic in texture In some varities thin layering is well developed. Euhedral to subhedral plagioclase and subhedral to anhedral augite with minor olivine and hornblende are arranged in subpoikolitic manner Plagioclase shows polysynthetic twining according to albite law. The anorthite content in plagioclase ranges from An_{54} to An_{68}. Small prismatic crystals of apatite occur as inclusions in plagioclase and subhedral to anhedral grains of magnetite are scattered throughout the groundmass Estimated mineral composition is as follows:-

Plagioclase	50 - 55%
Augite	35 - 40 %
Hornblende	3 - 5%
Olivine	2 - 3 %
Magnetite	1 - 2%
Apatite	Traces

ii) *Hornblende Gabbro:* Is melanocratic holocrystalline medium to coarse grained and subporphyritic in texture. In some varities layering is well developed. Large euhedral to subhedral crystals of hornblende and relatively small euhedral to subhedral and tabular crystals of plagioclase occur as alternate layering. Within plagioclase layers porphyritic texture is developed The anorthite contents in plagioclase ranges from An $_{64}$ to An$_{68}$ but majority of the grains are around An$_{64}$ Substantial amount of augite and olivine are also found interlocked with hornblende Apatite occurs as small accicular crystals within plagioclase. Euhedral to subhedral crystals of magnetite are scattered throughout the groundmass. The estimated mineral composition is as under.-

Plagioclase	50 - 55%
Hornblende	30 - 40%
Augite	3 - 5%
Olivine	1 - 3%
Magnetite	1 - 2%
Apatite	Traces

Sheeted dykes

As mentioned earlier sheeted dykes are represented by at least four phases of metadolerites Originally these rocks were dolerites (contains 48-53% SiO_2) but during emplacement metamorphosed into amphibolites Several textural varities of amphibolite are identified which include coarse and fine grained, layered and non layered, foliated and nonfoliated

Main minerals identified in these rocks include hornblende, ferro-hornblende, ferro-actinolite, ferro-tremolite, plagioclase and minor quartz The hornblende occurs as small prismatic euhedral to subhedral crystals Plagioclase found as euhedral to subhedral and tabular crystals, and shows polysynthetic twining according to albite and combined albite and carlsbad laws The anorthite contents in plagioclase range from An$_{12}$ to An$_{54}$ and majority of them are around An$_{45}$.

The hornblende shows minor chloritization and plagioclase is occasionally dusted with argllization and sericitization Small prismatic grains of apatite are found as inclusions

in plagioclase. Small subhedral to anhedral grains of ilmenite, magnetite and hematite are scattered throughout the groundmass.

Plagiogranite: Several textural and compositional varities are identified which include foliated mylonitized and nonfoliated varities with medium to coarse grained and poikolitic textures.

The main minerals found in plagiogranites include plagioclase (An_{8-30}), quartz with minor hornblende and biotite Hornblende and biotite are partially chloritized whereas plagioclase is dusted with argillization and sericitization Small prismatic crystals of apatite and rutile occur as inclusions in plagioclase and quartz respectively. Small euhedral crystals of hematite are scattered throughout the groundmass. Some varities of plagiogranites grade into granodiorite and quartz diorite with gradual increase in hornblende and reduction in quartz and plagioclase.

Pillow lavas

Under microscope these pillow lavas are hypocrystalline subporphyritic and sub-intersertal in texture. Partially resorbed phenocrysts of augite, plagioclase (An_{54-68}) and antigorite pseudomorph after olivine with minor diopside and hornblende occur in micro to criptocrystalline groundmass Other minerals in groundmass include crystallites and tinny crystals of plagioclase, augite and devitrified volcanic glass. Apatite, ilmenite and magnetite occur as accessories.

Mineral Chemistry

The present microprobe studies on orthopyroxene, clinopyroxene and olivine (Figure 2) from the whole Ophiolite Complex show that orthopyroxene ($Fs_{7.14-8.94}$ $En_{90.19-91.96}$ $Wo_{0.56-2.04}$), Mg # (91 13-92 90) from the harzburgite of ultramafic tectonite has lower Al_2O_3 (1.1-3.75%) relative to its mid oceanic ridge (MOR) type counterpart and its wollastonite contents are also found very low (0 56-2 04) Similarly olivine from the harzburgite of ultramafic tectonite ($Fo_{92.50-94.36}$, Mg # 91 32-92 83) and dunite ($Fo_{92.50-94.36}$) from the same sequence have higher Mg # (92 62-94 41) and higher (0.37-0 47) NiO contents . All the above features indicate a residual upper mantle origin for these rocks (Mysen and Kushiro 1977, Dick and Fisher 1984). The clinopyroxenes in wehrlite ($Fs_{4.27-10.36}En_{43.29-48.19}Wo_{45.37-49.88}$, Mg # 81.56-92.01), pyroxenite ($Fs_{4.07-4.58}En_{47.32-47.89}Wo_{47.79-48.35}$, Mg # 91.44-92.89) and dunite ($Fo_{89.68-91.83}$) from ultramafic cumulate sequence have higher Mg # which are consistent with a higher degree of partial melting (30-45%) of a depleted mantle source and high pressure ($\geq$ 10 kbar) crystal fractionation (Elthon et al , 1982) contrary to these rocks in oceanic crust which generally crystallize in a low pressure

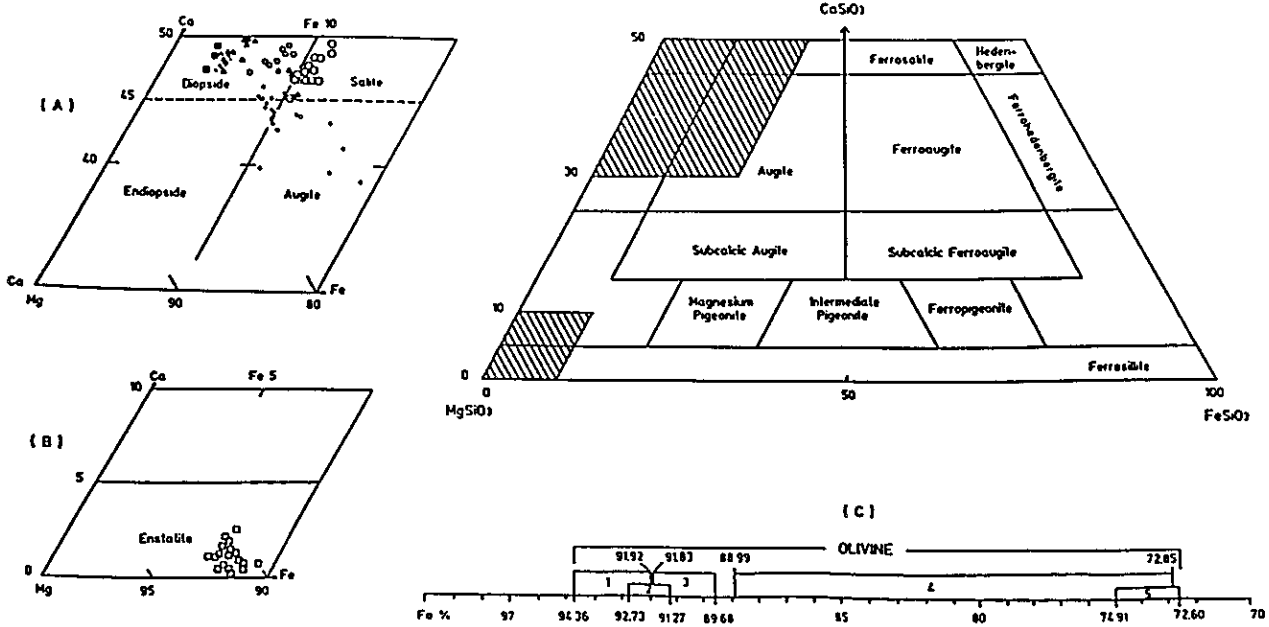

Figure 2. (A) Clinopyroxene composition in harzburgite from ultramafic tectonite (■), in wehrlite from ultramafic cumulate (▲), in pyroxenite from mix-mafic and ultramafic cumulate (·), in gabbro from mix-mafic and ultramafic cumulate (O), in Pillow basalt from melange zone (o) and in diabase from dyke swarm (+). (B) Orthopyroxene composition in harzburgite from ultramafic tectonite (□). (C) Forsterite contents of olivine in dunite from ultramafic tectonite (1), in harzburgite from ultramafic tectonite (2), in dunite from ultramafic cumulate (3) in wehrlite from mix-mafic and ultramafic cumulate (4) and in gabbro from mafic cumulate (5).

(≤ 2.5 kbar) environment (Flower et al , 1977, Dewey and Kidd, 1977) The Cr # of chromian spinel in harzburgite and dunite from the mantle peridotites is also higher (> 0.56) with a few exceptions, which are not consistent with the values found in mid oceanic ridge-type or abyssal-type peridotites (Dick and Bullen 1984).

The microprobe data (Figure 2) on clinopyroxene from pyroxenite ($Fs_{4\,07-4\,58}$ $En_{47.32-48\,19}$ $Wo_{47\,79-48.35}$, Mg # 91 44–92.89), wehrlite ($Fs_{4\,27-10\,36}$ $En_{44\,27-48\,14}$ $Wo_{45.37-49\,88}$, Mg # 81.56-92.01) and gabbro ($Fs_{9\,70-11\,93}$ $En_{39\,44-44\,44}$ $Wo_{45\,21-49\,24}$, Mg # 77.56-82.07) from the ophiolite suites, diabase from dyke swarm and pillow basalt from melange zone plot in the overlapping fields of volcanic arc basalt, within-plate basalt and ocean floor basalt (Figure 3,4A & 4B). Such overlapped plots are considered to have formed by back-arc basin or supra-subduction type ophiolitic rocks (Nisbet and Pearce, 1977; Saunders and Tarney, 1991). Similarly microprobe data on chromian spinel from mantle and crustal peridotites plot within the fields of Semail and Troodos ophiolite (Figure 5A & 5 B) which have already been considered to have formed in back-arc basin or supra-subduction zone type environments (Pearce, 1984).

Petrochemistry

The petrochemical study of metadolerites from sheeted dyke complex and pillow basalts from the melange zone show that they belong to low-K quartz tholeiite series (Figure 6A & 6B). In trace elements chemistry they are enriched in LILE and depleted in HFSE relative to N-MORB, and their average Nb/Y, Zr/Nb, K/Rb, Ba/Zr, Ce/Ba, La/Sm, La/Ce and La/Nd ratios are more consistent with back-arc basin basalt relative to N-MORB or island arc tholeiite (IAT). Their LILE enriched N-MORB and primordial mantle normalized patterns (Figure 7 & 8) and moderately LREE enriched Chondrite normalized REE patterns are also consistent with back-arc basin basalts (Figure 9). The N-MORB normalized patterns of metadolerites and pillow basalts show close resemblance with the back-arc basin basalt patterns of East Scotia Sea and Lau and Fiji basins (Figure 10). The Zr versus Zr/Y plot (Pearce 1984, in Figure 11) shows 15 to 45 % partially melted depleted source for metadolerites and pillow basalts from Muslimbagh Ophiolite Complex which is almost consistent with the inference already reached by mineral chemistry The pillow basalts (tholeiitic) and gabbro found towards southeastern side of the melange zone show island arc like signatures exhibited by their lower K/Rb (138-360), Zr/Nb (1-26), Rb/Sr (0.014-0.063) and Ti/V (10 65-20.97) ratios The lower Zr/Y ratios in these pillow basalts (2.25 to 3.0) and gabbros (0 14-1 15), indicate higher degree of partial melting of a depleted mantle source which are consistent with island arcs.

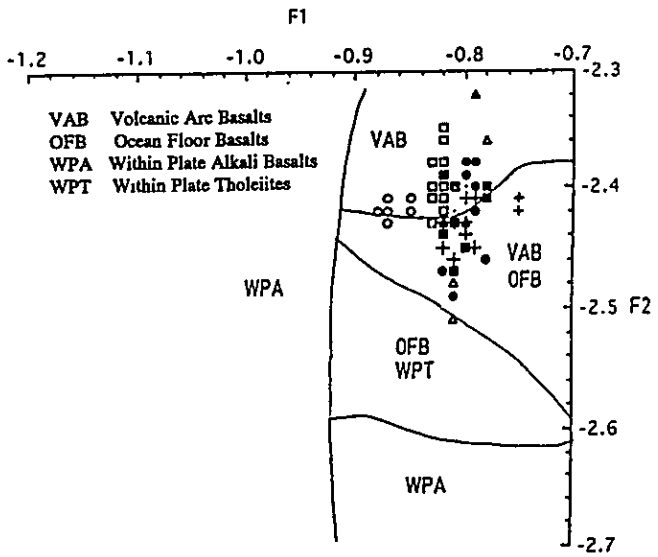

Figure 3 The plot of discriminant function F1 and F2 (after Nisbet and Pearce, 1977) for the clinopyroxenes from wehrlite (Δ) and gabbro (□) from the Muslimbagh Ophiolite Complex and pillow basalt (O) from melange zone and diabase (+) from dyke swarm transecting the whole Ophiolite Complex. The equivalent filled symbols and smaller cross is for Waziristan Ophiolite Complex (the Waziristan data is from Ahmad and Hameedullah,1987).

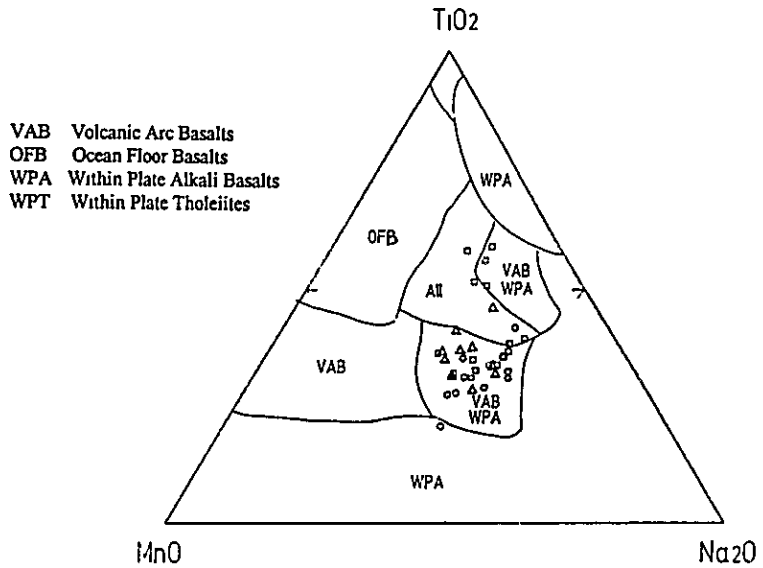

Figure 4A TiO_2-MnO-Na_2O tectonomagmatic discrimination plot (after Nisbet and Pearce 1977) based on clinopyoxene chemistry of gabbro (□),wehrlite (Δ) and pyroxenite (○) from mafic and mix mafic and ultramafic sequence of the Muslimbagh Ophiolite Complex

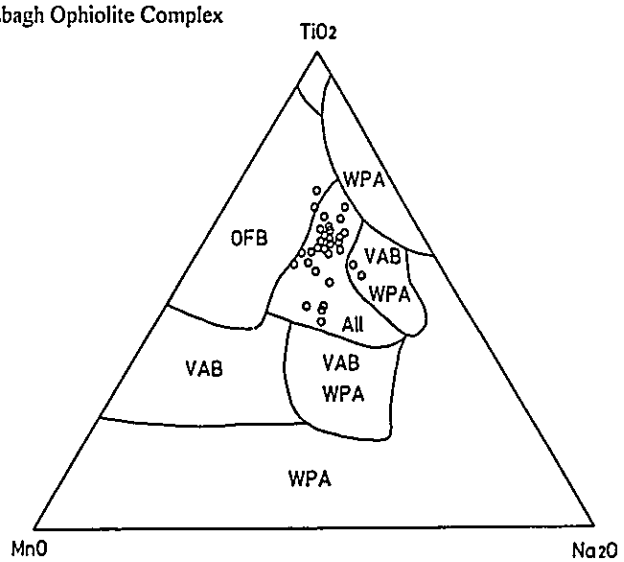

Figure 4B TiO_2-MnO-Na_2O tectonomagmatic discrimination diagram based on clinopyroxene chemistry of diabase dyke swarm transecting the Muslimbagh Ophiolite Complex (after Nisbet and Pearce 1977)

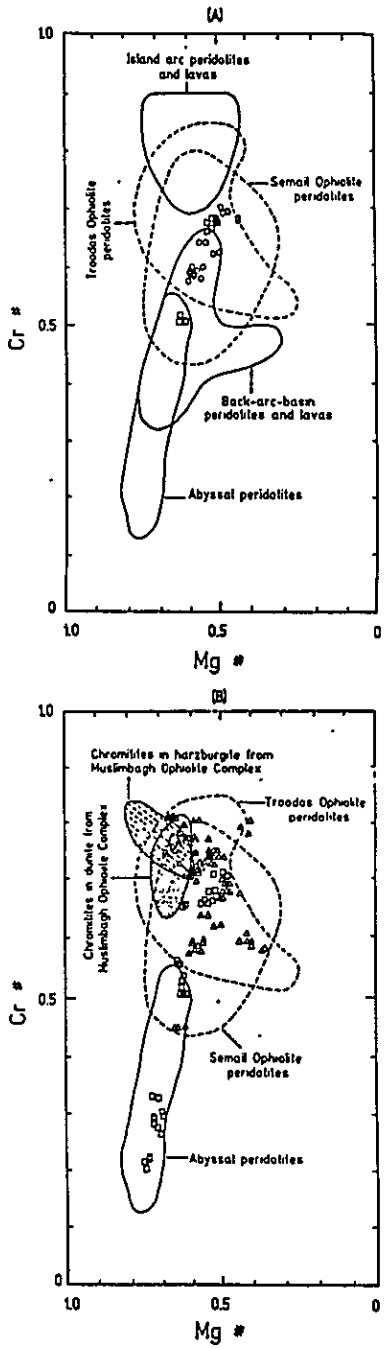

Figure 5 Cr# (Cr/Cr+Al) versus Mg# (Mg/ Mg+Fe^{2+}) plot of chromian spinel from mantle harzburgite (□) and dunite (○) from the Muslimbagh Ophiolite Complex All the boundaries are after Dick and Bullen (1984) (B) The same diagram showing the plot of chromian spinel from mantle harzburgite (□) and dunite from both mantle and crust (△) sequences of the Muslimbagh Ophiolite Complex. The samples for plot (B) are from Hoshino and Siddiqui (unpublished data 1989,1992).

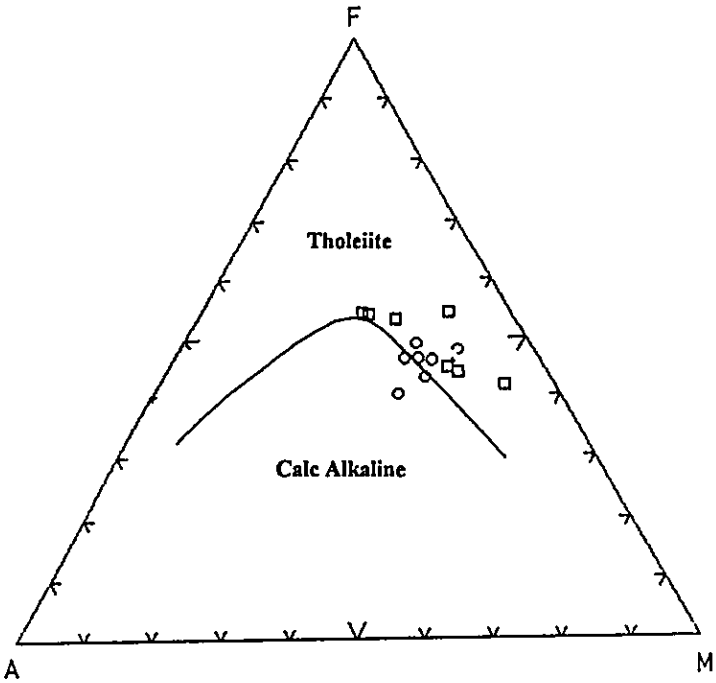

Figure 6A. FAM diagram for the pillow basalts (o) and metadolerites (□) from the Muslimbagh Ophiolite Complex with boundaries from Irvine & Baragar (1971)

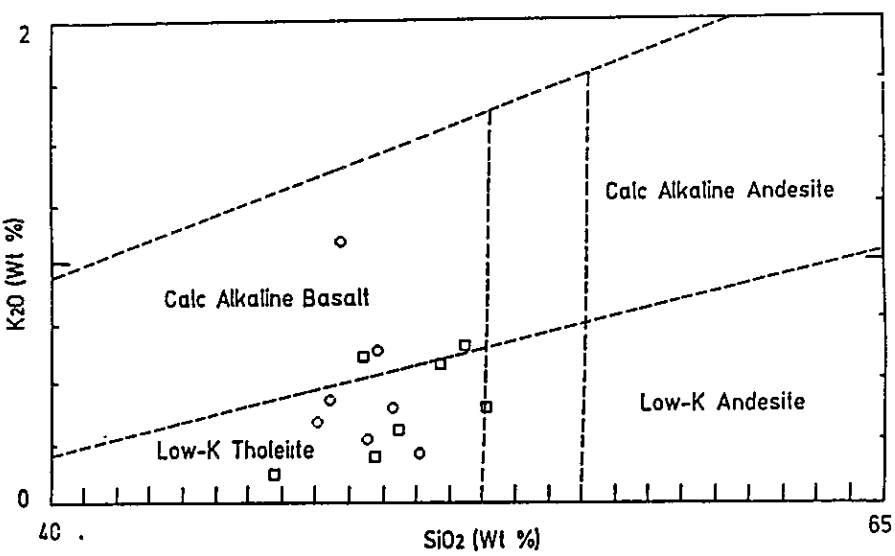

Figure 6B. SiO_2 versus K_2O plot for the pillow basalts (o) and metadolerites (□) from Muslimbagh Ophiolite Complex (boundaries are from Evart (1982), modified after Peccerillo & Taylor 1971).

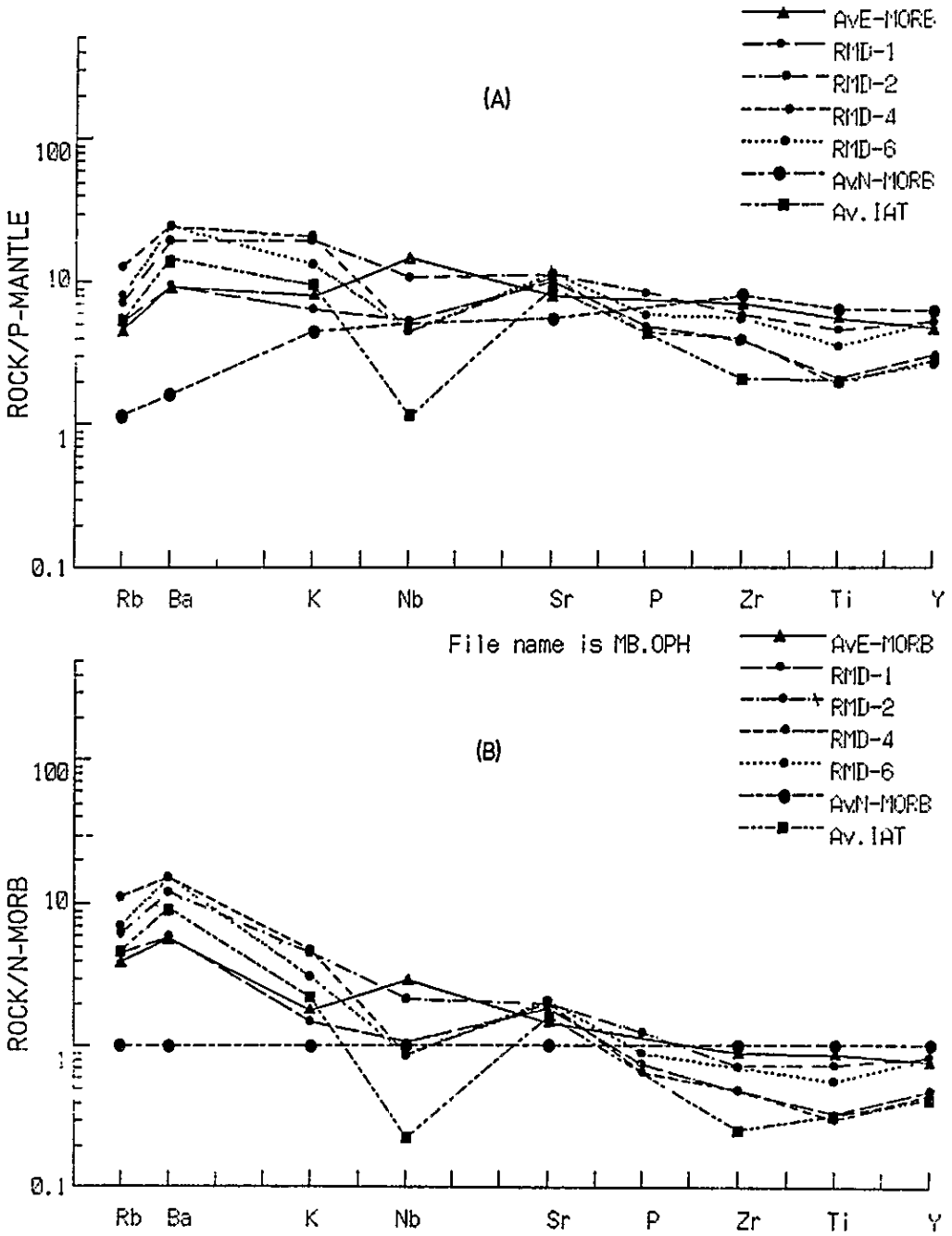

Figure 7. The primordial mantle (A) and N-MORB (B) normalized spider diagrams for metadolerites (RMD) from sheeted dyke complex of the Muslimbagh Ophiolite Complex and average basalts from enriched MORB (Av. E-MORB), normal MORB (Av. N-MORB) and island arc tholeiite (Av. IAT) after Wood et al, 1979.

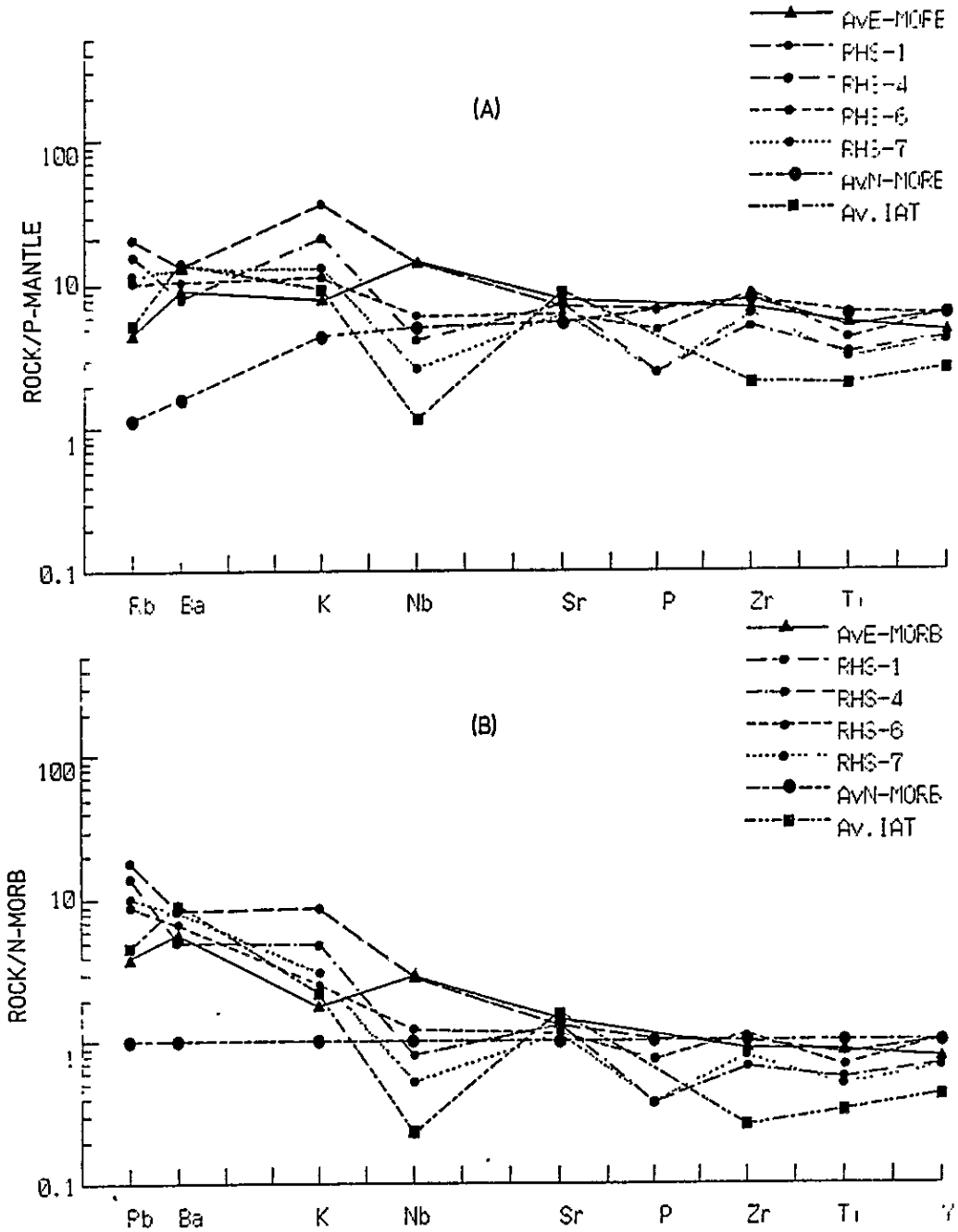

Figure 8. The primordial mantle (A) and N-MORB (B) normalized spider diagrams for pillow basalts (RHS) from melange zone of the Muslimbagh Ophiolite Complex and average basalts from enriched MORB (Av.E-MORB), normal MORB (Av. N-MORB) and island arc tholeiite (Av.IAT) after Wood et al, 1979.

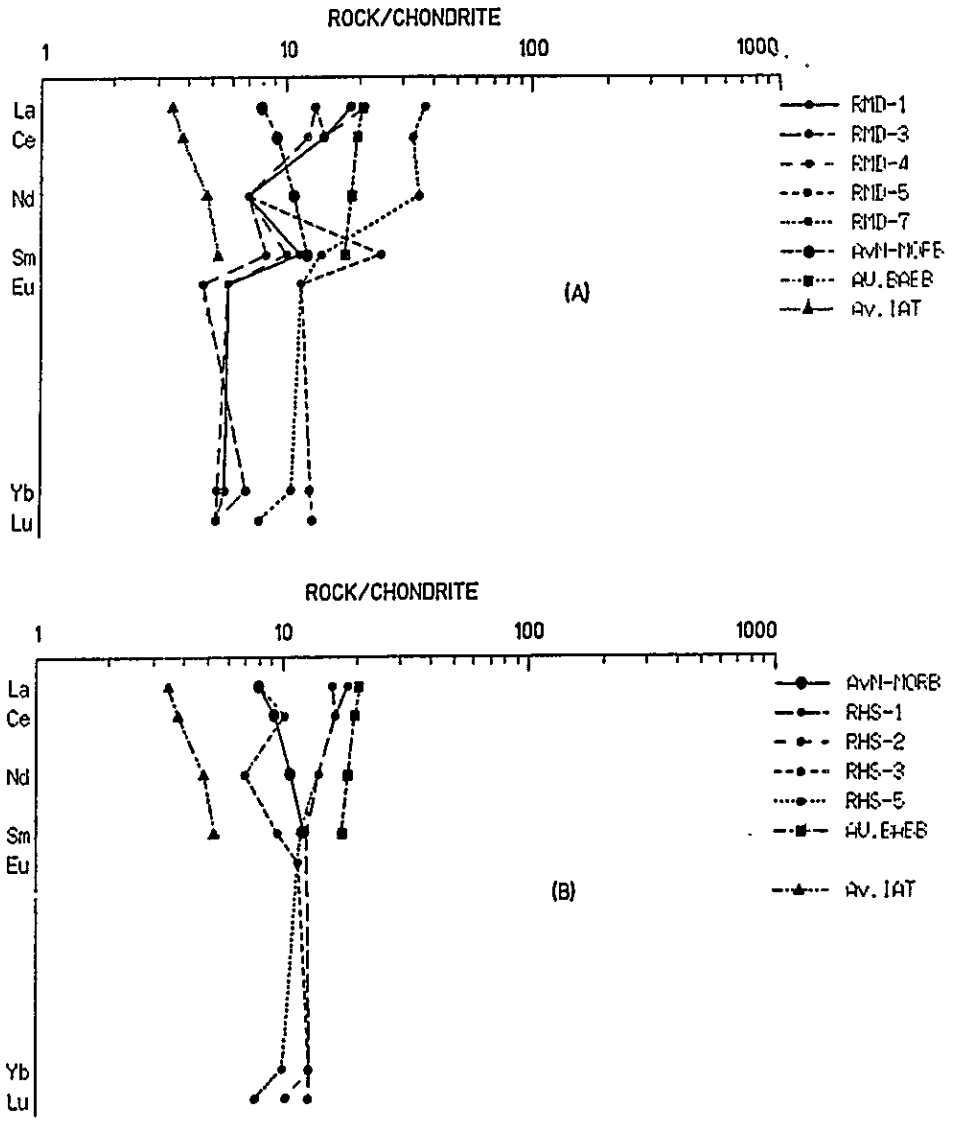

Figure 9. Chondrite normalized REE patterns for metadolerites (A) and pillow basalts (B) from Muslimbagh Ophiolite Complex (after Thompson et al., 1984).

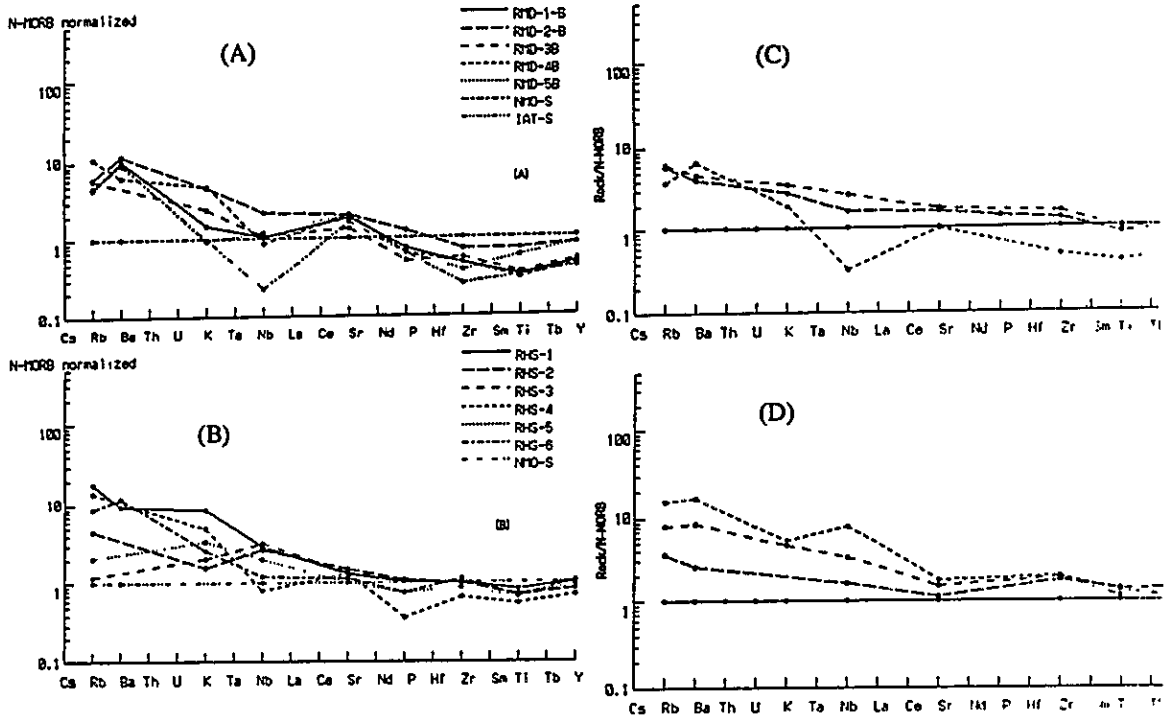

Figure 10 . Comparison of N-MORB normalized spider diagrams for metadolerites (A) and pillow basalts (B) from the Muslimbagh Ophiolite Complex and East Scotia Sea (C) and Lau-Fiji basin (D) basalts.

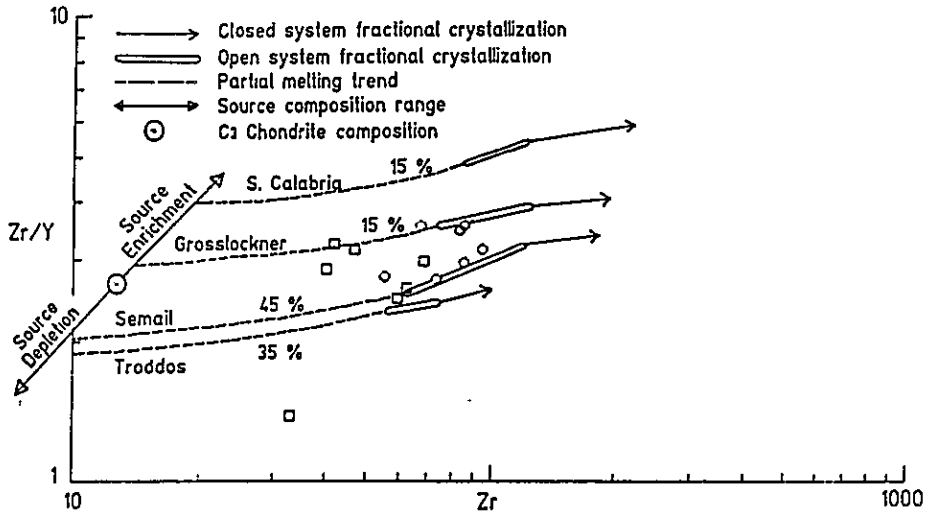

Figure 11. Zr versus Zr/Y diagram for metadolerites (□) and pillow basalts (○) from the Muslimbagh Ophiolite Complex. (After Pearce 1984).

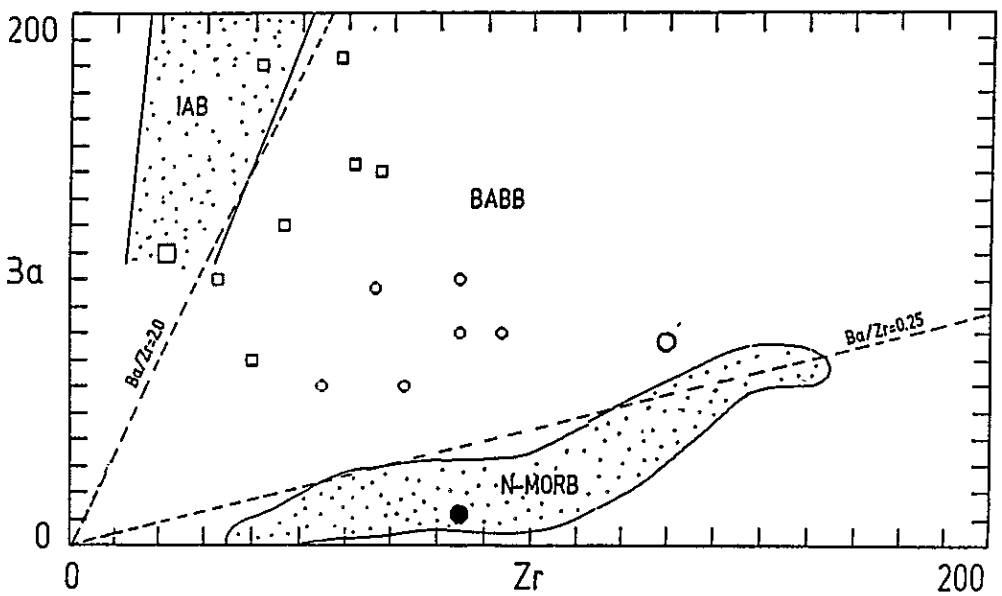

Figure 12. Ba versus Zr tectonomagmatic discrimination plot for metadolerites (□) and pillow basalts (○) from the Muslimbagh Ophiolite Complex and average N-MORB (●), island arc basalts (□) and back arc basin basalt (○) (after Saunders and Tarney 1991).

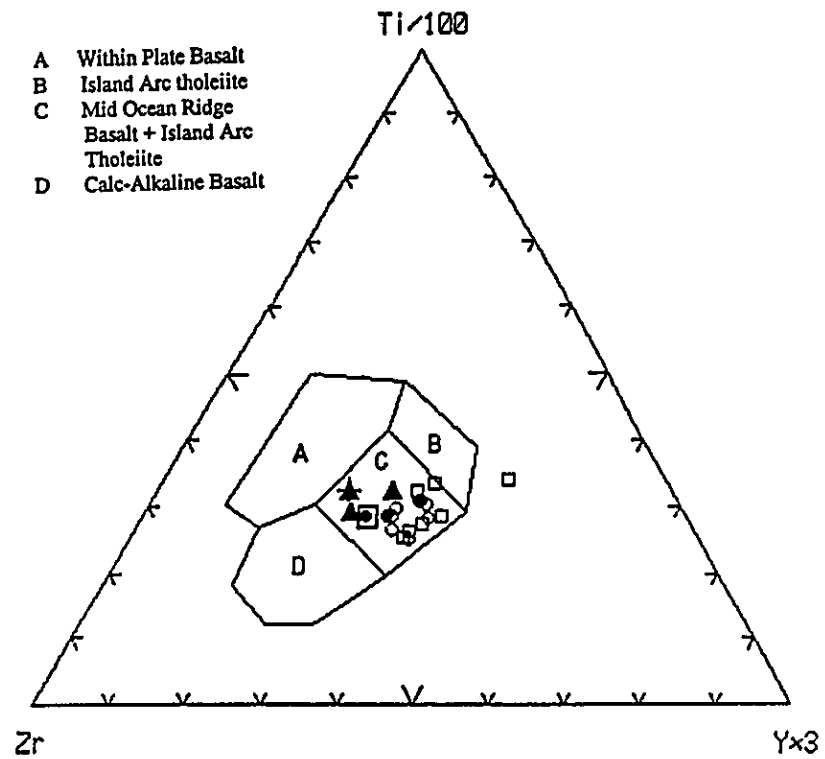

Figure 13. Ti-Zr-Y plot for metadolerites (□) and pillow basalts (o) from Muslimbagh Ophiolite Complex, average Bela Ophiolite Pillow basalt (+), East Scotia Sea (▲), Fiji and Lau (●) back arc basin basalts and average back arc basin basalt (□), after Pearce and Cann, 1973.

Discussion and Conclusion

The Muslimbagh Ophiolite Complex is studied by several past and present workers Vredenburg (1901), Jones (1960) and Bilgrami (1964) have considered it as an intrusive complex Shah (1974) named it as an extrusive complex. Rossman et al., (1971b) first designated it as an ophiolite complex, later on Khain et al., (1973), Gansser (1979), Sillitoe (1974), Andrieux and Brunel (1977), Ahmad and Abbas (1979) also favoured the Rossman et al, (1971b) nomenclature and described it as an ophiolite complex. On the basis of field studies Sillitoe (1974), Otsuki et al., (1989) and laboratory studies Ahmed (1975) and Sawada et al, (1992) have considered that this ophiolite complex was formed in an oceanic ridge setting in the Noe-Tethys ocean Jan et al., (1983 and 1984) have reported high chromium Al-chromitites from the Muslimbagh Ophiolite Complex and correlated it with the alpine type peridotites and stratiform complexes, Hoshino and Siddiqui (1993) on the basis of higher Cr # in the chromitite and chromian spinel found in ultramafic tectonites and cumulates from Muslimbagh Ophiolite Complex suggested that these were not originated in a mid oceanic ridge setting.

The age of origin of Muslimbagh Ophiolite Complex as proposed by Sawada et al., (1993) is Late Cretaceous (82 to 67 m y). The paleotectonic data (Dietz and Holden, 1970; Powel, 1979, Clark, 1990) on southern Neo-Tethys suggest an island arc rather than a mid oceanic ridge type environment during this period. The Bela Ophiolite has recently been interpreted to have formed in a supra-subduction zone (Ahmad, 1991), and the Waziristan Ophiolite Complex was proposed to have formed in an island arc setting by Ahmad and Hameedullah (1987) (although the plot of clinopyroxene from Waziristan Ophiolite Complex in Figures 3 and 4C lead to the similar tectonic setting as for Muslimbagh Ophiolite Complex) The Petrological studies of Muslimbagh Ophiolite Complex reveal that the harzburgites are poor in modal clinopyroxene, the dunites are poor in pyroxene The mineral chemistry of orthopyroxene and olivine of harzburgite and dunite from ultramafic tectonites is consistent with residual upper mantle origin whereas mineral chemistry of clinopyroxene and olivine from ultramafic cumulates posses high Mg # and chromian spinels, have high Cr #. All these feature are are consistent with a higher degree of partial melting of a depleted upper mantle source. (most probablly plagioclase lherzolite) The mafic rocks are enriched in LILE and depleted HFSE in their bulk chemistry and have lower K/Rb Ti/V Zr/Y ratios relative to N-MORB which suggests that primitive magma of Muslimbagh Ophiolite Complex was more depleted and more residual in nature and was modified by subduction related fluids enriched in LILE and LREE. The plots in figures 12 & 13 based on trace element chemistry leads to interpret

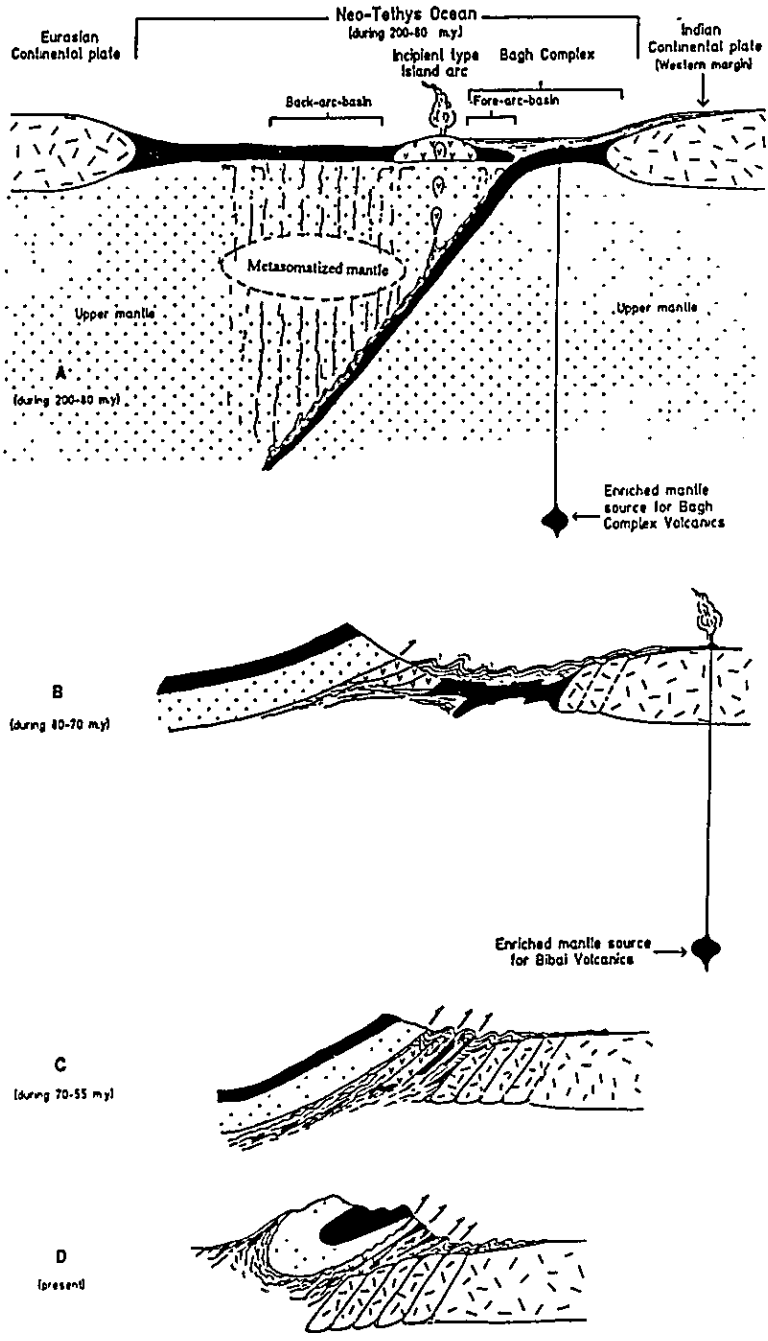

Figure 14. Sketch showing the formation and tectonic evolution of the Muslimbagh Ophiolite Complex in the southern Neo-Tethys.

that the Muslimbagh Ophiolite Complex was formed in a back-arc basin environment which developed in the southern Neo-Tethys during Late Cretaceous. The pillow basalts (tholeiitic) and gabbro found towards southeastern side of the melange zone show island arc like geochemical signatures. The Muslimbagh Ophiolite Complex was emplaced sporadically onto the continental shelf of Indian continental plate during Late Paleocene to Early Eocene (Allemann 1979) or Latest Cretaceous to Paleocene (Kojima et al ,1994). A new tectonic model (Figure 14) is proposed, based on the aforementioned data for the origin and evolution of Muslimbagh Ophiolite Complex. It is suggested that the sediments of the Bagh complex (Melange Zone) were deposited in the western continental shelf of Indian plate, ocean floor of Neo-Tethys ocean, and in a trench of an incipient type island arc during 200 to 80 m.y The incipient type oceanic island arc was developed at about 80 m.y in the Neo Tethys ocean, which got back and fore arc separations. The Muslimbagh Ophiolite Complex represent the oceanic lithosphere of this back arc basin The tholeiitic pillow lava and gabbro found towards southeastern side of the melange zone might have been developed in this arc and the tholeiitic pillow lavas found towards southwestern side of melange zone might have been developed in the fore-arc basin The within plate alkali basalts (Sawada et al., 1993) might have been developed as oceanic islands in the ocean floor of the Neo-Tethys ocean (the oceanic part of the Indian plate). These tholeiitic and alkali basalts and adjacent sediments were scraped off during subduction and accreted as subduction complex. During 80 to 55 m.y the above back arc oceanic lithosphere, subduction complex and other adjacent sediments were sporadically emplaced onto the western margin of the Indian continent due to the oblique collision of Indian plate with the Afghan micro continent

Acknowledgment

The authers are greatly indebted to Tahir Karim, of the Geoscience Laboratory G.S.P, Islamabad for critically reviewing the manuscript. A. Minami is gratefully thanked for carring out the microprobe analyses in Hiroshima University, Japan.

References

Ahmad, Z., 1975, Geolgy and Petrochemistry of a part of the Zhob Valley Ignous complex, (Baluchistan) Pak Geol., Surv. Rec. Vol. 24.

Ahmad, Z., 1992, Basalt geochemistry and surasubduction zone origin of the Bela Ophiolite , Pakistan Acta Mineralogica Pakistanica v 5 pp 83-98.

Ahmed, W. and Hameedullah., S , 1987, Island arc signatures from the Waziristan igneous Complex, N W.F.P., Pakistan Geol. Bull. Uni. Peshawar.vol 20.

Ahmed, Z , and Abbas, S G., 1979, The Muslimbagh Ophiolites,In,Farah, A and DeJong, K.A. (eds) GEODYNAMICS OF PAKISTAN pp 243-250

Allemann, F. 1979, Time of Emplacement of the Zhob Valley Ophiolite and Bela Ophiolite. In Farah A. and DeJong K A (eds) GEODYNAMICS OF PAKISTAN pp 215-242.

Andrieux, J and Brunel, M, 1977, Evolution des chaines ochidentales du Pakistan, e n h s Soc. Geol Franc No. 8 pp 189-208.

Bilgrami, S.A., 1964, Mineralogy and petrology of the Central part of the Hinddubagh Igneous Complex, Hindubagh Mining District Zhob Valley, West Pakistan. Geol. Surv. Pakistan Rec Vol 10, 28p

Clark, M.H.,1974, Omans Geological Heritage" published by the Petroleum Development,Oman. 247p

Dewey, J.F. and Kidd, W.S.S., 1977, Geometry of plate accretion. Bull.Geol. Soc. Amer.88, 960-968

Dick,H.J.B and Bullen,T., 1984, Chromian Spinel as a petrogenetic indicator in abyssal and alpine type peridotites and spatially associated lavas Cont. Min. & Petrol 86, pp 54-76

Dick,H.J.B.and Fisher,R L., 1984, Mineralogic studies of the residues of mantle melting: Abyssal and Alpine type peridotites pp 295-308 In: J. Kornprobst (Ed) Kimberlites vol.2 The mantle and crust-mantle relationships Elsevier

Dietz R.S and Holden J.C 1970, The Breakup of Pangea Soi Am , 221 pp 126-137

Elthon, D., Casey, J.F and Komor, S., 1982, Mineral chemistry of ultramafic cumulates from the north Arm Mountain massif of the Bay of island ophiolite: evidence for high pressure crystal fractionation of oceanic basalts Jr Geophys Res 87,pp 8717-8734.

Farah, A. Abbas, S G. DeJong, K A and Lawrence, R D , 1984, Evolution of the Lithosphere in Pakistan. Tectonophysics, 105 pp 207-227. Frey Clauge 1983

Flower,M.F.J., Robinson, P.T , Schminki, H.U and Ohnmacht, W. 1977, Magma fractionation systems beneath the Mid-Atlantic Ridge at 36-37 N Contrib Miner Petrol 64, 167-1995.

Gansser, A., 1979, Reconnaissance visit to the Ophiolites in Baluchistan, In Farah, A and DeJong, K.A. (eds) GEODYNAMICS OF PAKISTAN pp 193-213

Hawkesworth, C.J., O'Nions, R K , Paukhursat, R J , Hamilton, P J and Evensen 1977, A geochemical study of island arc and back-arc tholeiites from the Scotia Sea Earth Planet. Sci Lett. 36, pp 235-262

Hoshino, K., and Siddiqui, R H ,1993, Chromite deposits in Muslimbagh Ophiolite (in preparation)

Hunting Survey Corp. Ltd. (H.S.C.)., 1960, Reconnaissance Geology of Part of West Pakistan, Publ. under Colombo Plan Coop. Project, Govt. of Canada, Toronto, Canada.

Jan, M.Q ,Khattak, M.U K and Tahirkheli, R A K ,1983, A comparison of chemistry of chromites from the Zhob valley, Harichand and Waziristan Ophiolite Complexes of Pakistan

Jan, M.Q , Windley, B F and Abbas, G , 1984, Microprobe analytical data on Chromitites from the Muslimbagh Opiolite, Balochistan, Pakistan, Geol Bull. Univ Peshawar v 17 pp 1-16

Jones, A. G., ed, 1960, Reconnaissance geology of a part of west Pakistan A Columbo Plan Co-opreative Project Rpt Toranto, Gorernmt of Caneda 550 p.

Khain, V., Kats, Ya G. and Selitskiy, A G , 1973, Tectonic regionalization and main features of modren structures of alpine belt in the near and middle part East Int Geol. Rev. 15, pp. 117-133

Kojima, S , Naka, T., Kimura, K , Mengal J M , Siddiqui, R H , and Bakht, M S 1993, Mesozoic Radiolarians from the Bagh Complex in the Muslimbagh area Pakistan Their significance in reconstructing the geologic history of ophiolites along the Neo Trthys suture zone Bull Geol Surv Japan 45 (2) pp 63-97

Mengal, J.M & Siddiqui, R H , 1993, Geological map of Bagh quadrangle Killa Safullah District Balochistan Pakistan Geol, Surv Pak Map Ser (in press)

Miyashiro, A 1974, Volcanic rock series in volcanic arcs and continental margins Am Jour Sci 274 pp 321-55

Mysen, B O and Kushiro, I , 1977, Compositional variations of coexisting phases with degree of melting of peridotite in the upper mantle Am Mineral 62 pp 843-65

Nisbet, E G. and Pearce, J A , 1977, Clinopyroxene Composition in Mafic Lavas from Different Tectonic Setting Cont Min Pet 63 pp 149-160.

Otsuki, K , Anwar, M , Mengal J M, Brohi, F A , Hoshino, K , Fatmi, A N and Okimura, Y., 1989, Breakup of Gondwanaland and Emplacement of Ophiolite Complex in Muslimbagh Area of Baluchistan Geol Bull Univ Peshawar 22· pp 103-126.

Pearce, J.A , 1980, Geochemical evidence for the genesis and eruptive setting of lavas from Tethyen ophiolite Proc Int Ophiolite Symp. , Cyprus1979,pp 261-272.

Pearce, J.A. and Cann, J.R. 1973, Tectonic setting of basic volcanic rocks determination using trace element analysis. Earth Planet. Sci Lett. 19 pp 290-300.

Pearce, J.A., Lippard,S.J and Roberts, S., 1984, Characteristic and tectonic significance of supra-subduction zone opiolites . In· B.P Kokelaar and M.F Howells (Edts)Marginal Basin Geology .Volcanic and associated sedimentary and tectonic processes in modern and anciant marginal basins. Spec. Pub. Geol. Soc. London,16: pp 77-94.

Powel, C.M.A, 1979, A Speculative Tectonic History of Pakistan and Surroundings:Some Constraints from the Indian Ocean. In: Farah, A. and DeJong, K.A.(eds) GEODYNAMICS OF.PAKISTAN.pp.5-24

Rossman, D. L. Ahmad, Z., and Abbas, S G., 1971b, Geology and Chromite deposits of the Saplai Tor Ghar and Nisai area Zhob velly complex, Hindubagh Qulta Divisrion west of Pakistan Pak Geol Surv and U.S Geol Surv Interim Report Pk-51,47p.

Saunders, A.D., and Tarney,J., 1984, Geochemical characteristics of basaltic volcanism within back-arc basin. In Kokelaar, B.P & Howells, M.F.(eds) MARGINAL BASIN GEOLOGY. Geol Soc. London. Spec ;Publ. 16 pp. 59-76.

Saunders, A.D. and Tarney, J. 1991, Back-arc basins. In Floyd. P A (ed) OCEANIC BASALTS, Blackie London pp 219-263

Sawada, Y., Kubo, K and Siddiqui R.H., 1993, K-Ar ages of the igenous and metamorphic rocks from Muslimbagh area, Pakistan (in preparation)

Sawada, Y., Siddiqui R.H., Aziz, A and Rahim S.M., 1992, Mesozoic Igneous activity in Muslimbagh area, Pakistan, with special reference to hotspot magmatism related to the break-up of the Gondwanaland. Proc of Symp. on Himalayan Geology Shimane Japan 42 p.

Searle, M.P., Windley, B.F.,Coward,M P., Cooper, D J.W., Rex,A.J., Rex,D., Lit., Xiao, X., Jan, M.Q., Thakur,V.C and Kumar, S 1987, The closing of Tethys and the tectonics of Himalaya.Geol. Soc Am. Bull.98 pp 678-701.

Shah, S. H. A., 1974, The structurs of chromite bearing ultramafic complex of Muslimbagh and its control on ore grade: Geonews, v 4 pp. 20-23.

Siddiqui, R.H and Mengal, J.M., 1995, Island arc affinities of cumulate gabbro and pillow basalts found towards southeastern side of the Bagh Complex, Balochistan, Pakistan (in preparation)

Sillitoe. R.H, 1974, Metallogenic evolution of a collisional mountain belt of Pakistan,Geol. Surv. Pak. Rec. 34, 16p

Sun, S.S. and Nisbitt. R.W. and Sharaskin, A N., 1979, Geochemical characteristics of mid-oceanic ridge basalts Earth Planet. Sci. Lett. 44, 119-38.

Sun, S.S., 1980, Lead Isotop study of young volcanic rocks from mid-oceanic ridges, ocean islands and island arcs. Phil. Trans R. Soc. Lond. A297, 409-445.R.N .,

Thompson,R.N., Morrison, M.A., Hendry, G.L and Parry, S.J 1984, An assessment of the relative roles of crust and mantle in magma genesis. an elemental approach. Phil Trans. R.Soc. London A 310, pp 549-590.

Vredenburg, E., 1901, A geological sketch of the Balochistan desert ant part of eastern Persia Mem. Geol. Surv. India v 31 pp 179-302.

Wilson, M.,1989, IGNEOUS PETROGENESES. Unvin. Hyman, London UK. 466p.

Wood, D.A., Joron, J.L. and Trevil, M. 1979, A reapparaisal of the use of trace element to classify and discriminate between magma series erupted in different tectonic setting. Earth Planet.Sci.Lett. 45, pp. 325-336.

Proceedings of Geoscience Colloquium, Geoscience Lab ,GSP, 9, 51-58

Modes of Plagioclase Twinning in the Chilas Complex and Kohistan Batholith, Northern Pakistan

Yuhei Takahashi, Yutaka Takahashi*, Allah Bakhsh Kausar**, Tahseenullah Khan** and Kazuya Kubo**

**JICA Expert, Geological Survey of Japan*
***Geoscience Laboratory, Geological Survey of Pakistan, Islamabad*

INTRODUCTION

Feldspars are the most abundant minerals in the earth's crust and the rheology of feldspars is representative for that of the crust as a whole (Olsen and Kohlstedt, 1985). In addition to this, feldspars have often recorded important information of plutonism and metamorphism (Gorai, 1951). In this manuscript, we present the results of the studies on plagioclase twinning of the Chilas Complex and the Kohistan Batholith, which are large plutonic bodies in the Kohistan terrain, northern Pakistan. At the end of the manuscript, the geological implications of the results are discussed.

GEOLOGICAL SETTING

1. General

Kohistan encompasses most of the country along the middle Indus Valley in northern Pakistan. Geologically, the Kohistan terrain is bounded along the south by the Main Mantle Thrust zone (MMT) and along the north by the Main Karakoram Thrust (MKT) (Tahirkheli et al., 1979). The rocks of the Kohistan terrain have been interpreted as representing an island-arc sequence caught up between the Indian and Asian plates and deformed during the collision of the two plates (e.g., Coward et al., 1982; Petterson and Windley, 1985).

The Kohistan terrain can be divided broadly into a few components (e.g., Searle, 1991). Southern Kohistan includes the Jijal Complex, which is composed of high grade metamorphosed ultramafic body, and the Chilas Complex, which is composed of mafic and ultramafic rocks. These two complexes are separated by the Kamila shear zone.

Northern Kohistan is dominated by numerous large-scale granitic plutons (Kohistan Batholith) and a sequence of arc-type volcanic rocks and meta-sediments.

2. Chilas Complex

The Chilas Complex comprises a very thick mafic-ultramafic stratiform plutonic complex (Jan et al., 1984). Dominant components (host rocks) are gabbro and gabbronorite, and minor components include layered gabbro, anorthosite, troctolite, chromite-layered dunite, pyroxenite and peridotite (Khan et al., 1989). The extensive calc-alkaline gabbronorites of the Chilas Complex were derived from partial melting of a mantle diapir emplaced into a mature arc (Khan et al., 1993). After crystallization, the Chilas Complex underwent a granulite facies re-equilibration at ca. 800°C at 7-8 kbar (Jan and Howie, 1980). Ar-Ar and K-Ar ages from the Complex indicate cooling through 500°C, the hornblende blocking temperature, at around 80 Ma (Treloar et al., 1989).

3. Kohistan Batholith

The composition of the Kohistan batholith varies from hornblende gabbro to leucogranite, but it is dominantly composed of granodiorite to quartz-diorite. Based on the degree of deformation and radiometric dating, the Kohistan batholith is divided into three stages (Petterson and Windley, 1985, 1991; Petterson et al., 1993; Treloar et al., 1989); strongly deformed plutons in the early stage(76-102 Ma), weakly deformed to undeformed plutons in the second stage(40-62 Ma), and swarms of leucogranite sheets in the final stage(29-34 Ma).

DESCRIPTION FOR EXAMINED SAMPLES

Eight rock samples, four each of the Chilas Complex and Kohistan Batholith, were collected in the vicinity of Chilas town and near Gilgit, respectively (Fig. 1).

Rock samples of the Chilas Complex are medium-grained gabbronorite. Main constituents are plagioclase, orthopyroxene and clinopyroxene with subordinate amount of quartz, biotite and hornblende. Accessories are apatite and opaque minerals. Plagioclase is subhedral and up to 2 mm. Plagioclase composition is mostly 40 to 55 % in anorthite component (Fig. 2). Pyroxenes are subhedral to anhedral and up to 1 mm. Quartz is interstitial and up to 2 mm, and shows very weak wavy extinction.

Present samples of Kohistan Batholith are undeformed to weakly deformed, corresponding to the second stage of the batholith. Rock samples are medium-grained

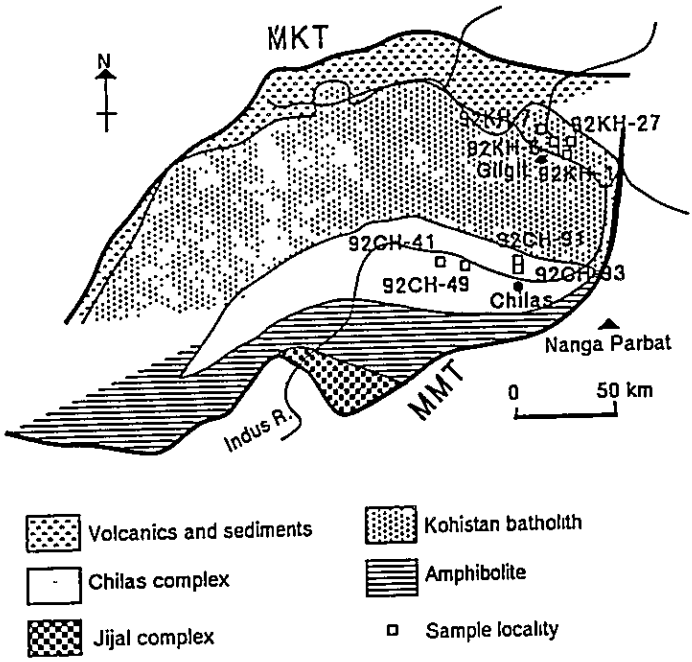

Fig.1 Simplified geologic map (modified from Khan and Coward, 1990) showing locations of examined samples

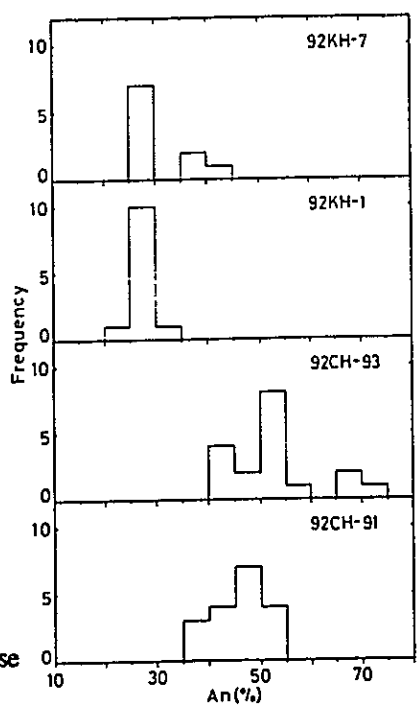

Fig.2 Frequency of An composition in plagioclase

quartz-diorite to tonalite. Main constituents are plagioclase, quartz, hornblende, biotite and epidote with or without K-feldspar. Accessories are sphene, apatite and opaque minerals. Plagioclase is subhedral and up to 3 mm. Plagioclase composition is mostly 25 to 40 % in anorthite component (Fig. 2). Quartz is up to 1 mm and shows very weak wavy extinction. Hornblende is subhedral to anhedral and up to 2 mm, and shows pale green to brownish green Z-axial color. Biotite is subhedral to anhedral and up to 3 mm, and shows greenish brown Z-axial color.

PLAGIOCLASE TWINNING LAWS

1. Method for determining twinning laws

Plagioclase twinning laws were determined by optical method using a universal stage. The way to determine the plagioclase twinning laws was described in Takahashi and Nishioka (1994) and Takahashi et al. (1994). The procedures are summarized as follows.

The composition plane can be determined by referring to the crystallographic relationship between composition plane and optical elastic axis. The twinning laws having the composition plane (010) can be determined by measuring the extinction angle in the zone perpendicular to (010) (Suwa et al., 1974). By this method, albite, Carlsbad, albite-Carlsbad, albite-Ala B and Ala B twins can be distinguished. In our study, the other composition plane was (001) or rhombic section. In this case, if twinned plagioclase is simple twin and shows symmetrical extinction, the twinning is identified as Manebach law. Twinned plagioclase not having symmetrical extinction is now identified pericline twin though this cannot be separated from Acline twin for all plagioclase of 0 to 70 % in anorthite composition.

Table 1 Frequency of plagioclase twin laws (%)

Name of body	Chilas Complex				Kohistan Batholith			
Sample No.	92-CH				92-KH			
	41	49	91	93	6	7	1	27
Numbers of measurements	(60)	(50)	(59)	(50)	(50)	(50)	(50)	(50)
Carlsbad	3.3	4.0	0.0	4.0	2.0	0.0	2.0	2.0
albite-Carlsbad	0.0	0.0	5.1	0.0	12.0	4.0	10.0	24.0
albite	56.7	62.0	71.2	74.0	74.0	58.0	58.0	58.0
albite-pericline	28.3	30.0	15.3	16.0	2.0	18.0	20.0	10.0
pericline	11.7	4.0	8.5	6.0	8.0	16.0	10.0	6.0
others	0.0	0.0	0.0	0.0	2.0	4.0	0.0	0.0

2. Result

Plagioclase twinning laws were determined in mostly up to 50 grains of twinned plagioclases along systematic lines in one thin section. Results are shown in Table 1 and Fig. 3. In gabbronorite of Chilas Complex, albite twin is common, followed by albite-pericline composite twin and pericline twin. Carlsbad twin and albite-Carlsbad twin are minor. In tonalite and granodiorite of Kohistan Batholith, albite twin is common, followed by albite-Carlsbad twin, albite-pericline composite twin and pericline twin. Carlsbad twin and others (albite-Ala B twin and Manebach twin) are minor.

DISCUSSION

Assignment to a particular mechanism of formation is often hazardous, and consequently discussion of the frequency of twinning in plagioclase is severely handicapped (Smith, 1974). However, from practical viewpoint, frequency of plagioclase twinning is useful for characterization of the plutonic rocks and metamorphic rocks, especially in high grade metamorphic terrain.

Gorai (1951) found that it is profitable to group the twin laws into two categories; A twins and C twins. The A twins, comprising the albite and pericline laws, occur in all rock types, while the C twins, comprising all the other laws, are frequent only in volcanic and plutonic rocks. Frequency of C twins, particularly Carlsbad and albite-Carlsbad twins, is low, especially in the schist and gneisses.

On the other hand, it is suggested that the pericline twin is generally produced by mechanical deformation. Wenk (1969) heated an albite-twinned oligoclase at 5-15 kbar and 800-1000°C and found very fine-scale pericline twinning developed in the albite lamellae. Albite and pericline twins have been produced at a strain rate of 2×10^{-5}/sec at 1073°K and 0.8-1.0 GPa in low and transitional plagioclase of 32 to 95 % in anorthite composition (Borg and Heard, 1970).

Now we use the ratio of C twins and the ratio of pericline twin in twinned plagioclases to discuss the implication of frequency of plagioclase twinning in the Chilas Complex and the Kohistan Batholith (Fig. 4).

The ratios of pericline twin of both are overlapped, suggesting that these are deformed under same physical condition. The ratios of C twins in the Kohistan Batholith are more than those in the Chilas Complex. The ratios of C twins of the Kohistan Batholith are more than 8 %, indicating mostly within the igneous field of Gorai(1951) and Suwa (1956). The ratios of C twins of the Chilas Complex are less than 5 %, indicating within metamorphic field (Suwa, 1956). It is noted that the Chilas Complex has been emplaced at depth first and subsequently metamorphosed, which is

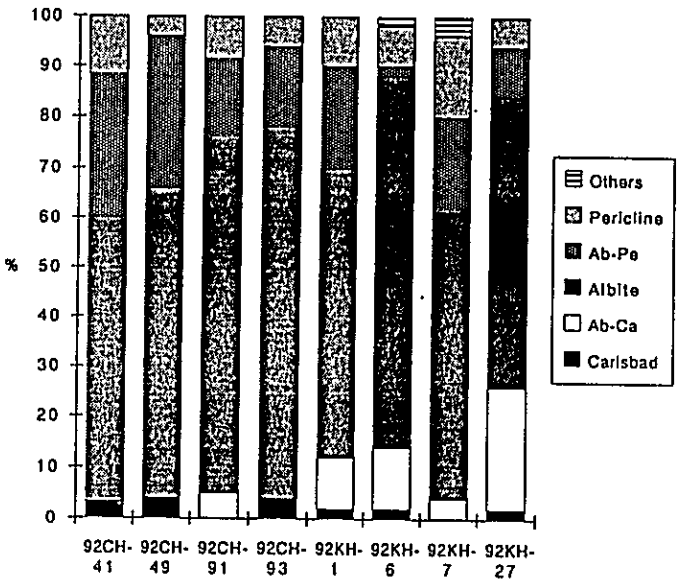

Fig.3 Ratios of plagioclase twin laws

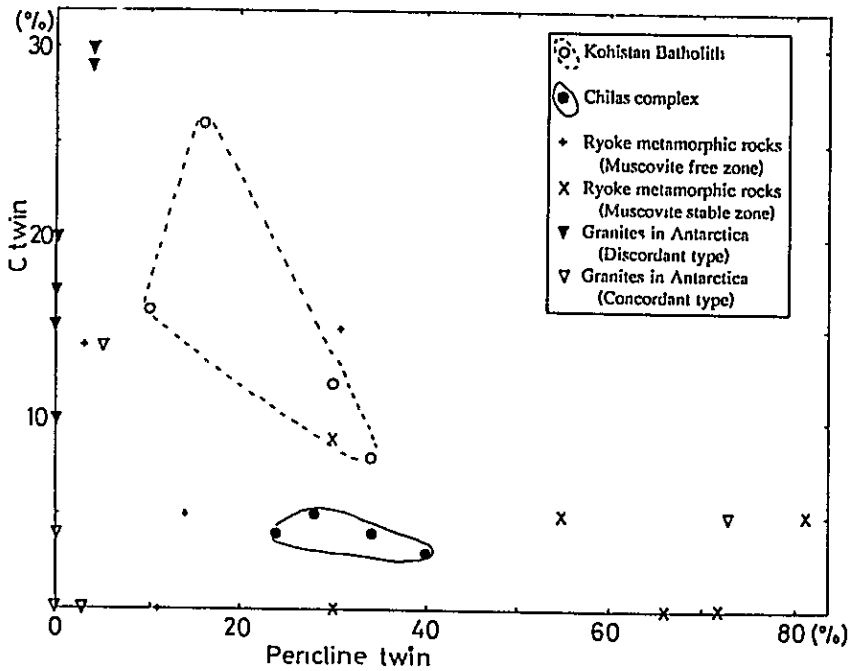

Fig.4 Ratios of C twins and pericline twin in twinned plagioclases
Pericline twin of this figure is both simple pericline twin and albite-pericline composite twin. C twins are defined as all the other laws except albite and pericline laws.

characterized by low ratio of C twins. On the other hand, the Kohistan Batholith shows high ratio of C twins suggesting comparatively shallow depth of emplacement and has not been metamorphosed after intrusion.

Acknowledgments

We acknowledge Japan International Cooperation Agency (JICA) for giving us the chance of this collaborative project as one of the technology transfer programs for Geoscience Laboratory. We also thank Dr. Teruo Shirahase for his critical reading our rough manuscript.

References

Borg,I.Y., and Heard,H.C., 1970, Experimental deformation of plagioclases:in Paulitsch(ed.)"Experimental and Natural Rock Deformation", Springer-Verlag, 375-403.

Coward,M.P., Jan,M.Q., Rex,D., Tarney,J., Thirlwall,M., and Windley, B. F., 1982, Geotectonic framework of the Himalaya of N. Pakistan:J. Geo. Soc.London, Special Publication , 19, 203-219.

Gorai,M., 1951, Petrological studies on plagioclase twins:Am. Min., v.36, 884-901.

Jan, M.Q., and Howie,R.A., 1980, Ortho- and clinopyroxene from pyroxene granulites of Swat, Kohistan, northern Pakistan: Min. Mag., v.43, 715-728.

Jan, M.Q., Parvez, M.K., Khattak, M.U.K., and Windley, B.F., 1984, The Chilas stratiform complex: field and mineralogical aspects: Geol. Bull. Univ. Peshawar, v.17, 153-169.

Khan,M.A., and Coward,M.P., 1990, Entrapment of an intra-oceanic island arc in collision tectonics: A review of the structural history of the Kohistan Arc, NW Himalaya: Phys. Chem. Earth, v.17, no.11, 1-18.

Khan,M.A., Jan,M.Q., and Weaver,B.L.,1993, Evolution of the lower arc crust in Kohistan, N. Pakistan: temporal arc magmatism through early, mature and intra-arc rift stages: J. Geo. Soc. London, Special Publication , 74, 123-138.

Khan,M.A., Jan,M.Q., Windley,B.F., Tarney,J., and Thirlwall,M.F.,1989, The Chilas mafic-ultramafic complex; the root of the Kohistan island arc in the Himalaya of northern Pakistan: Geol. Soc. Amer. Special Paper, 232, 75-94.

Olsen,T.S., and Kohlstedt,D.L., 1985, Natural deformation and recrystallization of some intermediate plagioclase feldspars:Tectonophysics, v.111, 107-131.

Petterson,M.G., and Windley,B.F., 1985, Rb-Sr dating of the Kohistan arc-batholith in the Trans-Himalaya of north Pakistan, and tectonic implications: Earth and Planetary Science Letters, v.74, 45-57.

Petterson, M.G., and Windley,B.F., 1991, Changing source regions of magmas and crustal growth in the Tran-Himalayas: Evidence from the Chalt volcanics and Kohistan batholith, Kohistan, N. Pakistan: Earth and Planetary Science Letters, v. 102, 326-341.

Petterson, M.G., Crawford, M.B., and Windley, B.F., 1993, Petrogenetic implications of Neodymium isotope data from the Kohistan batholith, North Pakistan: J. Geol.Soc. London, v.150, 125-129.

Searle,M.P.,1991, Geology and Tectonics of the Karakoram Mountains: John Wiley & Sons, 358p.

Smith,J.V.,1974, Feldspar Minerals 2 (Chemical and Textural Properties): Springer-Verlag, 690 p.

Suwa,K., 1956, Plagioclase twinning in Ryoke metamorphic rocks from the Mitsue-mura area, Kii peninsula, central Japan: J. Earth Sci., Nagoya Univ., v.4, 91-122.

Suwa,K., Mizutani,S., and Tsuzuki, Y.,1974:Proposed optical method of determining the twinning laws of plagioclase:Mem. Geol. Soc.Japan, no.11, 167-250.

Tahirkheli,R.A.K., Mattaur,M., Proust,F., and Tapponnier,P., 1979, The India-Eurasia suture in northern Pakistan: Synthesis and interpretation of data on plate scale. In Farah, A., and Dejong, K.(eds.) Geodynamics of Pakistan. Geol. Surv. Pakistan, Quetta, 125-130.

Takahashi,Y., and Nishioka,Y., in press, Mode of plagioclase twinnings in Ryoke metamorphic rocks in the western area of Tsu City, Mie Prefecture: J. Min. Petr. Econ. Geol.(in Japanese with English abstract)

Takahashi,Y., Tainosho,Y., Osanai,Y., and Tsuchiya, N., in press, Mode of plagioclase twin laws in the granitic rocks in Sor Rondane Mountains: Proc. NIPR Symp. Antarct. Geosci.

Treloar, P.J., Rex,D.C., Guise,P.G., Coward, M.P., Searle, M.P., Windley, B.F., Petterson,M.G., Jan,M.Q., and Luff, I.W.,1989, K-Ar and Ar-Ar eochronology of the Himalayan Collision in NW Pakistan: Constraints on the Timing of Suturing, Deformation, Metamorphism and Uplift:: Tectonics, v.8, 881-909.

Wenk,H.R.,1969, Annealing of oligoclase at high pressure:Am. Min., v.54, 95-100.

Proceedings of Geoscience Colloquium, Geoscience Lab.,GSP. 9, 59-72

Determination of Arsenic and Antimony in Geochemical Samples Using Hydride Formation System by Atomic Absorption Spectrometry

Muhammad Naseem, Adnan Iqbal*, Komi Kato** and Shiro Itoh***

**Geoscience Laboratory, Geological Survey of Pakistan, Islamabad*
***JICA expert, Geoscience Laboratory, Islamabad*

INTRODUCTION

The trace amount analysis of As and Sb in geological samples has been considered to be difficult, because of their poor detection limit in available analytical instruments and volatile character in reducing conditions. Recently, hydride generation accessory combined with AAS or ICP-AES has been developed and provides a rapid and very sensitive method to determine the elements, forming gaseous hydrides This method has been successfully applied to analysis of geochemical samples for As and Sb (Aslin, 1976)

A field survey in Swat area was conducted in September, 1994 to collect some geochemical samples from an area where Kaolinite deposits are being exploited and the area went through a hydrothermal activity in past and the sampling of B horizon was done for the path finders As and Sb for Au.

This report is intended to determine the optimization of a suitable procedure for the determination of As and Sb in geochemical exploration samples in Geoscience Laboratory.

EQUIPMENT

The Geoscience Laboratory is housing Hitachi model Z-8100 atomic absorption spectrophotometer with a magnetic field of one tesla for applying Zeeman effect to correct the background (Fig 1). The hydrides of the As and Sb are atomized in a quartz tube over a low flame in the absence of magnetic field. The principal spectral lines of the element are emitted by a cathode lamp and the absorbence of the spectral lines is detected through an optical path as shown in the Fig 2.

The power supply of graphite furnace is used if flameless atomization is required. The photometric section is housing a lamp turret of eight cathode lamps to provide the specific spectral lines. These spectral lines emitted by the hollow cathode lamps are absorbed by the target element excited in quartz tube/flame. The degree of absorption by

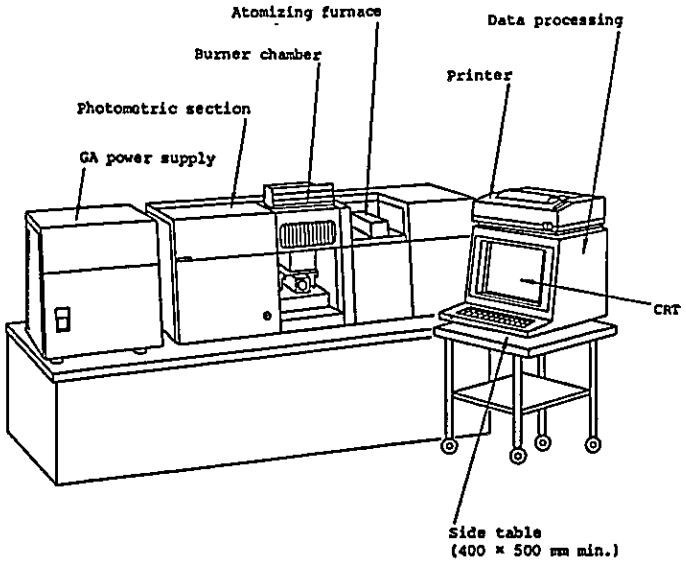

Figure 1. Arrangement of Z-8100 Polarized Zeeman Atomic Absorption Spectrophotometer

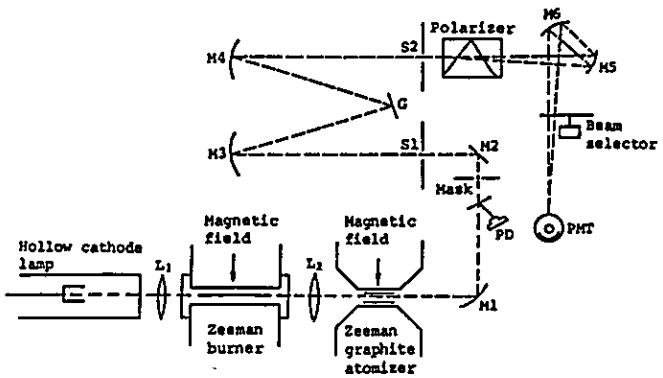

L_1, L_2 ..... Lenses

S1, S2 ..... Slits

M1 to M6 ..... Mirrors

G ..... Grating

PD ..... Photodiode (optical temperature control)

Polarizer ..... Wollaston prism

PMT ..... Photomultiplier

Figure 2. Optics of Z-8100 Polarized Zeeman Atomic Absorption Spectrophotometer

ground state atoms or the atomic absorption sensitivity differs according to the spectral lines. A solution of low concentration can be analyzed efficiently by using the spectral lines which will be absorbed intensively. The spectral lines not absorbed much, may be used when the concentration of target element is high. The illustration in Fig. 3 explains well these phenomena.

In the flame of burner head, target elements in sample solution will be dissociated from other elements and become free atoms which absorb the spectral lines emitted by the hollow cathode lamps. In case of hydride measurement, because it is gaseous, the hydride will be introduced into a quartz tube settled at the right position of beam axis and heated by the burner flame. Thus, free atoms will be produced in the tube similar to aerosol in the flame.

Absorbence of the spectral lines of specific element can be measured by a photomultiplier in spectrophotometer and compared to that of reference lines. All mechanical systems of the instrument are controlled by a computer which is also used as a data processor.

Hydride Generation Equipment: Accessory attachment Model HFS-2 for the Hitachi AAS was used. The equipment consists of three parts, suction pump, manifold and separator (Fig.4). By a peristatic pump, constant volume of sample solution and other solution of reagent for making hydrides are entered into the manifold in which all solutions are encountered and are reacted with each other resulting in hydride generation. At the separator, gaseous hydrides will be separated from liquid and constant flow of Ar gas will take the hydrides into a quartz cell on the burner head of AAS. The quartz cell is heated by air acetylene flame for atomizing the hydrides.

Reagents:

Experiments have been carried out using following reagents.

A) Sodium borohydride 1% solution: this solution is prepared by dissolving 5g of $NaBH_4$ in 500ml of 0.1% NaOH solution and renewed everyday.

B) Hydrochloric acid 5%: this is prepared by diluting 25ml of concentrated HCl to 500ml with distilled water.

C) Potassium iodide 50% solution: a 50g of KI is dissolved in distilled water and made it up to 100ml.

D) Arsenic standard solution, after drying reagent at 110°C, exact 132mg of As_2O_3 is dissolved in 50ml of water plus 0.2g of NaOH , then make it up to exact 100ml with water to give a 1000 mg/l in solution. Because the As_2O_3 powder used is guaranteed

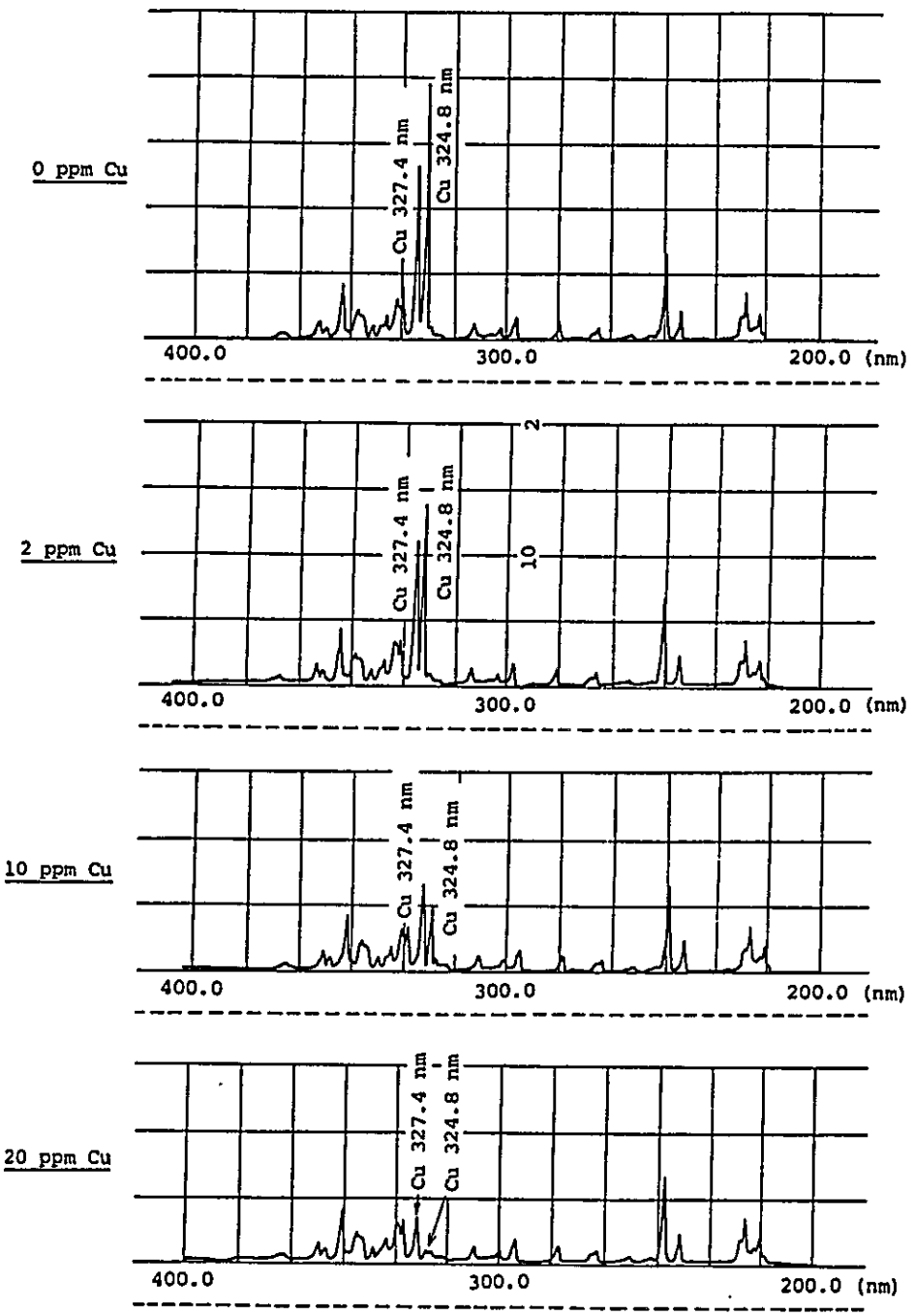

Figure 3. Spectral lines emitted from copper hollow cathode lamp and their absorbed status

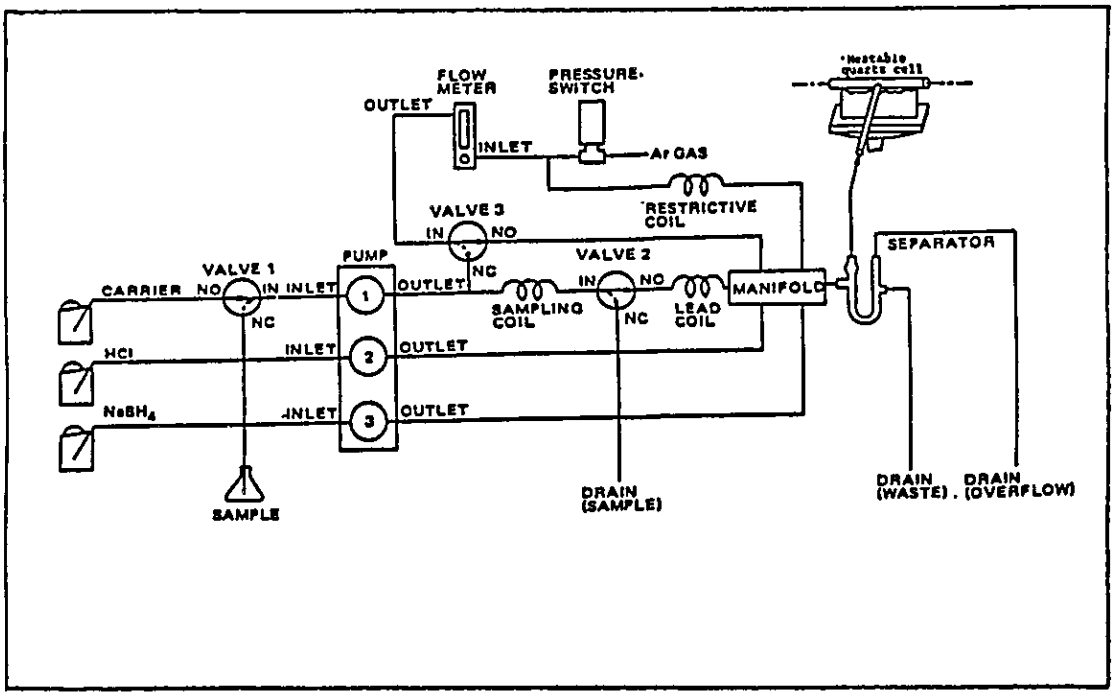

Figure 4. Flow diagram of hydride generation system (HFS-2)

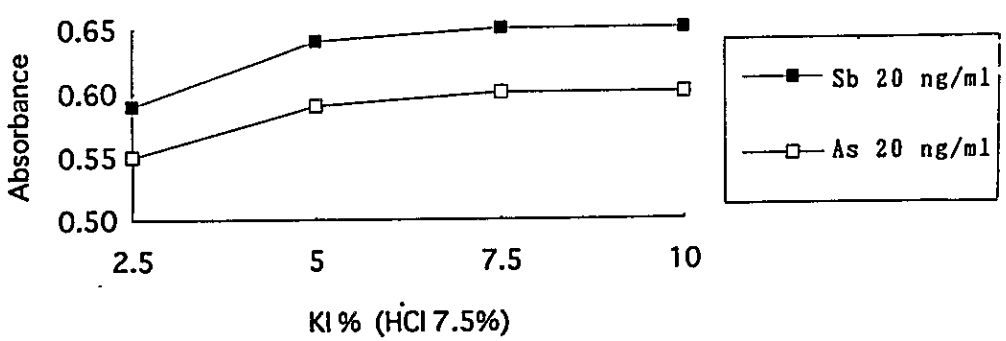

Figure 5. Absorbance in different concentration of KI

to be 98% by the manufacturer, 134 7mg was weighed. For working standard solution, the stock solution was diluted 100 times.

E) Antimony standard solution: 100mg of antimony metal (99.999% proof) is dissolved in 10ml nitric acid and then diluted to exact 100ml to give a concentration of 1000mg/l in solution. For working standard solution, the stock solution was further diluted 100 times.

OPTIMIZING THE ANALYTICAL CONDITIONS

1) Interferences

Early reports have proved the absence of interferences in the hydride generation method. However, Smith (1975) found in his detailed study that Cu, Ge, Au, Pt, Pd, Rh, Ru, Ni, and Co always suppressed hydride generation probably due to their preferential reduction and precipitation which might result coprecipitation or absorption of the analyte and consumption of reductant. Belcher et al. (1975) found that in 0.1 M hydrochloric acid media, suppression of the evolution of arsine (AsH_3) and stibine (SbH_3) by Co, Ni, Zn, Fe, Bi, Cd and Cu could be almost eliminated by addition of EDTA. In more strongly acidic media (5M HCl) no interference from up to a 10,000-fold excess of Cu on the evolution of arsine has been reported (Aggett and Aspell 1976) In the hydride generation of Bi, Se and Te, however, Thompson et al.(1978) found it necessary to avoid interference from Cu by their coprecipitation and separation on lanthanum hydroxide. Aslin (1976) found that Ni suppressed evolution of arsine from 1.5 M hydrochloric acid and both Ni and Ag suppressed stibine. The interferences could, however, be controlled by addition of EDTA and prereduction by KI

With hot acid decomposition of geochemical samples, it is necessary to prevent volatilization of As and Sb by maintaining them in their highest valency state which then must be reduced to the trivalent state for quantitative hydride generation. Large amounts of nitric acid remaining after decomposition can not be tolerated and should be removed by evaporation with perchloric acid.

2) Optimum concentration of hydrochloric acid and potassium iodide

The concentration of acid and potassium iodide in sample solution may affect on the hydride generation reaction. Figures 5 and 6 show the atomic absorbence of the same concentration of As and Sb but different concentration of hydrochloric acid and potassium iodide respectively. As shown in the figures, more than 5% in KI and 0.9M in hydrochloric

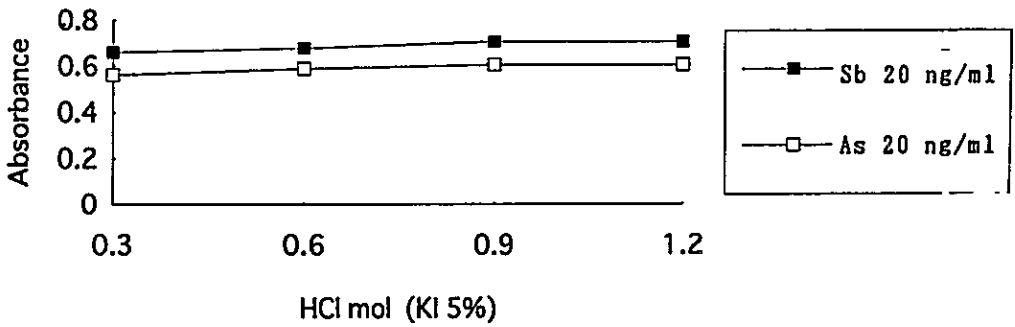

Figure 6. Absorbance in different concentration of HCl

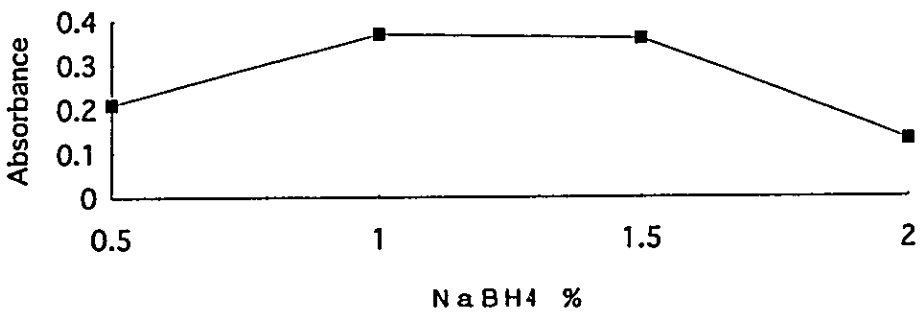

Figure 7. Absorbance in different concentration of $NaBH_4$

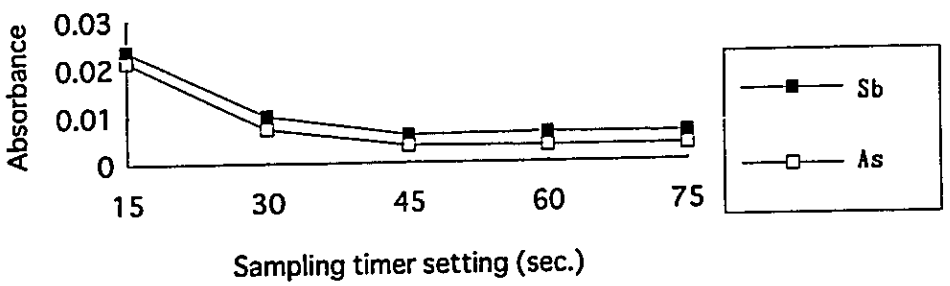

Figure 8. Diagram showing carryover after measuring Sb and As

acid concentrations gave maximum absorbance for both elements. Accordingly. in following experiments the sample solutions always contained 5% of KI and 0.9M of HCl.

3) Optimum concentration of sodium borohydride

The sodium borohydride reacts with sample solution and generates hydrides. The solution containing 20 ng As in 1ml was reacted with various concentration of sodium borohydride solution. Results are shown in Fig. 7. Absorbance of AsH_3 generated from the solution of 1.0% and 1.5% in $NaBH_4$ concentrations showed the same and higher than those of 0.5 % and 2.0%. So that it is likely that 0.5% solution of $NaBH_4$ is not enough concentration for the generation of hydrides and 2.0% concentration of $NaBH_4$ gives excess free hydrogen which dilutes the concentration of hydrides in gas phase carried into the atomizer. In the following experiments, 1% solution of $NaBH_4$ was used.

4) Setting sampling timer

In the case of successive analysis, former sample solution remaining in the system will be mixed and alter the composition of next sample solution which is called as carryover. In order to minimize carryover, it is instructed that sample suction volume is set at sampling coil capacity (3ml) plus 2ml. However, carryover may remain after rinsing with 2ml of sample solution depending on viscosity of samples. To test the strength of this carryover, under the various time setting of sampling both As and Sb solutions of constant concentration and distilled water were sucked alternately and measured absorbance of the elements. The absorbance of the distilled water against time setting is shown in Figure 8, suggesting necessity of the suction time of more than 45 seconds. Accordingly, sampling timer was set on 60 second in the following experiments.

5) Setting reaction timer

In the manifold the reducing agent ($NaBH_4$) and the acid (HCl) are always reacted with each other to produce hydrogen. By operation of the REACTION timer the sample solution in the LEAD coil flows into the manifold at a high speed. The sample will react in the manifold with hydrogen (immediately after being produced) to form hydride. A reaction time also allows the absorption signal to return to the baseline level. Experiments in 15, 30 and 45 second setting showed the same peak height (Figure 9) and no difference So that 30 second setting of reaction timer was adopted.

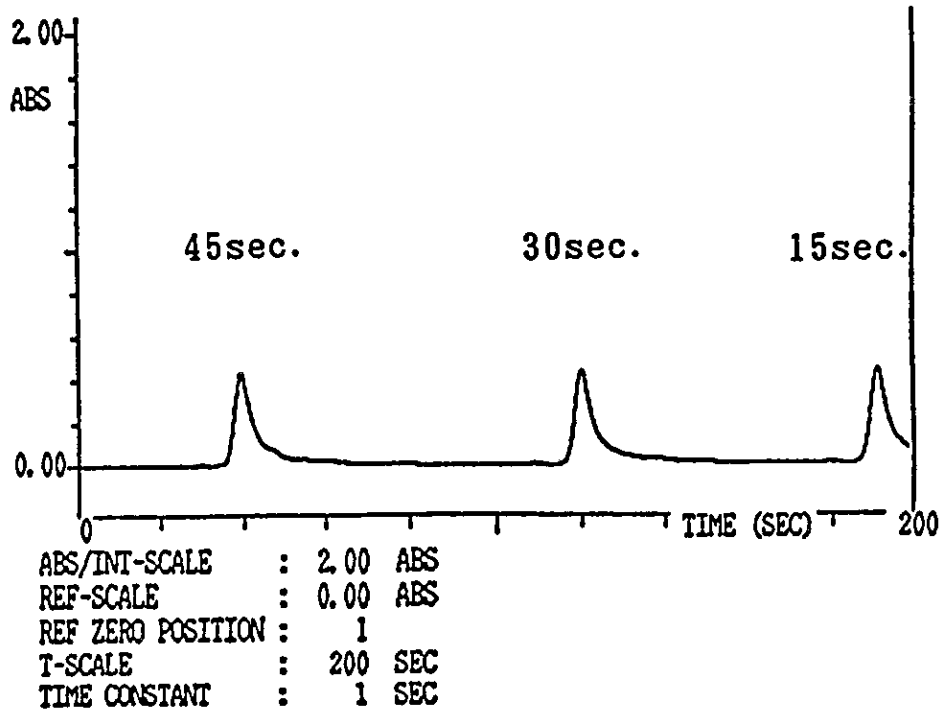

Figure 9. Absorbance on different reaction time

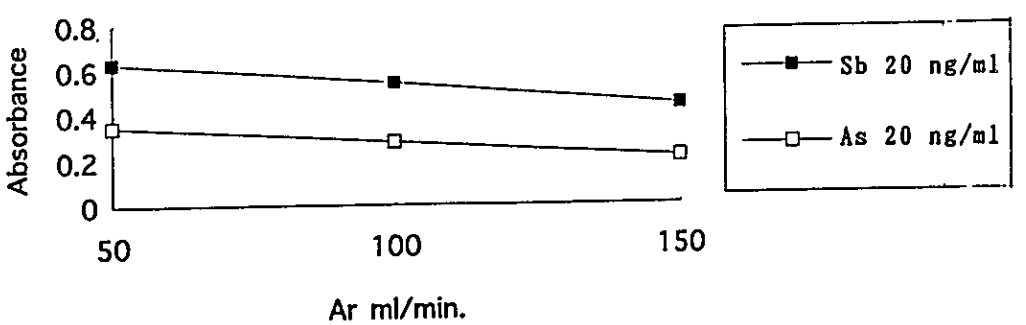

Figure 10. Absorbance in different Ar gas flow rate

6) Setting Argon gas flow rate

In general sensitivity of the measurement of hydrides absorption is dependent on flow rate of argon gas. A lower flow rate will result high concentration of gaseous hydrides in argon gas as carrier which will enhance sensitivity. In a higher flow rate of the carrier gas, the concentration of hydrides will be diluted and will make the signal waveform gentle. Signal form may also vary depending on composition of sample Therefore, an optimum argon flow rate should be selected through practice. The practice for the 20 ng/ml concentration of As and Sb in silicate sample solutions is carried out in 50 ml/min., 100ml/min. and 150ml/min. of gas flow rate, respectively. Figure 10 shows the results of the practice, suggesting the optimum flow rate of less than 50 ml/min. However, an attached flow meter to the hydride generator showed unstability in the range of less than 50 ml/min. Therefore the argon gas flow rate of 50 ml/min. was adopted in the following experiments.

ANALYTICAL PROCEDURES FOR CLAY SAMPLES

Some clay samples including a few soil samples were analyzed for As and Sb by following procedures which were subjected to the elaborate experimental study. Flow chart of the procedures is shown in Figure 11.

A 0.5 g of powdered sample is taken in a platinum dish, 2 ml of conc. HNO_3, 5ml of conc. $HClO_4$, 1ml of 20% $KMnO_4$ and 10ml of HF are added to the dish. The dish is heated on a sand-bath up to dryness. If the color of $KMnO_4$ is disappeared during heating, some more solution of $KMnO_4$ should be added. After dry-up the inside wall of the dish is washed with water and add 2ml of $HClO_4$. Then the dish is heated to dryness again. Then, 8ml of conc. HCl and 20ml of water are added to the dish and digest by heating with a glass watch plate cover. After complete digestion, cool the dish to room temperature and transfer the solution into a measuring flask (100ml). Two other sample solutions are prepared as the same process. First sample solution (No.1) is added 10ml of 50% KI and make it exactly 100ml with water. Second one (No.2) is added 0.5 μg of Sb standard and 10ml of 50% KI, then make it exactly 100ml with water. Third one (No.3) is added 1μg of Sb standard and 10ml of 50% KI, then make it exactly 100ml with water.

The carrier bottle attached to the hydride generation equipment is filled with distilled water, similarly fill a HCl bottle with 5% HCl and also a $NaBH_4$ bottle is filled with 1% $NaBH_4$ solution. After making sure that the tubes are connected correctly to each bottle, set operating functions referring to the instruction manual for the atomic absorption spectrophotometer. The air-acetylene flame heatable cell is attached for measurement, air

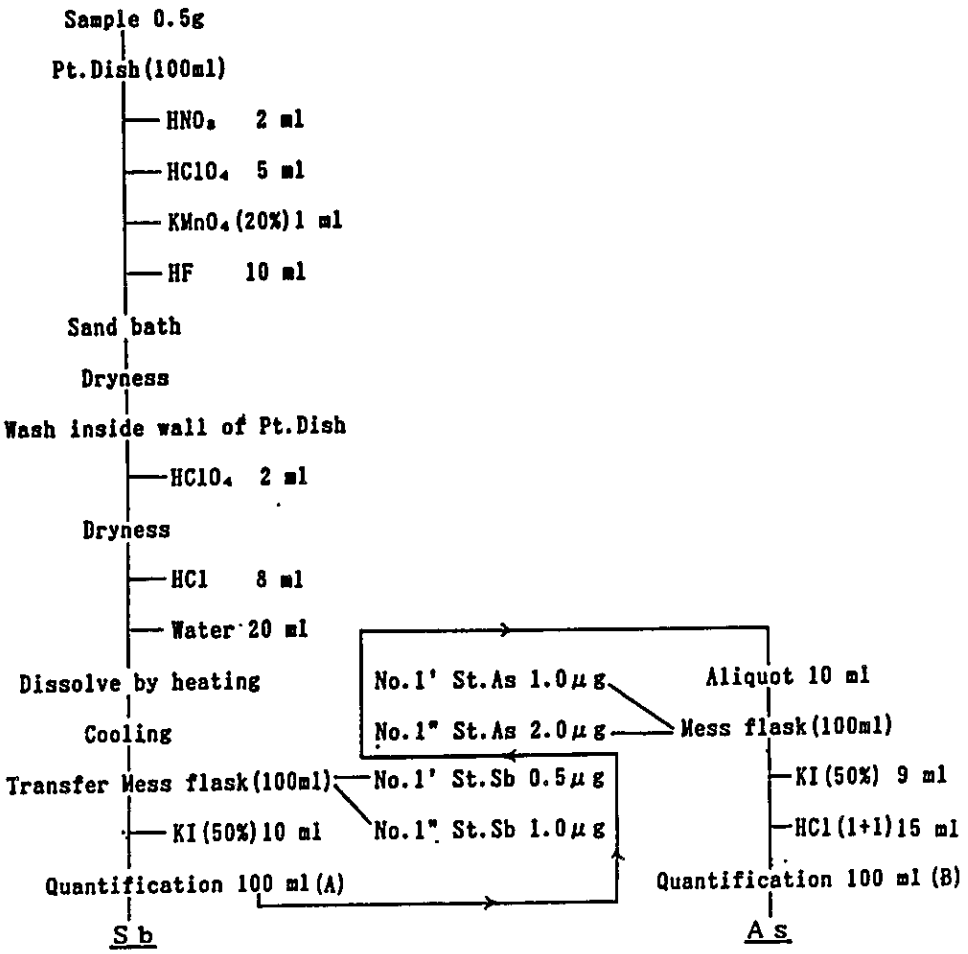

Wavelength	217.6nm	Wavelength	197.2nm
Atomizer	Quartz cell	Atomizer	Quartz cell
Flame	C_2H_2-Air	Flame	C_2H_2-Air
Measurement	Std.add.	Measurement	St.add.
Calculation	Peak height	Calculation	Peak height
Calc.time	20 sec.	Calc.time	20 sec.
Sampling time	60 sec.	Sampling time	60 sec.
Reaction time	30 sec.	Reaction time	30 sec.
Ar Flow	50 ml/min.	Ar Flow	50 ml/min.

Figure 11. System diagram of As and Sb hydrides analysis

Table 1. Analytical results of As and Sb in the samples from the Shah Dheri deposit, Swat.

Sample No.	As ppm	Sb ppm
1	7.45	0.24
2	10.40	0.77
3	8.50	0.36
4	3.15	0.22
5	1.04	0.07
6	2.53	0.64
7	0.62	0.02
8	1.08	0.09
9	0.67	0.09
JA-1	2.82	0.26
JA-1	3.02	0.30
(JA-1,recom.)	(2.92)	(0.26)

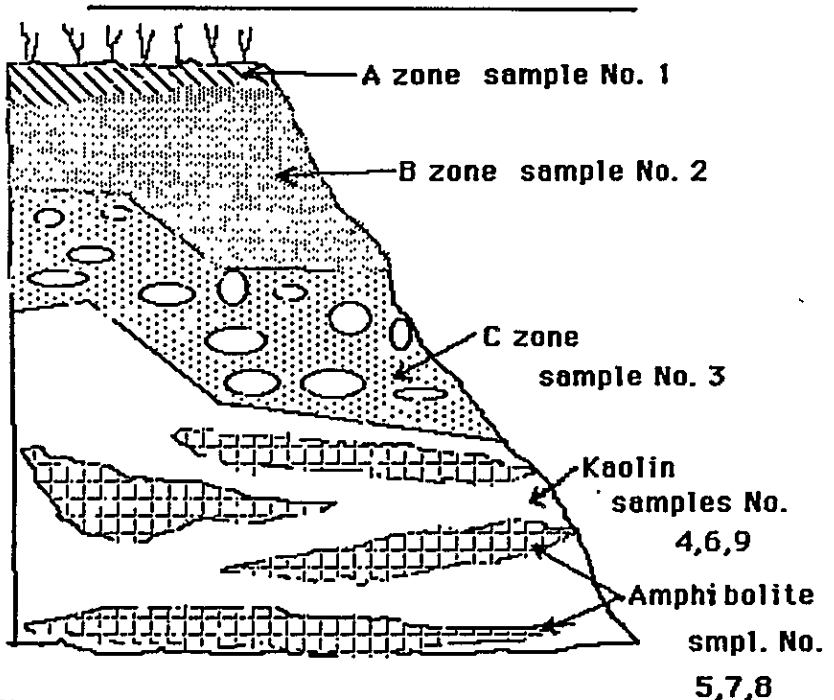

Figure 12. Locality of the analyzed samples from the Shah Dheri deposit, Swat.

and acetylene are to be flowed from the gas controller built in the atomic absorption spectrophotometer main unit, and argon gas through the gas control unit prepared separately in HFS-2. Ignite a flame. Set the support clamp lever in right position by turning it, and set the fixing lever. Turn ON the POWER switch, and flow reagents for about 10 minutes for running in. After setting the SAMPLING Timer 60 sec., REACTION Timer 30 sec. and Ar Gas Flow Rate 50ml/min., set a sample solution (from No. 1) in position and dip the sample suction tube into it. Make sure that the READY lamp is lit. Depress the START button.

Sb will be determined by measuring the absorption at the wavelength of 217.6nm and standard addition mode.

A 10ml of sample solution of No.1 bottle is exactly allocated each to other three measuring flasks namely No.4, No.5 and No.6. No.4 solution is added 9ml of 50% KI and 15ml of (1+1) HCl and make it exactly 100ml with water. No 5, solution is added 1 μg As standard and 9ml of 50% KI and 15ml of (1+1) HCl. Similarly, No 6 is added 2μg As standard and 9ml of 50% KI and 15ml of (1+1) HCl and make it 100ml with water. Then As will be determined by measuring the absorption at the wavelength of 197.2nm and standard addition mode.

Analytical results for the clay samples from Swat region are presented in Table 1, in which the results for JA-1 showed good agreement with a recommended value. The location of the samples analysed is shown in Fig.12, details of which will be discussed elsewhere.

REMARKS

1) By this empirical study, it is demonstrated that the trace amount of As and Sb in silicate samples down to 0.05 ppm can be determined with hydride generation system (Model HFS-2) followed by atomic absorption method.

2) Potassium iodide added to sample solution as pre-reductant works also as a preventive reagent for the interferences from Co and Ni.

3) It is learnt that the unseparated fine particles of liquid phase have caused breakage of the quartz cell which is positioned in acetylene air flame and in which hydrides are atomized. In the following experiments, a cooling system was installed between the cell and the outlet of the hydride generation system, and it is proved that the system has functioned well.

4) Ten samples could be analysed within five hours by this method.

5) The analytical results for As and Sb in standard rock sample (JA-1) of Geological Survey of Japan matched with a recommended value.

REFERENCES

Aggett. J. and Aspell. A.C., 1976. The determination of arsenic (III) and total arsenic by atomic absorption spectroscopy. Analyst. v. 100, 341-347.

Aslin, G.E.M 1976. The determination of arsenic and antimony in geological materials by flameless atomic absorption spectrometry. J. Geochem. Explor., v. 6, 321-330.

Belcher, R., Bogdanski, S.L., Henden E. and Townshend A. 1975. Elimination of interferences in the determination of arsenic and antimony by hydride generation using molecular emission cavity analysis (MECA). Analyst, v. 100, 522-523.

Smith A. E., 1975. Interferences in the determination of elements that form volatile hydrides with sodium borohydride using atomic-absorption spectrophotometry and the argon-hydrogen flame. Analyst' v.100, 300-306.

Thompson. M., Pahlavanpour. B., Walton. S.J. and Kirkbright. G.F., 1978. Simultaneous determination of trace concentrations of arsenic, antimony, bismuth, selenium and tellurium in aqueous solution by introduction of the gaseous hydrides into an inductively coupled plasma source for emission spectrometry. Analyst, v. 103, 705-713.

Proceedings of Geoscience Colloquium, Geoscience Lab ,GSP, 9, 73-100

Magnetic Granulometry by Hysteresis Loop Properties

- Alternating Gradient Force Micro-magnetometer for Rock Magnetic Studies -

Mitsuo Yoshida

JICA expert, Geoscience Laboratory, Geological Survey of Pakistan, Islamabad, Pakistan

INTRODUCTION

Alternating Gradient Force Micro-magnetometer System* which was recently equipped in the Geoscience Laboratory, Islamabad is new-generation high-sensitive magnetic hysteresis analyzer Hysteresis properties of geologic materials give us various kinds of magnetic information such as isothermal saturation magnetization, saturation remanence, coercive force, coercivity of remanence, magnetic susceptibility, magnetic hardness, and domain state of materials, which are indispensable parameters to assess stability and reliability in rock magnetism, and to evaluate industrial potentiality of magnetic materials In this paper, possible applications of hysteresis loop properties for rock magnetic studies, especially for magnetic granulometry of rocks, are described

MAGNETIC HYSTERESIS

Magnetic fields and forces originate from the movement of the basic electric charge, the electron When electrons move in a conducting wire, a magnetic field is produced around the wire Magnetism in materials is also due to the motion of electrons, but in this case the magnetic fields and forces are caused by the intrinsic spin of electrons and their orbital motion about their nuclei An external magnetic field acting on the atoms of a material slightly unbalances their orbiting electrons and creates small magnetic dipoles within the atoms which oppose the applied field. This action produces a small negative (antiparallel to the applied field) magnetic effect known as ***diamagnetism***. Most felsic minerals such as quartz and feldspars are diamagnetic minerals On the other hand, materials

* AGM MicroMag™ System, Model 2900-02, Princeton Measurements Corporation.

which exhibit a small positive (parallel to the applied field) magnetic effect in the presence of a magnetic field are called paramagnetic, and the magnetic effect is termed ***paramagnetism***. The paramagnetic effect in materials is produced by the alignment of individual magnetic dipole moments of atoms or molecules in an applied field, and it disappears when the applied field is removed Most mafic minerals (pyroxene, amphibole, etc.) show paramagnetic behaviors

Since the magnetization effect of these materials M is proportional to the applied field H, a proportionality factor, κ (kappa) is defined as:

$\kappa = M/H$
$\kappa < 0$: diamagnetic
$\kappa > 0$: paramagnetic

This physical quantity κ is called the ***magnetic susceptibility*** (volume susceptibility) and is dimensionless. The diamagnetic effect shows a very small negative magnetic susceptibility of the order of -10^{-6} (SI) and the paramagnetic effect yields positive magnetic susceptibilities ranging from about 10^{-6} to 10^{-2} (SI) Diamagnetism and paramagnetism are induced by an applied magnetic field, therefore the magnetization remains only as long as the field is maintained, but the effect is reversible.

A third type of magnetism, called ***ferromagnetism***, show significant irreversible properties, the hysteresis. A particular characterization of ferromagnetic materials is their magnetization reaches a saturated value within a strong external field. Figure 1 illustrates the relation between the intensity of magnetization J of a ferromagnetic material and the applied magnetic field H. The magnetization J increases along the curve O-A-B-C-D with the increase of applied field, reaching saturated value Js at C. After the saturation point C, the magnetization is constant (the ***saturation magnetization***, Js).

In the initial part of the curve (O-A), J changes *reversibly* with H. The initial slope of the curve is called as the ***initial susceptibility*** κ_0.

$\kappa_0 = dJ/dH$

When the strength of applied field H is increased from the portion of initial susceptibility, an irreversible behavior in magnetization appears. In this condition, a slight change in applied field at point B (a slight decrease) produces a minor loop B-B', the slope of B-B' being named the ***reversible susceptibility*** κ(rev).

On the other hand, a slope of the main magnetization curve at any point after the portion having initial susceptibility is defined as the ***differential susceptibility***, κ_{dif}. The difference between κ_{rev} and κ_{dif} is named as the ***irreversible susceptibility***, κ_{irrev}.

$$\kappa_{irrev} = \kappa_{dif} - \kappa_{rev}$$
$$\kappa_{dif} = \kappa_{rev} + \kappa_{irrev}$$

After reaching saturation level C-D, the magnetization decreases from Js with decrease of the applied field (demagnetizing, see the curve D-C-E in Figure 1) A finite amount of magnetization Jrs remains at H=0 (no applied field) The magnetization Jrs is called the ***saturation remanent magnetization*** (or simply called the ***remanent magnetization*** Jr) Then inverse magnetic field reduces the remanent magnetization, and the magnetization becomes zero (J=0) at point F where H = -Hc. The strength of Hc is named as the ***coercive force*** And further increase of inverse applied field results in saturation value -Js at point G Furthermore, the reverse process follows the curve G-H-I-C.

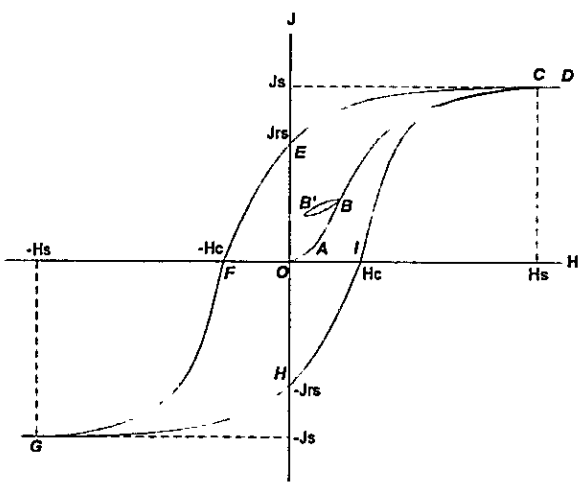

Figure 1: Magnetization curve (hysteresis loop) of ferromagnetic materials (modified from Nagata,1961).

This irreversible phenomenon of magnetization with respect to the applied field H is called the ***magnetic hysteresis***, and the S-shaped loop (Figure 1) is called the ***hysteresis loop***. Its internal area is a measure of energy lost or the work done

by the magnetizing and demagnetizing cycle (***hysteresis loss***). The hysteresis phenomenon takes place only with ferromagnetic materials.

Above mentioned hysteresis loop employs magnetization hysteresis loop where the ordinate is magnetization (or magnetic polarization). The induction hysteresis loop where the ordinate is magnetic induction has different shape and the induction coercivity has a different values (Figure 2).

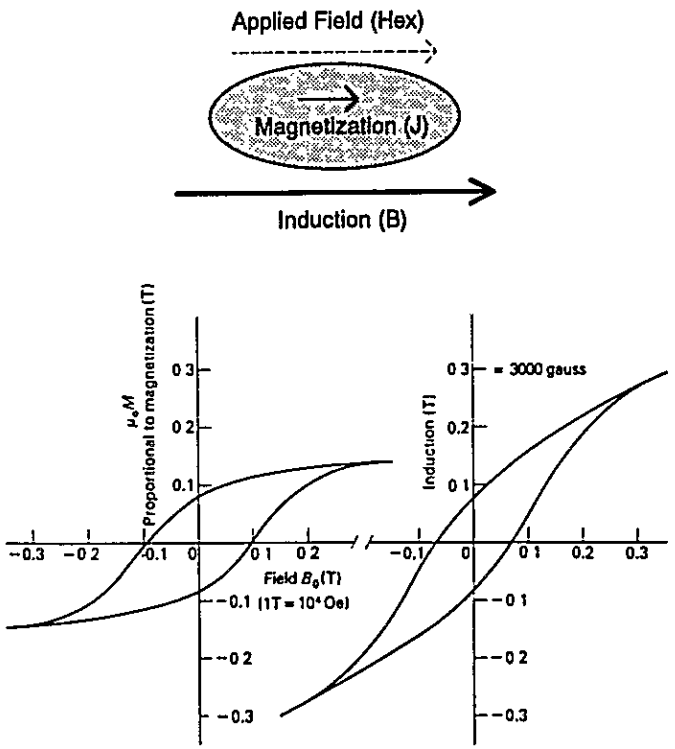

Figure 2: Schematic idea of magnetic induction and magnetization by external field (top), magnetization hysteresis loop (left) and induction hysteresis loop (right) (Crangle,J.,1977).

A ***soft magnetic material*** is easily magnetized and demagnetized, whereas a ***hard magnetic material*** is difficult to magnetize and demagnetize. Soft materials used in cores for transformers and motors have narrow hysteresis loops with low coercive forces, while hard magnetic materials used for permanent magnets have wide hysteresis loops with high coercive forces (Figure 3).

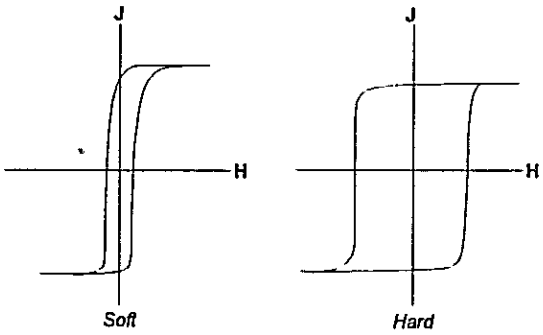

Figure 3: Hysteresis loops for soft and hard magnetic materials The soft magnetic material has a narrow hysteresis loop which makes it easy to magnetize and demagnetize, whereas the hard magnetic material has a wide hysteresis loop which makes it difficult to magnetize and demagnetized (modified from Smith,1990)

AGM MICRO-MAGNETOMETER SYSTEM

An alternating gradient force magnetometer system uses an alternating field gradient to produce a periodic force on a magnetized sample The sample is mounted on the tip of a vertical extension rod, which is taken to lie along the z-axis, and the gradient field is along the x- or the y-axis. The top end of the sample rod is attached to the bottom end of a piezoelectric element (Transducer, Figures 4 and 5) The top end of the piezoelectric element is rigidly clamped The force of the field gradient on the magnetized sample produces a bending moment on the piezoelectric element, which generates a voltage proportional to the force on the sample The output from the piezoelectric element is synchronously detected at the frequency of the gradient field. The amplitude of this voltage is proportional to the magnetic moment of the sample, which can be varied by changing an applied DC field Hx which is along x-axis (Flanders,1989). The micro-magnetometer system is a type of vibrating sample magnetometer (VSM) capable of sensitivity exceeding 10^{-8}emu ($10^{-11}Am^2$) which is thousand times more sensitive than conventional vibrating sample magnetometer (VSM) (Table 1)

Table 1: Specification of the AGM/MicroMag™ Model 2900-02

Magnetic Moment		**Field & Sample**	
Measurement Range	10^{-6} to 5emu (full scale)	*Maximum Field*	14000Gauss (1 4T)
Sensitivity	10^{-8}emu (standard dev.)	*Sample Size (P1)*	3x3x2mm (<50mg)
Resolution	0.005% (full scale)	*Sample Size (P2)*	5x5x2mm (<100mg)

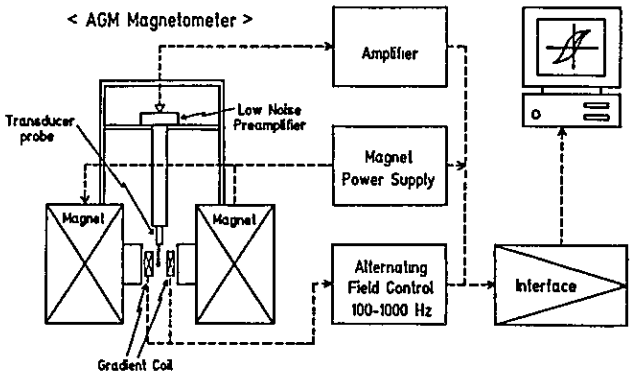

Figure 4: Block diagram of alternating gradient force micro-magnetometer (AGM) system.

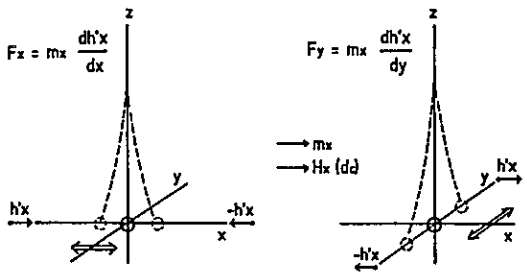

Figure 5: Configuration of the magnetizing and gradient fields (modified from Flanders,1988).

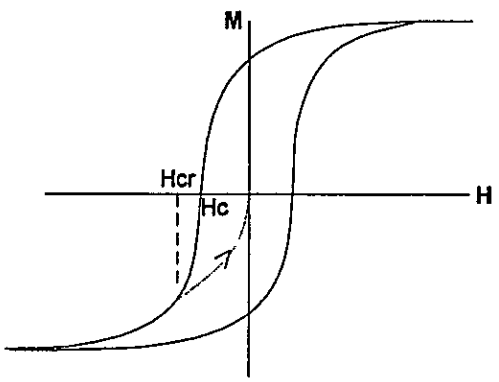

Figure 6: DC demagnetization parameters in a hysteresis loop. Hc: coercive force, Hcr: coercivity of remanence (sometimes expressed by "Hr" or "Hrc").

PARAMETERS OF HYSTERESIS LOOP

The following parameters derived from a hysteresis loop have been used to characterize the magnetic hysteresis loop

(1) ***Saturation magnetization*, Js**

The bulk magnetic moment of a sample when all atomic moments are aligned in their maximum ordered configuration This can be achieved by spontaneous alignment, as in a single-domain size grain, or by application of a sufficiently large magnetic field Js is temperature-dependent, the magnetization becomes zero at the Curie temperature (Tc)

(2) ***Saturation isothermal remanent magnetization (Remanent saturation Magnetization)*, Jrs**

The remanent magnetization left in the sample from a saturating field, when the applied field is reduced to zero

(3) ***Natural remanent magnetization*, Jrn**

The residual magnetization left from some natural process of magnetization acquisition other than the saturation IRM, e g. TRM and CRM.

(4) ***Coercive force*, Hc**

The required external-field to reduce a **Jrs** to zero This is sometimes termed the ***remanence coercivity (Remanent coercive force)*** The remanence is thereby not permanently reduced to zero, when the applied field removed, the magnetization curve will follow a path upward to a residual value on the vertical J-axis.

(5) ***DC demagnetization parameters*:**

Two parameters in DC demagnetization which applies reversed field to sample for demagnetizing the remanence are useful in classifying and identifying rock magnetic characteristics The first parameter is the reversed field **Hcn (NRM coercivity)** which will reduce the natural remanent magnetization (Jrn) to zero, and the second parameter is reversed field **Hcr*** **(coercivity of remanence)** which is required to reduce the residual remanence to zero when the applied field H has been removed (Figure 6). Normally the relationship Hcr>Hc>Hcn is recognized. The magnetic field strength required to magnetized a not-previously-magnetized magnetic material to one-half of the remanent saturation magnetization (Jrs/2) is named **H'cr (remanent acquisition coercive force)**.

(6) ***Magnetic susceptibility*, k**

This represents the ease of magnetization of the material in an external field. In general it is k=J/H, that is, the slope of the curve, however, this varies depending

* The coercivity of remanence is sometimes expressed by "Hr" or "Hrc".

on the location of H (abscissa) value. It is typically low at small fields, increases as the H increases, and then decrease as saturation is approached. Magnetic susceptibility can be measured anywhere on the curve, and experimental values can thus vary widely. Rock magnetism and paleomagnetism generally use an appropriate magnetic susceptibility (reversible susceptibility) not exceeding the Earth's magnetic field; H<0.05mT(0.5Oe). The ***initial susceptibility*** $\mathbf{k_0}$ is that for J=0, and the ***remanence susceptibility*** **kr** is for J=Jr,nrm.

(7) ***Remanence ratio (Jrs/Js) and Coercivity ratio (Hcr/Hc)***:

The form of loop and numerical values of the ratios **Jrs/Js** and **Hcr/Hc** depends on microstructure, principally grain size and shape.

MAGNETIC GRANULOMETRY

Hysteresis parameters are strongly dependent upon the grain size. The grain size of ferromagnetic minerals are generally classified into four groups: multidomain (MD), pseudo-single domain (PSD), single domain (SD), and the superparamagnetic size (SPM) on the basis of magnetic domain state.

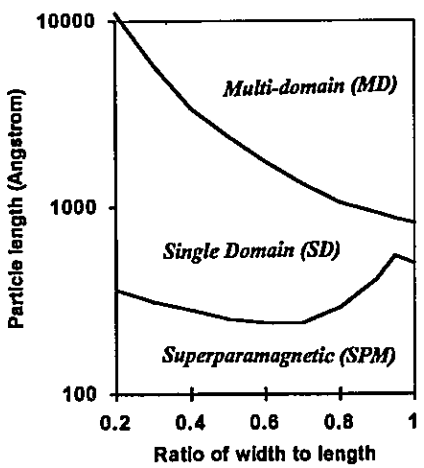

Figure 7: Theoretical size and shape ranges of MD, SD, and MD configurations for fine magnetite particles at room temperature. The shape is indicated by the ratio of width to length; cubic grains are at the right side and progressively elongated grains are toward the left. The boundary between SD and SPM is given on the basis of relaxation time τ=100sec (simplified from Butler and Banerjee,1975).

The MD/SD transition size for cubic-shaped magnetite (Fe_3O_4) at room temperature is around 1000Å (0.1μm) in diameter, and the SD/SPM transition size is 700Å (0.07μm) (Figure 7). Maghemite (γ-Fe_2O_3) shows similar but a little larger threshold values (Nagata,1961) The SD/SPM transition size for hematite is also several hundred angstrom, but the modeling of MD/SD transition size has not been carried out (O'Reilly,1984)

Among all the hysteresis loop parameters, saturation magnetization (Js) is not a function of grain size, while saturation remanent magnetization (Jrs), coercive force (Hc), coercivity of remanence (Hcr), and initial magnetic susceptibility (k), indeed depend upon grain size. The coercivity ratio (Hcr/Hc) and remanence ratio (Jrs/Js) are also grain size dependent. These parameters are functions of grain size not because of any intrinsic control of grain size on magnetization, but because they are influenced by the magnetic domain state of the sample. Therefore the grain size and domain state, ***magnetic granulometry***, of ferromagnetic particles in given sample can be analyzed by the parameters*. Table 2 summarizes general grain size dependence (=domain state dependence) of the hysteresis parameters.

Table 2: Grain size dependence for hysteresis loop parameters of magnetite particle The shape of "hysteresis loop" for SPM size particles is extremely thin and exhibit no remanence and no coercivity

Parameters	MD size →	PSD size →	SD size →	SPM size
Js	constant →	constant →	constant →	-
Jrs	very small →	small →	large →	-
Hc	small →	large →	very large →	-
Hcr	small →	small →	large →	-
Hcr/Hc	large →	small →	very small →	-
Jrs/Js	very small →	small →	large →	-
k_0	small →	small →	large →	small

Grain Size Dependence of Remanence Ratio

The saturation magnetization (Js) is independent of the grain size, but the saturation remanent magnetization (Jrs) strongly depends on the factor. Non-interacting uniaxial single-domain (SD) grains provides a theoretical value of the remanence ratio:

* Other methods in magnetic granulometry are reviewed by Torii(1993).

Jrs/Js = 0 5 (SD magnetite)

The remanence ratio yields the maximum value at SD size range and it decreases with increasing the grain size (→ PSD and MD) (Figure 8).

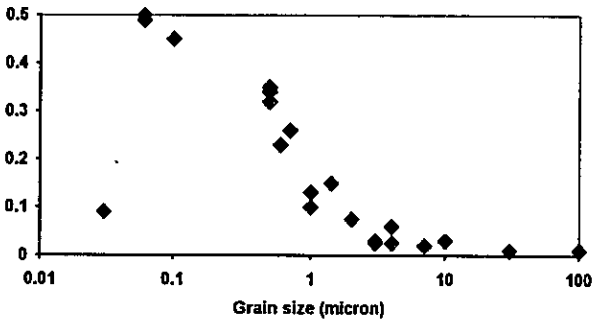

Figure 8: Grain size dependence of remanence ratio (Jrs/Js) for synthetic magnetite particles (data from Worm and Markert,1987).

Grain Size Dependence of Coercivity and Coercivity Ratio

The coercivity force is slightly different depending on the source of anisotropy, but for magnetite, theoretical values range from about 50 to 100mT. It also shows the maximum value at SD size and decreases with increasing the grain size (Figure 9) A theoretical value of the coercivity ratio is also predicted as follows.

Hcr/Hc = 1~2 (SD magnetite)

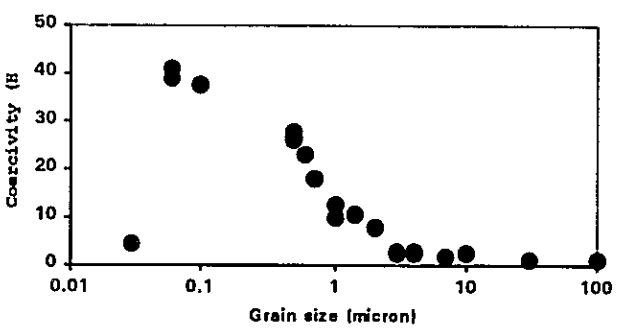

Figure 9: Change of Coercivity (Hc) with various grain size of magnetite particle (data from Worm and Markert,1987)

Mixture of different grain size, such as MD and SD particles, also shows complicated behavior of hysteresis properties For example, Day et al.(1977) prepared synthetic samples containing two population of grain sizes, a coarse fraction of MD sizes and a fine fraction of SD sizes. The result indicates that the coercivity ratio Hcr/Hc is biased toward the low-coercivity fraction as shown in Figure 10

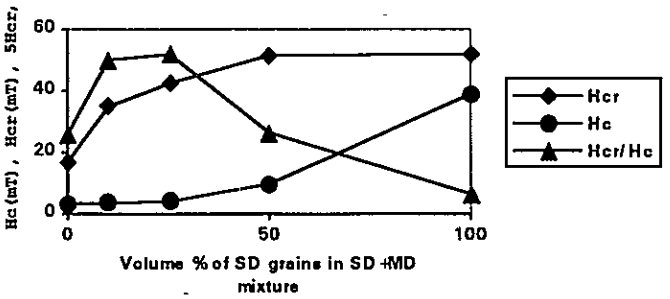

Figure 10: Hysteresis parameters in mixtures of MD and SD particles (after Day et al ,1977)

Remanence Ratio vs. Coercivity Ratio Plot ("Day Plot")

In general, hysteresis loops for SD particles are typically wider than loops for MD particles which means SD particles are much harder than the MD particles This is just a reflection of the higher coercivity and remanence in SD particles. On the basis of the hysteresis loop properties, Day et al.(1977) generalized the relationship between domain state and the distribution on the remanence ratio Jrs/Js *vs.* coercivity ratio Hcr/Hc diagram (so-called ***"Day Plot"***; Figure 11)

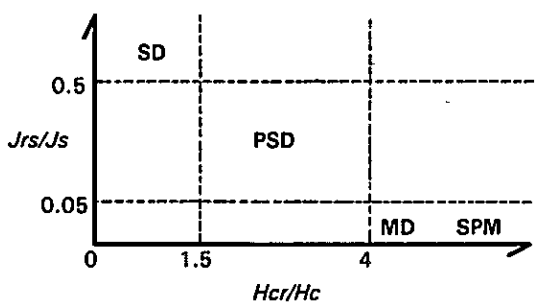

Figure 11: Classification of domain state of magnetic particles in terms of remanence and coercivity ratios (Jrs/Js *vs.* Hcr/Hc diagram) (after Day et al.,1977)

The Mrs/Ms *vs.* Hcr/Hc diagram (Day plot) provides us various information in rock magnetism. Channell and McCabe(1994) recognized an "age-dependent" trend within the PSD field of the Day plot for a number of limestone samples collected from a certain section (formation). Older samples from the base of the formation tend to have higher Mrs/Ms and lower Hcr/Hc. This trend manifests as an "age-dependent" shape variation in magnetic hysteresis loop; the more 'wispy' loops with smaller values of Mrs/Ms are associated with the upper (= younger) part of the formation. A logarithmic plot of Mrs/Ms *vs.* Hcr/Hc (logarithmic Day plot) is informative for assessing the condition of mixtures of SD and MD particles in rock samples. Parry(1982) found a power law relationship in the logarithmic diagram and suggested that the slope of linear trend possibly indicated a state of mixture of SD and MD particles.

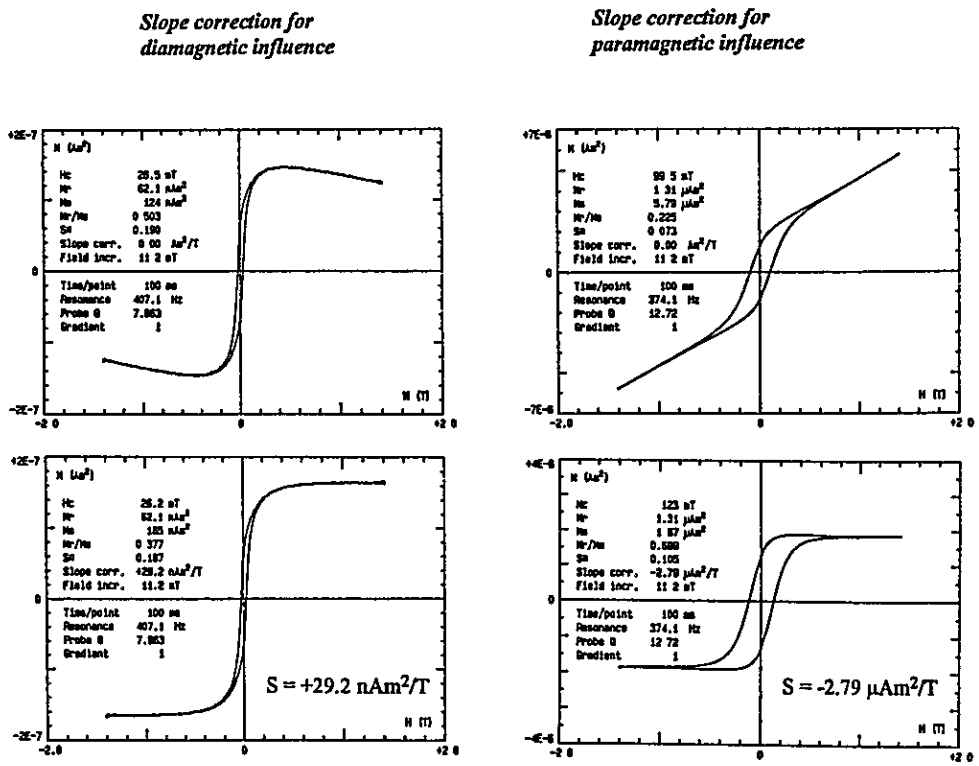

Figure 12: Slope corrections (***Slope Adjust*** function) to cancel diamagnetic or paramagnetic influences. Upper loops show raw data and the lower loops show the corrected loops. S: Slope correction fuctor

Slope Correction Factor

The hysteresis loop measurements of bulk rock specimens indicate both diamagnetic and paramagnetic influence at ,high applied fields. In the micro-magnetometer system, raw hysteresis data are generally slope-corrected (***Adjust Slope function***)* to cancel these effects by subtracting the constant-slope component at high fields from the raw data-set (Figure 12) The value of the slope correction (= a measure of the diamagnetic/paramagnetic influence) also appears to be "age-dependent" (Channell and McCabe,1994) Channell and McCabe(1994) found that limestone samples from a certain section (formation) tend to have diamagnetic slopes in the basal (oldest) part whereas upper (younger) samples have paramagnetic slopes They interpreted that the enhanced upward paramagnetic signal may corresponded to an increase of clay mineral. It means the slope correction factor (S; Figure 12) can give us some stratigraphic or sedimentlogical information.

Other hysteresis properties and related parameters possible to be measured by the micro-magnetometer system, such as property of minor loops, various DC demagnetization parameters, time-dependence property and so on, are probably informative for magnetic granulometry and for rock magnetism However the details still remain unknown and should be further studied.

Acknowledgments

This paper was prepared for the in-house lecture and practical training course on the micro-magnetometer system held in October and November,1994 I am grateful to Messrs. Iftikhar Mustafa Khadim, Mohammad Ali, and Mirza Naseer Ahmad, Geoscience Laboratory for their fruitful cooperation I would like to express my special thank to Dr Takayuki Katoh of Earth Science Co.Ltd., Sapporo, Japan for his suggestion about sample preparation technique. It is acknowledged that Japan International Cooperation Agency (JICA) financially supported to equip the Princeton/MicroMag Model 2900-02 AGM magnetometer system (1993F.Y. Supplementary Equipment Grant).

* see Appendix (4-6).

References

Butler,R.F. and Banerjee,S.K.,1975, Theoretical single-domain grain size range in magnetite and titanomagnetite. *J.Geophys.Res.*,80,4049-4058.

Channell,J.E.T. and McCabe,C.,1994, Comparison of magnetic hysteresis parameters of unremagnetized and remagnetized limestones. *J.Geophys.Res.*,99,4613-4623.

Crangle,J.,1977, *The Magnetic Properties of Solids - The Structure and Properties of Solid 6*. Edward Arnold Publ Ltd.,London.

Day,R ,Fuller,M. and Schmidt,V.A.,1977, Hysteresis properties of titanomagnetites: Grain-size and compositional dependence. *Phys.Ear.Planet.Inter.*,13,260-266.

Flanders,P.J.,1988, An alternating-gradient magnetometer. *J.Appl.Phys.*,63, 3940-3945.

Mauritsch,H.,Becke,M.,Kropacek,V.,Zelinka,T. and Hejda,P.,1987, Comparison of the hysteresis characteristics of synthetic samples with different magnetite and haematite contents. *Phys.Ear.Planet.Inter.*,46,93-99.

Nagata,T.,1961, *Rock Magnetism* Maruzen Co.Ltd ,Tokyo,350p.

O'Reilly,W.,1984, *Rock and Mineral Magnetism.* Blackie & Sons,Glasgow,220p.

Parry,L.G ,1982, Magnetization of immobilized particle dispersions with two distinct particle sizes. *Phys.Ear.Planet.Inter.*,28,230-241.

Princeton Measurements Corporation, 1993, *MicroMag 2900 Instruction Manual (08/18/93 version)*. Princeton Measurements Corporation,Princeton,83p

Schmidbauer,E and Schembera,N.,1987, Magnetic hysteresis properties and anhysteretic remanent magnetization of spherical Fe_3O_4 particles in the grain size range 60-160nm *Phys.Ear.Planet.Inter.*,46,77-83.

Smith,W.F.,1990, *Principles of Materials Science and Engineering.* McGraw-Hill Publ Co ,New York,864p.

Snowball,I.F.,1991, Magnetic hysteresis properties of greigite (Fe_3S_4) and a new occurrence in Holocene sediments from Swedish Lappland. *Phys.Ear.Planet.Inter.*,68,32-40.

Worm H.-U and Markert,H.,1987, Magnetic hysteresis properties of fine particle titanomagnetites precipitated in a silicate matrix. *Phys.Ear.Planet.Inter.*, 46,84-92

Yoshida,M.,1994a, *Magnetic Approaches to Geological Sciences. Part I. Geomagnetism and Rock Magnetism (Revised and Enlarged Edition).* Geoscience Laboratory, Geological Survey of Pakistan, Islamabad.151p.

Yoshida,M.,1994b, *Magnetic Approaches to Geological Sciences. Part II. Methods in Rock Magnetism and Paleomagnetism.* Geoscience Laboratory, Geological Survey of Pakistan, Islamabad 233p

<APPENDIX>

Operation Manual

Alternating Gradient Magnetometer (AGM)

Princeton Measurements Corporation / MicroMag™ Model 2900-02*

(1) AGM System Start

1-1. Turn on electrical power to the MicroMag controller

1-2 Open the faucet for supplying water to the electromagnet

1-3 Turn on electrical power to the magnet power supply

1-4. Turn on the computer power switch ***System Startup*** screen will be displayed first Press any key to leave this screen and enter the MicroMag operating software

1-5 ***Main Menu*** screen will be displayed Choose ***Measurements Menu*** and press [Enter]

1-6 ***Measurements Menu*** screen will be displayed

(2) Sample Preparation and Mounting on Transducer

2-1 Prepare sample to be measured
for ***P1 Transducer Probe*** up to 3×3×2mm (mass<50mg),
for ***P2 Transducer Probe*** up to 5×5×2mm (mass<100mg)

2-2 Clean up the ***Carrier*** (small glass plate attached with extension rods) on the probe by 91% isopropyl alcohol

2-3 Place the probe on ***Sample Handling Fixture***, and carefully apply a very thin coating of vacuum grease to one side of its ***Carrier***

2-4 Using a pair of non-magnetic tweezers, carefully place the sample on the ***Carrier***.

2-5 Make sure the Z axis (vertical) translation stage of the ***Micropositioner*** is in the UP position Pick up the ***Transducer Probe***, note orientation of the pins on the plug and the two white dots Carefully insert the plug into the receptacle on the bottom of the ***Micropositioner*** after releasing the vibration dampening suspension, then fix the probe.

2-6. Grasp the Micropositioner with one hand, press down to release the Z axis locking arm and slowly lower the micropositioner until the sample is located vertically in the center of the magnet-pole faces

* Based on the instruction manual for the MicroMag 2900 by Princeton Measurements Corporation (1993).

Appendix Figure 1: AGM micro-magnetometer system in the Geoscience Laboratory.

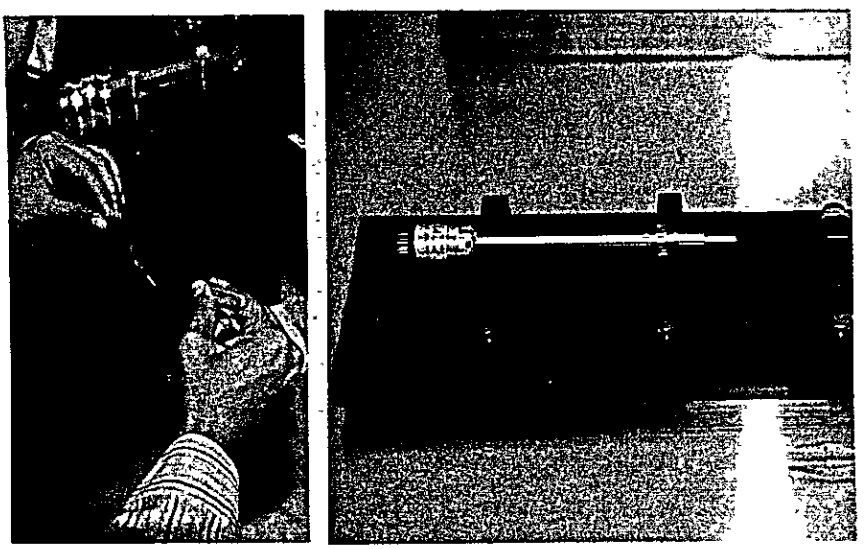

Appendix Figure 2: Mounting the sample on the carrier of transducer probe.

and gradient coils. Gently lift up on the locking arm and lock into position.

2-7. Check to see the sample is centered in the air gap along the X, Y, and Z axis If necessary rotate X, Y, and Z vernier knobs to position the sample in the center of the air gap. Setting sample is now completed.

(3) Autotune

3-1. In the ***Measurements Menu*** of the operating software, locate the cursor on ***Maximum Field*** and press [Enter]. Type in expected maximum field (≤1.4T), for example [0.5] for H_{max}=0 5(T), and press [Enter].

3-2. Locate the cursor on ***Autotune*** and press [Enter] Press [F1] key (***Initial***) to start the autotune routine which tunes the system to the condition of given sample

3-3. The system will enter ***search*** state and set the operating frequency (several ten seconds), then it signals completion with beep. The sensitivity range, probe Q and phase will also be updated upon completion of this function. The results of autotune will be displayed at the bottom of screen If the message ***Overload*** is appeared on the screen, dislocate the probe (follow the process (5)) and reduce the mass of sample and try the autotune again.

3-4 Press [Enter] to accept the initial autotune data. Press [F2] key (***Incremental***) to conduct an incremental fine tune After the incremental autotune, the system will be completely tuned.

(4) Hysteresis Measurement

4-1. In the ***Measurements Menu***, locate the cursor on ***Magnetization vs. Field*** and press [Enter]

4-2. Select function [F2] (***loop***) and press [Enter] for ***single scan***.

4-3. An M(=magnetization)-H(=applied field) diagram will appear on the screen and the measurement will start. When the hysteresis loop measurement is completed, computed parameters are displayed.

4-4 Press [F1] (***Enter description***) and input description of the sample up to 80 character. Press [Enter] to confirm the description.

4-5. Press [F2] (***Save***) and input the file name. For the raw data the following style of naming is recommended.

□□□□□□□□.DAT

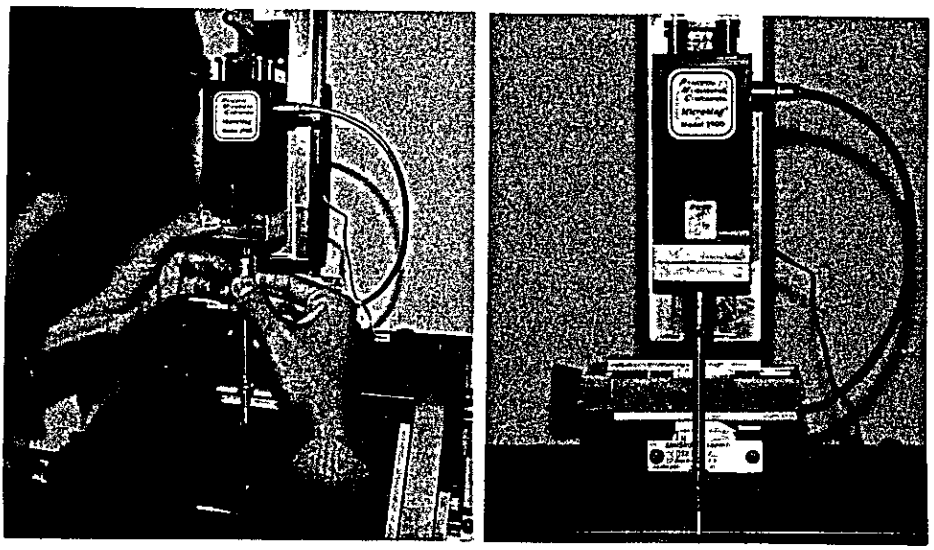

Appendix Figure 3: Setting the transducer probe on the micropositioner.

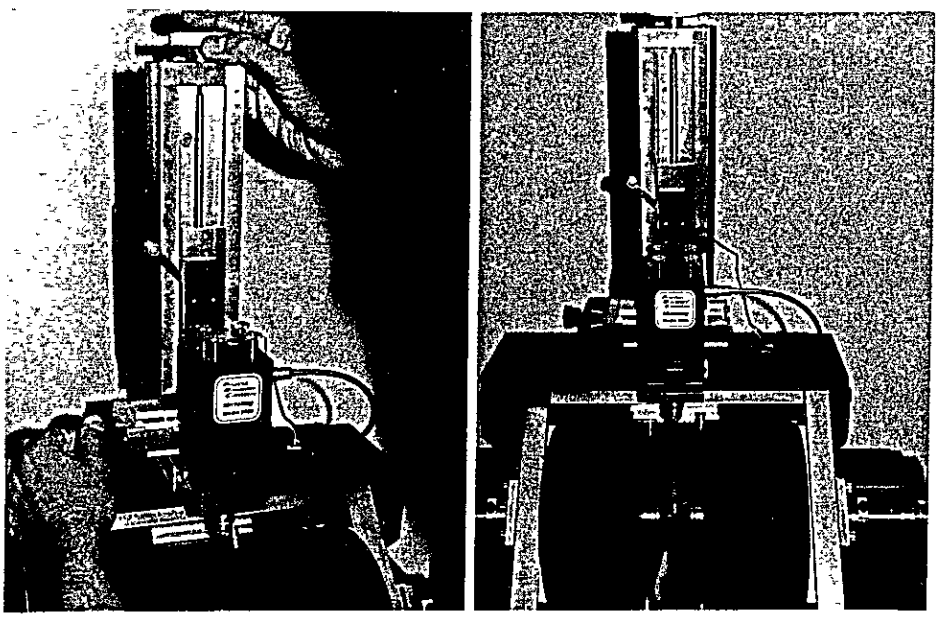

Appendix Figure 4: Centering the carrier of transducer probe in the air gap.

It is also recommended to save the data on specified floppy disk or directory on the hard desk Press [Enter] to save the raw data

4-6 Press [F5] (***Adjust Slope***), (use the 70% default setting), press [Enter] to correct data This function corrects the effects of strong diamagnetic or paramagnetic (linear slope) signals Adjusted loop will be redrawn soon on the screen Press [F9] for canceling the process Press [F7] (***Expand***) for changing scale of horizontal and vertical axes

4-7. Press [F2] (***Save***) and revise the file name as follows.

□□□□□□□□ HLP

4-8 Press [Enter] to save the corrected loop data Other optional measurements (***Initial permeability***, ***Initial permeability and hysteresis loop***, and ***Minor loops***) are explained in **(6)**.

4-9. Power on the plotter and set a paper. Press [F3] (***Plot***) for sending data of hysteresis loop to the plotter, note sub functions appearing below the screen Press [F1] to plot only loop, [F2] to plot only loop, [F3] to plot only annotations, and [Enter] to plot all

4-10 Press [Esc] to return ***Measurements Menu***

(5) Termination of Operation

5-1 Press [Esc] to return Main Menu Press [Alt]-[Q] to quit the operation program and to enter MS-DOS mode

5-2 Turn off power switches of the computer, MicroMag controller, and electromagnet power supply

5-3 Close the faucet for supplying water to the electromagnet

5-4 Relocate the ***Micropositioner*** in the UP position and release the vibration dampening suspension, then carefully disconnect the ***Transducer Probe*** from the receptacle

5-5 Remove the sample from the transducer probe and clean up the sample carrier by using 91% isopropyl alcohol (Do not use acetone)

5-6 The probe should be stored in the probe box

(6) Optional Measurement-1 <Initial Permeability>

6-1. Demagnetize the sample first

6-2 Follow the procedure until the step 4-1, and press [F1] (***Initial***) for the measurement of initial permeability "only" ($H=0 \rightarrow H_{max}$) For

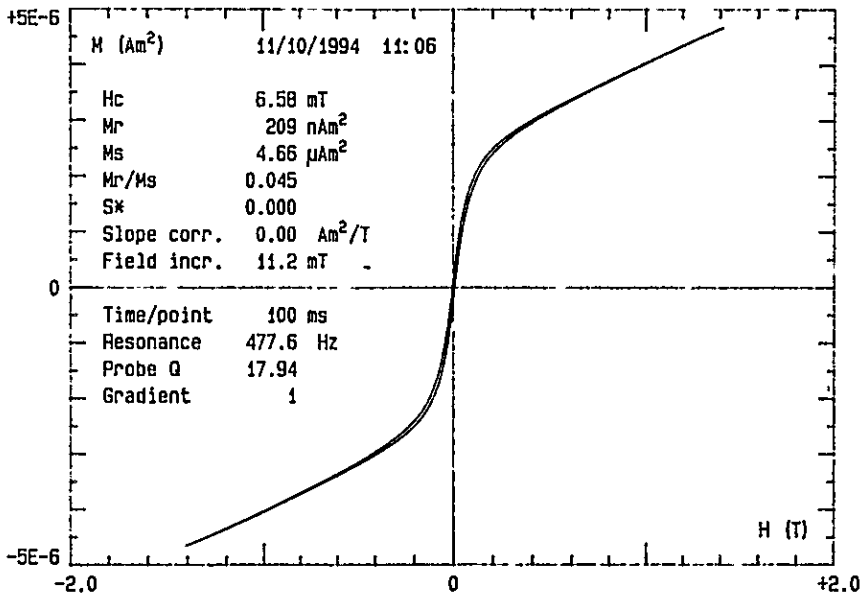

Appendix Figure 5: Result of hysteresis measurement (raw data). Measured sample is bulk specimen of "hematite oolite" collected from Bagnotar, Hazara area.

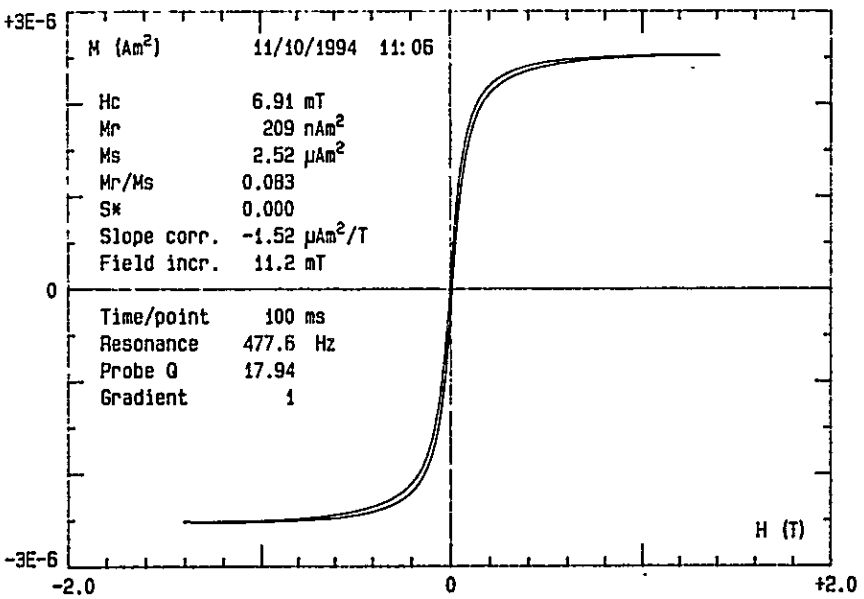

Appendix Figure 6: Hysteresis loop processed by *Adjust Slope* function. Used raw data is the same described in Appendix Figure 5

initial permeability and hysteresis loop "combined" ($H \rightarrow H_{max} \rightarrow -H_{max} \rightarrow H_{max}$), press [F3] (***Initial & Loop***)

6-3 Press [Enter] and the measurement will start Follow the process from the step 4-3. It is recommended to use the following style of data file naming.

for initial permeability "only"	□□□□□□□□ INI
for raw "combined" data	□□□□□□□□.DAT
for its corrected data	□□□□□□□□ INL

(7) Optional Measurement-2 <Minor Loops>

Executing this function, a group of hysteresis loops (up to 19) will be acquired in ascending order The user sets Hmax of the first and last curve in the group Loops within the group will be spaced equally

7-1 Demagnetize the sample first

7-2 Follow the procedure until the step 4-1, and press [F4] (***Minor loops***)

7-3 Input initial H_{max} value for the first minor loop and press [Enter]

7-4 Input final H_{max} value for the last curve and press [Enter]

7-5 The last prompt sets the total number (2~19) of loops to be acquired. Make a selection and press [Enter]

7-6. The system will start at zero field and run from the first minor loop to the last minor loop Upon completion, computed parameters are relative to the last loop in the group

7-7 It is recommended to use the following style of data file naming of the minor loop data:

for raw data	□□□□□□□□ MLP
for its corrected data	□□□□□□□□ CML

(8) Optional Measurement-3 <Remanence Measurements>

8-1. Follow the procedure until the step 3-4 In the ***Measurements Menu***, locate the cursor on ***Remanence Measurements*** and press [Enter]. ***Remanence Measurements Menu*** will appear on the screen

8-2 Two selections are available: "***Isothermal remanent Magnetization***" and "***DC Demagnetization Remanence***". Demagnetize the sample before conducting an ***Isothermal Remanent Magnetization*** measurement (see the process 10-2).

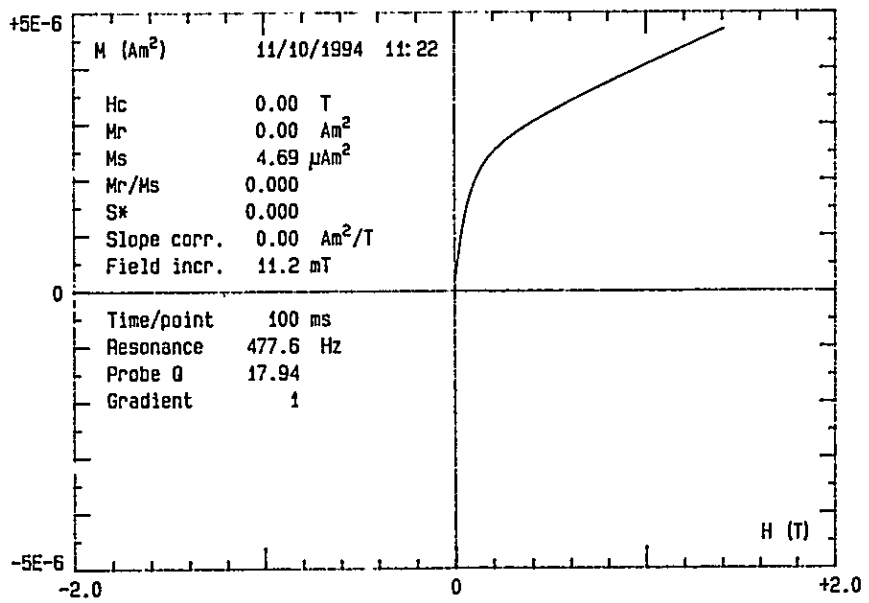

Appendix Figure 7: ***Initial permeability*** curve of a bulk sample of the "hematite oolite" measured after the demagnetization treatment.

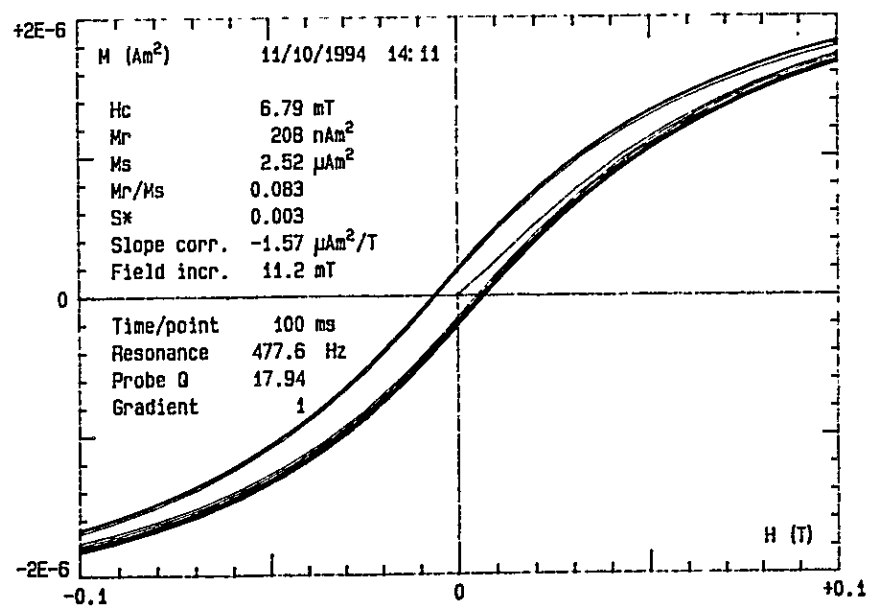

Appendix Figure 8: ***Minor Loops*** of 9 steps from Hmin=0.14T to Hmax=1.4T for a bulk sample of the "hematite oolite".

8-3. Change the setting of ***saturating field, applied field maximum, applied field increment***, if it is necessary.

8-4. Move the cursor bar to the desired function and press [Enter]. This start the measurement

8-5 Upon the completion of ***Isothermal Remanent Magnetization*** measurement, the following parameters and curves will be displayed on the screen

M(=magnetization)-H(=field) curve

Mr(=remanence)-H(=field) curve

Mr. saturation remanent magnetization

Ms: saturation magnetization

Press [F1], [F2], and [F3] for sample description, file save, and plotting the result, respectively It is recommended to use the following file name for isothermal remanence measurement data

□□□□□□□□ IRM

8-6. Upon the completion of ***DC Demagnetization Remanence*** measurement, the following parameters and curves will be displayed on the screen

M(=magnetization)-H(=field) curve

Mr(=remanence)-H(=field) curve

Hc coercive force

Hcr: coercivity of remanence (|Hcr|>|Hc|)

Mr: saturation remanent magnetization

Ms saturation magnetization

8-6 The ***DC Demagnetization Remanence*** measurement contains six additional curve-processing functions as follows

- [F1] (ΔM) Plot of M at field H and remanence at H=0 *versus* H
- [F2] (ΔM/2Mr) Previous curve ([F1]) normalized
- [F3] (ΔM_{irrev}) Plot of irreversable magnetization *versus* applied negative field
- [F4] ($\Delta M_{irrev}/2Mr$) Previous curve ([F3]) normalized
- [F5] (ΔM_{rev}) Difference between magnetization (M) and remanence (Mr) curve
- [F6] ($\Delta M_{rev}/2Mr$) Previous curve ([F5]) normalized

8-7. Press [Space] key and get another menu Select appropriate menu and save the data (results of processing)

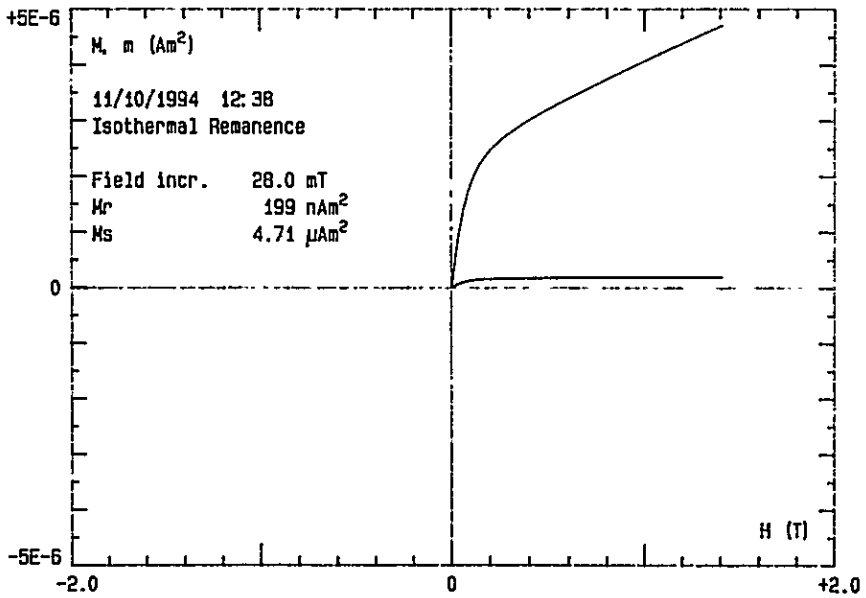

Appendix Figure 9: Result of ***Isothermal Remanence*** measurement for a bulk sample of the "hematite oolite". M-H curve (magnetization acquisition curve; upper curve) and Mr-H curve (change of remanence; lower curve) are displayed.

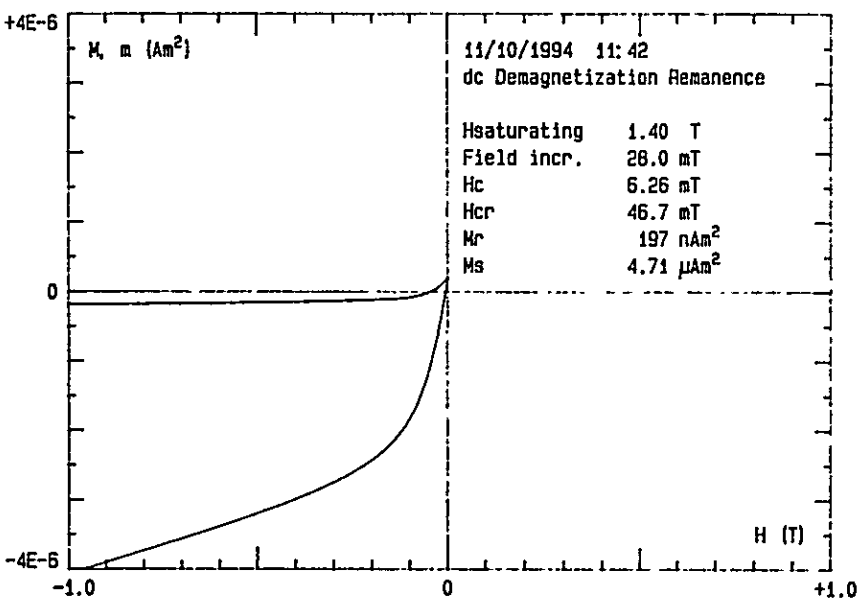

Appendix Figure 10: Result of ***DC Demagnetization Remanence*** measurement for a bulk sample of the "hematite oolite". M-H curve (Magnetization acquisition curve; lower curve) and Mr-H curve (Change of remanence; upper curve) are displayed. The field of Mr=0 is the value for Hcr (Hrc; coercivity of remanence)

8-8. It is recommended to use the following style of data file naming of the measurement data.

for DC demagnetization raw data	□□□□□□□□.DCD
for (ΔM)	□□□□□□□□ DC1
for (ΔM/2Mr)	□□□□□□□□ DC2
for (ΔM_{irrev})	□□□□□□□□ DC3
for (ΔM_{irrev}/2Mr)	□□□□□□□□.DC4
for (ΔM_{rev})	□□□□□□□□.DC5
for (ΔM_{rev}/2Mr)	□□□□□□□□.DC6

(9) Optional Measurement-4 <Time Dependence>

9-1 Follow the procedure until the step 3-4 In the ***Measurements Menu***, locate the cursor on ***Time dependence*** and press [Enter] ***Time Dependence Measurements Menu*** will appear on the screen. Executing this function, time decay curve of magnetization can be measured

9-2 Set the ***Sensitivity***, ***Applied field*** (a static field if required), ***Magnet sweep dwell time***, ***Initial field*** (field to be applied prior to the measurement), ***Applied initial field for*** (duration which initial field is applied prior to the measurement), ***Final field*** (field to be applied during measurement), ***Averaging time*** (per point averaging time, 1ms~1ks), ***Timebase*** (duration of measurement in second).

9-3 Locate the cursor on ***Measure time dependence*** and press [Enter]

9-4 Upon the completion of the measurement, M(=magnetization)-t(=time) diagram will be displayed It is recommended to use the following style of data file naming of the time dependence data·

□□□□□□□□.TDM

(10) Other Functions

10-1 **Optimize:** This function provides the operator with an alternate method of locating the sample in the "electrical center" of the sample zone and gradient field coil Move the cursor to ***Optimize*** in the ***Measurement Menu*** and press [Enter]. Adjust the vernier knobs on the ***Micropositioner*** for setting

X-position in *minimum* output signal

Y-position in *maximum* output signal

Z-position in *maximum* output signal

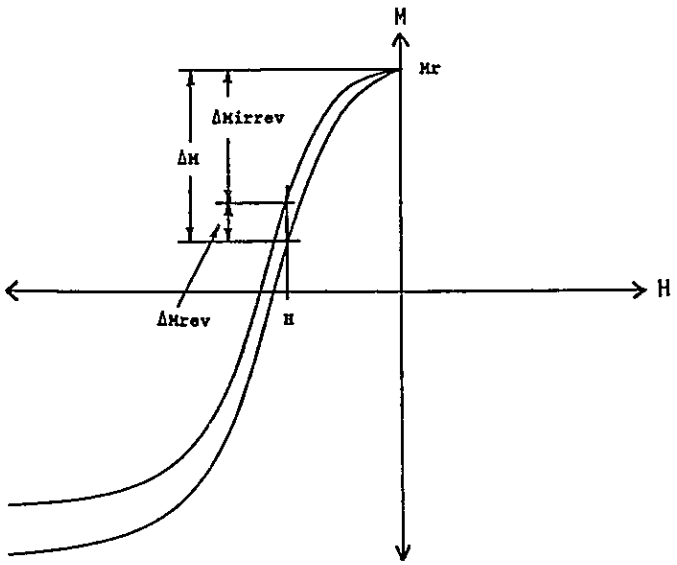

Appendix Figure 11: Three parametric values, ΔM, ΔMrev, and ΔMirrev, for the additional curve-processing functions (Princeton Measurements Cooperation,1993).

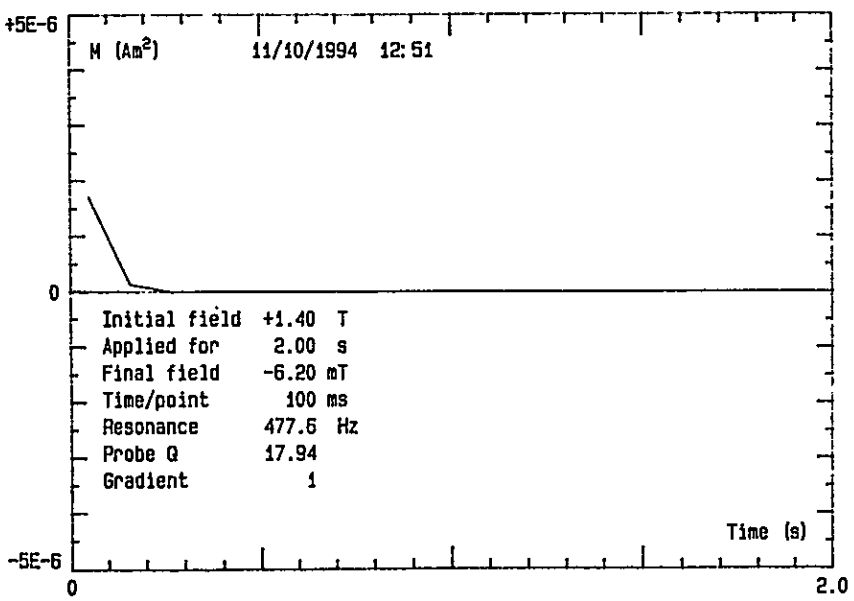

Appendix Figure 12: Result of ***Time Dependence*** measurement for a bulk sample of the "hematite oolite". The curve shows time decay of 1.4T IRM under -6.2mT field. It showed that the remanence can be completely demagnetized after 0.3 seconds

10-2. **Demagnetize:** Executing this function, most samples installed in the MicroMag system will be automatically demagnetized. Locate the cursor on ***Demagnetize*** in the ***Measurement Menu*** and press [Enter]. Select [F1] (field demagnetization), [F2] (moment demagnetization), or manual demagnetization.

10-3. **Noise Measurement:** Two noise measurement screens, ***Moment noise*** and ***Field noise***, are available. Move the cursor on ***Noise Measurement*** in the ***Measurement Menu*** and press [Enter]. Select [F1] (***Moment***; useful to measure acoustic noise in the laboratory) or [F2] (***Field***, useful to measure magnetic noise in the laboratory).

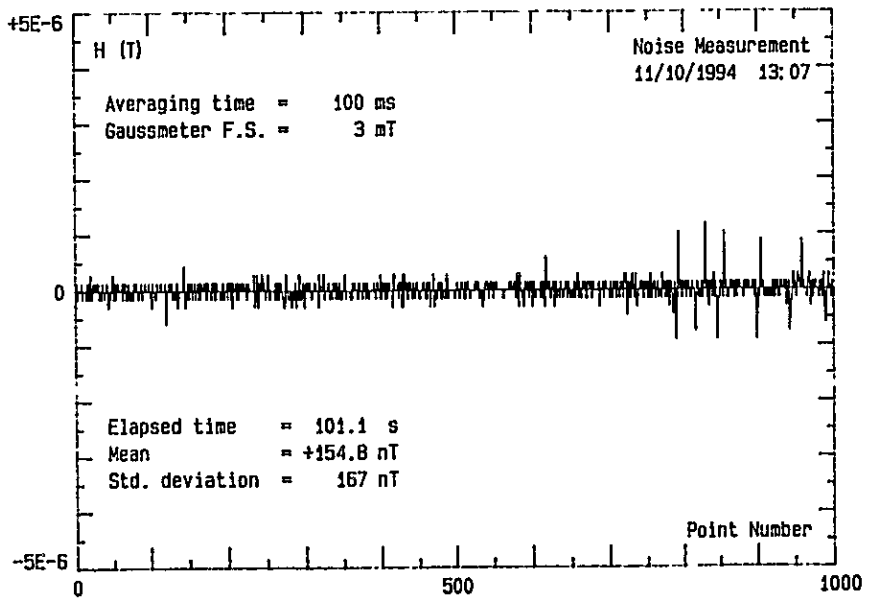

Appendix Figure 13: Noise of magnetic field in the laboratory during 101.1 seconds measured by the ***Noise Measurement*** function.

Proceedings of Geoscience Colloquium, Geoscience Lab ,GSP, 9,101-111

CAN WE DEVELOP OUR "DATA PROCESSING ROOM" TO A REAL "DATA PROCESSING CENTRE "?

Ibrar H. Khan, Tahir Karim* , Iftikhar Mustafa Khadim* and Yoshiki Fujiwara***

** Geoscience Laboratory, GSP, P.O.Box 1461, Islamabad*
*** JICA Expert, Division of Earth and Planetary Sciences, Hokkaido University, Sapporo 060, Japan*

ABSTRACT

With a view to the above commonly considered question, the computer facility available in the Data Processing Section, Geoscience Laboratory is reviewed according to the past and present nature of the job. The hardware and software provided by JICA at the time of inauguration of this laboratory and later addition to this is also assessed. The recent addition of hardware and software are given for the better understanding. The existing computer section setup is considered insufficient to meet the present day challenges and up gradation is required to cope with the future requirement along with the effective usage. The two stage up gradation is proposed: LAN Stage - Local Area Networking of high capacity, newly added machines in the first stage, and WAN Stage - Wide Area Network with computer facility extended to each researcher's table and linked to the world computer systems. This two - staged up gradation is considered necessary even for the near future developments in the computer hardware and software. The acquaintance of the researchers to the networked system is also considered before the second stage development.

INTRODUCTION

The Geoscience Laboratory was established in 1991 as grant-in-aid JICA Project with the installation of excellent and most modern analytical facilities. The latest instruments are purchased according to financial resources available, at that time. All the machines were opted by the renowned scientists of various Japanese organizations. Soon after the completion of installation phase and handing over of the facility by JICA, it was felt that working output can be bettered by the addition and modification of certain machines. The critical review resulted in many good additions, not only to the analytical equipment but also to the output data handling system. The Data Processing Section of this laboratory was considered a little bit unlucky, as the computer hardware facility was insufficient for even the limited number of scientists working at that time. Immediately after the inauguration, some computers, softwares and printers were added. Still the facility was just sufficient for word processing and limited data processing. The JICA provided some

etc. There is common question that , " Can we develop our Data Processing Room to a real Data Processing Centre"? This question was tried to be answered in post computer training Geoscience colloquium. The critical review of computer facility and proposal is given through this report. The requirement is changed with time and due to the advancement in the field of computer science. With a view to the future need of at least five years the present proposal is submitted. A brief resume' of the existing facility is included in this report.

1. FACILITY DONATED BY JICA IN 1991

1.1 Hardware

IBM Computers PS/2 Model 70 (M–60)		3 sets
80387 processors, 20 MHz. machines, HDD–60MB		
Floppy Disk drive—1, 4MB RAM, and VGA monitors		
Printers		3 pcs.
IBM Laser 4019	1 pce.	
IBM Proprinter XL24E	2 pcs.	
Plotters		2 sets
Graphtec ™ FP–7100 (8–pen, large size)	1 pce.	
Graphtec ™ FP–6400 (8–pen, small size)	1 pce.	
Digitizer		1 set
Graphtec ™, KD–6450 with 4–button cursor pad		

1.2 Software	3 pcg
WordStar 6.0, Lotus 1 2 3, ver. 2.2 dBase III+	

2. FACILITY ADDED BY GEOLAB

2.1 Computers:

Macintosh IIci:	1 set
25 MHz, RAM—5MB, HDD—80 MB, FDD—1.44 MB,	
DCM (IBM Compatible):	1 set
80387 processor, 33 MHz, RAM—4 MB, HDD—80 MB	
FDD—2 (3.5"–1.44 MB & 5.25"–1.2 MB)	

Toshiba Laptop: 1 set

80386 Processor, 20 MHz, RAM—2MB, HDD—80 MB,
FDD—3.5" 1.44 MB, 9" LCD display

IBM PS/2, Model-70 (A-16) 1 set

80387 Processor, 25 MHz, RAM—4 MB,
HDD—153 MB, FDD—3.5"(1.44MB),
EXT.FDD—5.25"(1.2 MB)

2.2 Input and Output Devices

Printers 6 pcs.

HP LaserJet III	1 pce.
Panasonic KX-P1624 24 pin	2 pcs.
Brother M4018(Color)	1 pce.
Apple Style Writer	1 pce.
Toshiba Express Writer 301	1 pce.

Scanner 1 pce.

HP ScanJet

3. RECENTLY ADDED

3.1 Hardware

Macintosh Quadra 800 1 set

33 MHz, RAM—16MB, HDD—500MB,
2- External Hard Disks—1GB each, Tape Drive—3GB,
ODDrive—1GB with 5 spare cartridges Re-writeable—1GB
each & 5 spare once-write—970MB each, CDD—650MB

Printer 1 pce.

Cannon Apple Color

Scanner 1 pce.

Apple Color Scanner

CD ROM Drive 1 set

For IBM Computer through SCSI interface with card

3.2 Software

Geological , Geophysical & Geochemical Software

IBM PC Software

1. Rockworks	2. COREL 4.0	3. Micrografix Designer
4. IGPET	5. Z-Con	6. Graph-Cad
7. MAG-CAD	8. MAG-CALC	9. INTERPEX

Mac Software

1. MapGrafix	2. MapCon Contouring	3. 4th Dimension
4. M.S Word 5.2	5. Aldus Persuasion	6. Quark Express

7. Claris Field Maker Pro.

DIFFICULTIES IN WORKING WITH EXISTING FACILITY

1. **Insufficient Memories**

The hard disk capacities of the existing computers are smaller (60~153 MB) as compared with the present day available software which normally needs much bigger hard disk capacities, 250~500 MB (approx.) in each computer. Various effectively used software, both for scientific data processing / management and routine office administrative use are now shifting to Windows based applications Windows is basically a multitask operating system and its applications are fundamentally color graphics based, therefore large computer memories are necessary to run these. Hence the up gradation of the present systems seem to be necessary. Besides the future requirement will be much more than the present day requirements, hence to meet the challenges of the future, the up gradation of this facility is essential. The bigger softwares also require much bigger random access memories (RAM) for effective running.

2. **Slow Processing Speed**

The presently available software in the market are developed on faster systems whereas our hardware is very slow. Hence while running the large memory graphics software, like Corel 4.0 or Micrografix Designer, the operator has to wait most of the time when the machine is busy in processing.

3. **Less Number of Computers and Output Devices**

The computers are less in number to process the data generated in this laboratory. Hence the researchers need better access to the computers for word processing and scientific data processing.

4. **Unavailability of Faster Input and Output Devices**

After the completion of training phase the rate of data generation is becoming faster and require the faster input and output devices compatible with the computer facility. These devices include Color scanner, digitizer, fast printers (both color and monochrome)—Laser or Thermal Vax type, Styler Pens for figure tracings, etc.

5. **Lack of Backup Facility**

There is no backup facility available at present and in case of any hard disk perishing or infection by viruses, all data will be lost or corrupted . The Magnetic Optical Disks or Tape Drive Backup facilities are presently becoming popular for backup.

6. **No Desktop Publication Facility**

The desktop publication is a specialized job whereas previously the Proceedings of Geoscience Colloquia and Proceedings of Geoscience Laboratory are being composed on normal word processing software. The desktop publication software facility should be available for the perfection of this job.

7. **Limited Maps and Figure Drawing Facility**

The map making with IBM systems is limited and the software need up gradation. The Rockware software is good for normal geologic work. If the large sized maps are to be prepared then new software should be added.

PROPOSAL FOR NECESSARY IMPROVEMENTS IN DATA PROCESSING

The present proposal is suggested in two stages. The first stage seems to be the immediate requirement and second stage is included as "future dream" in the end. This two staged up gradation is considered necessary so that the researchers of this laboratory should be first acquainted with the network system and to acquire knowledge for solution of day to day problems. The improvements are suggested after the detailed discussions also with the short-term and long-term JICA Experts.

First Stage - PRESENT REQUIREMENT

The small local area network (LAN) is suggested for the present requirement and the effective utilization of the facility. The purchase of new machines is recommended for the up gradation of the existing hardware as the up gradation of available machines will cost too much. Already a market survey has been conducted for the availability and working of various machines The proposed facility will enhance our Data Processing Section to qualify as a "Real Data Processing Centre". The facility should locally be networked at present to share the input and output devices. The telephone line can be connected through modem card for electronic mail service at present. The previously existing computer facility, being slow to respond the present software, may be transferred to the researchers for their word processing and other routine jobs. The proposed setup is shown in figure 1 and summarized below:

Main Server Machine[1] 1 set

80586–processor based or Pentium type machine
Speed >60 MHz, RAM >32 MB, HDD 2~3 GB, Opt. DD >500MB,
CD Drive >500MB, FDD—2 (at least), Tape Drive Backup >2GB,
connected through SCSI interface

Intelligent Terminals/Work Stations 4 set

Each with 80486–based processor, Speed 40~60 MHz, RAM 8~16 MB,
HDD 250~500 MB, FDD—2 (1.44MB & 1.2 MB), CD drive

LAN Requirements

1. Modem Card (Baud rate 9600 or more)	1 pce.
2. Ethernet cable thin type	15~20 m
3. T-sockets for cable connection on each NODE	8 pcs.
4. Network Cards NE-2000 for Work stations	6 pcs.
5. Network Card NE–32 for Main Server	1 pce.
6. Network Software for 8 stations	1 pcg.
Novel Netware 4.2 or higher version	

[1]Presently many machines are available from many world renowned companies like IBM, COMPAQ, AST, Digital or HP with 66~150 MHz speed, RAM 16~256MB, Vidio RAM 1~4 MB, HDD 500MB~19 GB, along with various capacity, Compact Disk ,Optical Disk, Magnetic Optical Disk and Backup Tape Drives, .

7. Network Security Software. 1 pcg.

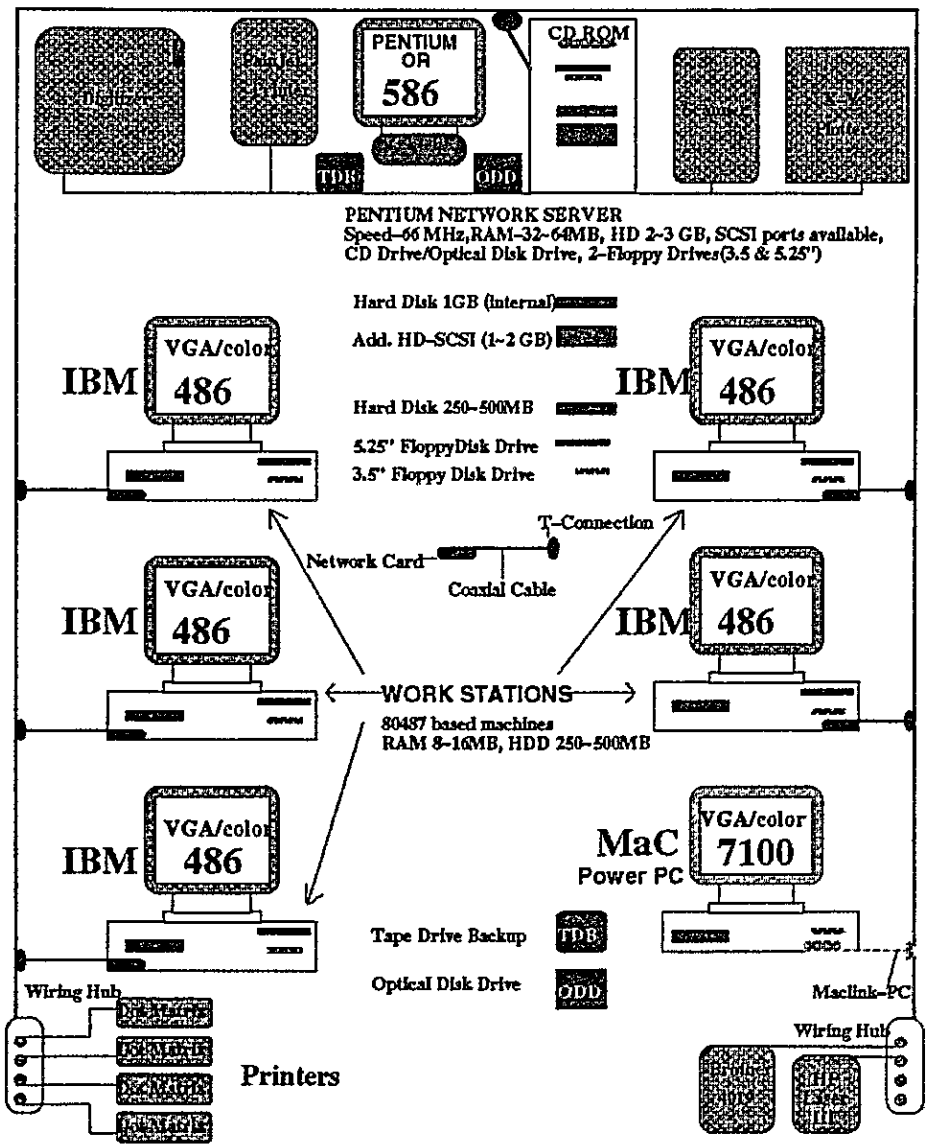

Fig.1 Schematic Diagram showing the setup of LAN in Data Processing Section.

Software requirement

This laboratory needs different types of software for the word processing, data processing, database management, desktop publication and preparation of illustrations and maps. The software available are barely sufficient for the map making and database management and the licensed to run on network or multisystem use have to be purchased. The following software are proposed:

1. Microsoft Windows 3.1 Upgrade
2. Word for Windows 2.0 or later version
3. Microsoft Access
4. Ventura Publisher 4 0
5. Harward Graphics for Windows
6. Aldus Page Maker Pro

Input/Output Devices

Digitizer — 1 set

HP or Summa Graphics, size 40"×48" with 16 button cursor pad

Color Printer — 1 pce.

PaintJet or Thermal Vax type for printing of figures in color

Plotter — 1 pce

DraftPro series, size 40" × 48",with multicolor and multisized pens (sizes 0.1mm~1.5 mm)

Second Stage: FUTURE NETWORK DREAM

With the advancement in the computer science and the automation in the analytical equipment the data generation is very fast these days. Such high technology instruments are installed in this laboratory which are being operated effectively to their output capacities. With the passage of time, the data generation will become much faster. Hence up gradation of the computer facilities will be required. The facilities extended to all sections and researcher, beside quick processing will also need faster acquisition of the output data as hard copies

For the effective utilization of such high technology equipment, the foreign collaborations are always necessary to keep up with the world research pace. Such collaborations need faster communication system and nothing is faster than the digital communication through data connections. This communication is possible if we develop our gateway system with special computer facility working under UNIX environments. To run UNIX environment, the mini or mainframe computer system is needed which can be

networked to each researcher's personal computer working in Windows or DOS based operating systems.

It is understood that minimization of unnecessary mobility of the research results in the effective increase in the output. The future network configuration is proposed in such a manner that the researchers need not to move around for the acquisition of data from others.

With increase in wages and inflation the hiring of large number of manpower is becoming difficult day by day. Hence the less number of manpower with highly efficient computer setup can produce much better results.

B. Proposed Setup

The proposed setup is given in the following and is illustrated in figure 2.

1. Hardware Requirement

1.1 Main Server Machine[2] 1 set

Mini or Mainframe type machine
Speed 100~150MHz, RAM 500MB~1GB, VRAM 5~10MB, HDD 20~50GB, ODD 1GB (RW), MODD 128~512MB, CDD 500MB~1GB, FDD >2, TDB 3~5GB, connected through SCSI interfaces.

1.2 Work Stations 37 set

Already Existing 8 set

To be Purchased 29 set

Desktop PCs 486–processor, Speed 40~60MHz, RAM 8~16MB, HDD 250~500MB, FDD—2 (1.44MB & 1.2MB), CDD

1.3 Laptop (for outdoor or field use) 5 set

386 or 486 processors, RAM 5~10MB , HDD 80~200MB, FDD 2 (1.44MB each),

1.4 WAN Requirements

1. Gateway System with stand by facility	1 set.
2. Major Optical Loop System for WAN linked to Gateway	1 set
3. Optical/Ethernet Coaxial cable for Network	250m
4. Network Cards for Major Server	2 pcs

[2] Presently big machines like IBM RISC System/6000s Or AS/400 are available with such facilities which can run in UNIX environments. The new abbreviations used above are MODD magnetic optical disk, RW for re-writeable, VRAM for vidio RAM.

5. Network Cards (NE-2000 or other) for Work stations 40 pcs

6.Socket for cable connection on each NODE 40 pcs

1.5 Input/Output Devices

Digitizers 2 set

HP or SummaGraphics, or Calcom Series size 40"×48" with 16 button cursor pad

Printers 42pcs

Dot-matrix Type 35

Laser Printers 4 pcs.

Color Printer 3 pcs.

PaintJet or Thermal VAX type for printing of figures in color

Plotters 3 set

DraftPro series, size 40" × 48", with multicolor and multisized with color Pens (sizes 0.1mm~1.5mm)

Color Scanners 3 pcs

LaserJet Scanners

2. Software Requirements

2.1 UNIX with networking capacity for 40 PCs.

2.2 DOS/WINDOWS with networked environment

2.3 DB2/400 Integrated database system for mainframe type systems

2.4 CICS/400 (Client Server) for AS/400 support software

2.5 Rockware or Other Software for Complete Geological, Geophysical, Geochemical and Cartographic application

2.6 Aldus Page Maker Pro(Organization Licensed)

2.7 Winword for organizational/network setup

2.8 Ventura for multivendor systems

3. Manpower Requirement

The proposed setup require full time system analyst and programmer for the effective operation, system security and maintenance. The access levels and coding systems are necessary for the setup. Hence one system analyst and one professional programmer are proposed who should be responsible for the development of certain software also. The solution of day to day problems and trouble shootings will also be necessary. In case of system shut down or any other failure immediate restoration is needed.

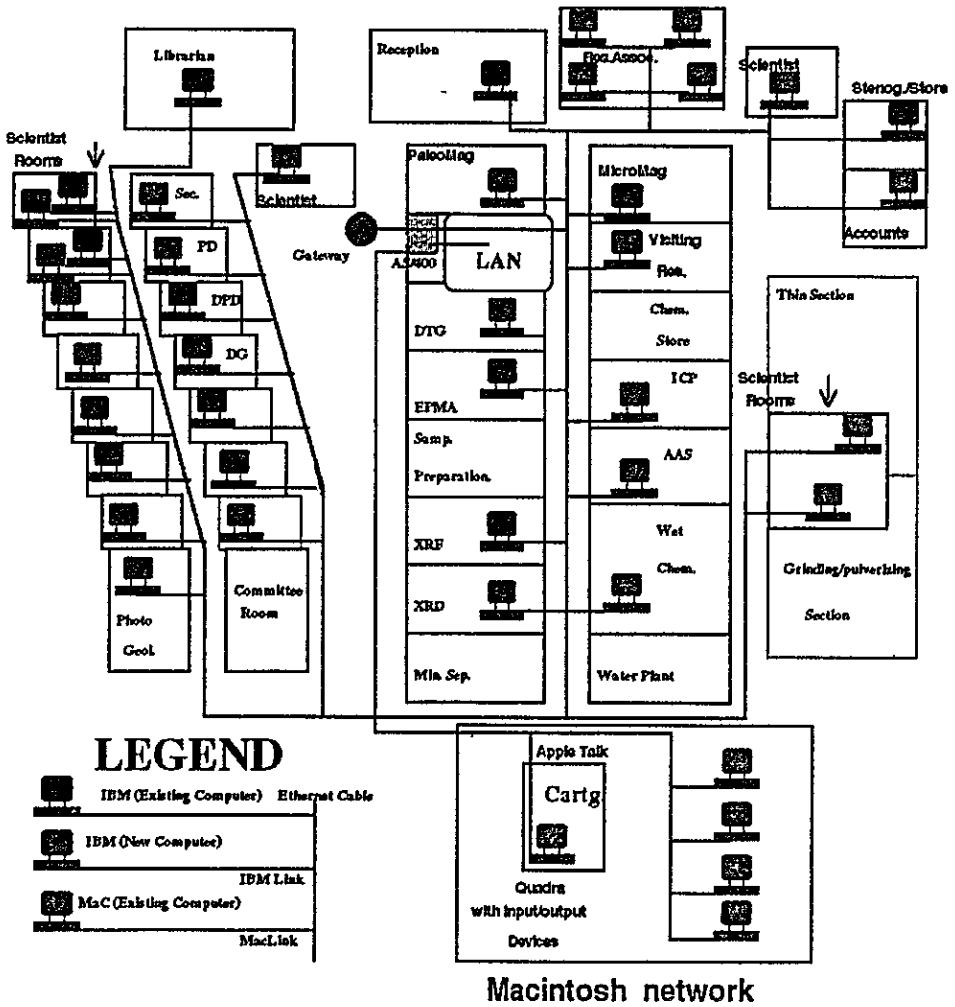

Fig. 2 Schematic diagram of Proposed Future Plan for Expansion of Computer Facility.[3]

[3]The abbreviations used above are DG–Director General, PD–Project Director, DPD–deputy Project Director, Sec.–secretary to PD/DG, DTG–Differential Thermal Analyzer/Gravimetery, EPMA–Electon Probe Micro-Analyzer, XRF–X-Ray Fluorescence Spectrometery, XRD–X-Ray Diffractometer, ICP– Inductively Coupled Plasma Spectrometery, AAS–Atomic Absorption Spectrometery, Chem. Chemistry, Min. Sep.–Mineral Separation.

PART II. FACT FILE

GeoLab Research / Training Activities
(MARCH - NOVEMBER, 1994)

In-House Training

Two computer trainings on the use of Map-Grafix system (mapping software) on the Mac and training on the map making, preparation of figures and illustrations and other geological data interpretation softwares on the IBM, were completed.

A month long physical geology course for the Geochemists and Geophysicists of the Geoscience Laboratory was completed. The course was conducted by Dr.Tahseenullah Khan, Assistant Director, Geoscience Laboratory.

One week special course on the use of universal stage and study of plagioclase twinning was given by the visiting short term JICA Expert in October, and two weeks training on basic optical mineralogy was also given by Dr.Yuhei Takahashi in November to the geophysicists.

Foreign Training

Three Geoscience Researchers visited Japan for the training in their respective fields. Mr. Muhammad Sakhawat, Geophysicist / Deputy Project Director, stayed in Japan for about three weeks in August-September. He visited different manufacturers and factories, Shimadzu, Rigaku, Seiko, Nichika, and Horiba companies. He discussed about the maintenance and availability of the spare parts of the existing instruments in the GeoLab.

Mr.A.B.Kausar, Deputy Director, stayed in Japan for about two months, August-October. During his stay he presented a paper in the IGCP symposium held in Hokkaido University, Sapporo. He worked on the EPMA and studied Chilas Complex rocks in the Shimane University, Matsue. He also delivered a talk on "REE variation across the Kohistan Batholith, Gilgit, northern Pakistan". In the last part of his visit he worked in the Geological Survey of Japan, Tsukuba, and presented a paper entitled "Temporal variation in Mineralogy Petrology, Kohistan Batholith, northern Pakistan".

Mr.Iqbal Hussain Haidri, Assistant Director, stayed in Japan for about two months, August-October, and practiced special techniques for preparation of thin sections, polished blocks and sections for the fluid inclusion study. He worked in the Geological Survey of Japan offices in Sapporo and Tsukuba.

Mr. Haider Zaman, Assistant Geophysicist, continued his Ph.D study in Kyoto University, Japan.

Mr.Shehzad Hassan, Research Associate, joined two years M.Sc. course in Shimane University, Matsue, Japan from October. His research topic is the "Geochemistry and Paleoenvironmental study of Permo-Triassic boundary in Salt Range area, Pakistan".

Field Work

First phase of field work on the Waziristan ophiolite complex is completed in July and about 650 sq. km area was mapped on scale 1:50,000. In the later part of the field work the a group from the Paleomagnetic Section joined the field for for some paleomagnetic studies in the ophiolite bearing area.
(Party members: Said Rahim, Tahseenullah Khan, Iftikhar M.Khadim, Muhammad Ali, Mirza Naseer)

A Geoscience researchers field party carried out field work in the Gilgit, Hunza, Yasin and Sassi areas in August. The party collected the samples to study the back-arc assemblages in Kohistan, Northern Pakistan.
(Party members: Dr.Tahseenullah Khan, Muhammad Naseem)

The Chemical Section has completed the field work and sampling for the second reference sample in October. They also made a short field trip to the Shah Dehri China clay deposit, Swat, NWFP. Sampling is done on the grid pattern for the geochemical exploration.
(Party members: Dr.T. Shirahase, Dr.H. Kaneda, Dr.S. Itoh, Mr.K. Kato, Muhammad Naseem, Muhammad Zafar)

A 10 days field work was carried out in Salt Range area by Mr.Shahzad Hassan, as a part of his studies on the Permo-Triassic boundary. He measured a section along Namal gorge and collected samples.

Mr.Shahzad Hassan, along with JICA Expert, before leaving for Japan made his second field work in Salt Range area and measured a section and collected samples from each lithological unit for the laboratory study in Japan.
(Party member: Dr.T. Naka, Shahzad Hassan)

A short field trip was made in the month of May to Swat, Malakand and Jijal areas for the exploration of the PGE minerals. During this field work special sampling techniques were demonstrated by the JICA Expert and stream-sediments samples for the laboratory study were collected.
(Party members: Dr.M.Nakagawa, M.Ujiie, JICA short term Experts, Said Rahim, Ibrar-ul-Hasan)

Another field work for the exploration of the PGE mineral in Jijal and adjecent areas was made in themonth of July. During this field detail sampling of the ultramafic rocks was done.
(Party members: Said Rahim, Muhammad Yousaf)

A field mapping training to geophysicists and geochemists was carried out in Margala Hills for few days during the months of June and July. During this field they were trained to identify major sedimentary rocks, and to read the map.
(Party members: Iqbal Haidri, Dr.T. Naka, JICA Expert, Iffat Jabeen, Arshad Ali, Adnan Iqbal, Mirza Naseer, Muhammad Ali.)

Paleomag group made a short trip in November, to collect samples from the iron ore occurences in NWFP and Punjab. The party sampled the iron ore body at Nizampur, Samana area, Kohat, Kalabagh, and the Sargodha.
(Party members: Dr.Mitsuo Yoshida, Iftikhar M. Khadim, Mirza Naseer, Muhammad Ali)

Short Term JICA Experts

Eight short-term experts visited the Geoscience Laboratory. These include Dr.Yoshiki Fujiwara, from Hokkaido University visited as a computer expert and organised and gave training on the mapping and other scientific softwares. (March-May)

Dr.Mitsuru Nakagawa, from GSJ, Hokkaido worked on the ultramafic rocks and gave training to the GeoLab researchers on the exploration of the PGE minerals. (April-May)

Miss Masumi Ujiie, from GSJ, Tsukuba, worked on the Chilas complex and gave a short training to the chemical section researchers on the application of Compton Scattering method on XRF. (April-May)

Two experts Mr.Shinichi Takada and Mr.Kuniyuki Mitsube from the SEIKO Electric. Co. visited the GeoLab for about one week to give operational and maintenance training on the ICP. (April)

Dr.Yuhei Takahashi, from GSJ, Hokkaido, arrived in Pakistan in the end of September, 1994. He will stay for about three months. In October, he gave training on the techniques to study the plagioclase twining by using Universal Stage.

GeoLab Visitors

A three member JICA Experts mission led by Mr. N. Okamura visited Pakistan on a three week study tour to see the prospects of Fused Magnesium Phosphate (FMP) Project. Beside field work in the phosphate and magnesite bearing areas in Hazara the mission also visited and held meetings with organizations belonging to public and private sectors.

A team of Metal Mining Agency of Japan (MMAJ) visited the GeoLab and discussed the prospects of developing the Duddar Zinc-Lead deposits. They were briefed about the general geology and metalogenic set up of Pakistan.

Laboratory Work

The Sample Preparation and Chemical Section gave full support to the GeoLab researchers in their research activities. More than 500 points qualitative and quantitative analyses were performed on the Electron Micro Probe Analyser, on the rock all over Pakistan specially the Swat, Malakand, Chilas and Waziristan areas. This also include analyses of the new mineral standards received in early this year.

The Sample Preparation Section during this period made more than 270 normal and polished thin sections. They also crushed / pulverized about 820 samples for the XRF, XRD and DTA/TG studies.

The analytical lab analysed about 570 samples for more than 10,000 estimations of major and trace elements on XRF, ICP and AAS.

Lectures / Seminars / Courses

Geoscience Lab arranged special lectures by the visiting scientists. Under the Distinguished Lecture Series of the Geoscience Laboratory on 8th August, 1994 Professor Dr.Patrick Le Fort delivered a lecture on "Closure of Tethys & the Formation of Himalayas". This talk was arranged in a local hotel and more than 150 earth scientists attended. Another lecture from the same professor was organised in the GeoLab on "Himalaya - Karakuram Junction in Chogo Lungma to Turnik area, Baltistan, northern Pakistan".

Two courses were organised in the Geoscience Laboratory under the Australian International Development Assistance Bureau (AIDAB) programme. First course was one-week long started on 26th June,1994, on "Mineral Development Practices for Senior Executives". The course was attended by 15 participants from 10 different organizations. The second course was on "GEMAP Photogeological Workshop" from 12th to 22nd September,1994. This course was attended by 14 participants from 6 organizations.

New Equipment

An Alternating Field Gradient Magnetometer (AGM), PRINCETON / Micro Mag Model 2900-02 was installed in Paleomagnetic Section, Geoscience Laboratory, under a financial support of JICA (F.Y. 1993 Supplemental Equipment Grant). The AGM micro-magnetometer is one of the latest magnetic property analyser which has been equipped only in few geological institutes in the world. Intensive training course for the operation and analytical techniques was held in September - November by Dr.M. Yoshida, JICA expert.

Programs of the Geoscience Colloquium held from March to November, 1994

The 26th Geoscience Colloquium
April 4, 1994 (Sunday)

1. *Tahir Karim*
   Data Processing System in the Geoscience Laboratory - the Status Quo and Proposal -

2. *Yoshiki Fujiwara*
   How to Use Personal Computer System for Geological Sciences
   - A Case Study: Landslides in Hokkaido, Northern Japan.

3. *Mitsuru Nakagawa*
   PGE Mineralization of ophiolite.

4. *Masumi Ujiie*
   Petrochemical Studies of the Orikabe Zoned Pluton, Kitakami Mountains, Northeast Japan.

5. *Teruo Shirahase*
   Perspective of the studies on the Chilas Complex.

6. *Muhammad Ali, Mirza Naseer Ahmad, Iftikhar M. Khadim, and Mitsuo Yoshida*
   Total Gamma-ray Observation along the Karakorum Highway, Northern Pakistan: An Attempt of Geological Interpretation by Radioactivity of rocks

***

The 27th Geoscience Colloquium
April 14, 1994 (Thursday)

1. *Muhammad Naseem*
   ICP training by Seiko engineers.

2. *Shinichi Takada*
   The feature of ICP-AES analysis.

3. *Mirza Naseer, Iftikhar Mustafa Khadim, Mohammad Ali and Mitsuo Yoshida*
   Geomagnetic survey of the Northern Suture along Hunza River.

The 28th Geoscience Colloquium
April 20, 1994 (Wednesday)

1. Research on Platinum-group Mineralization in Northern Pakistan

(1) *Said Rahim Khan, Ibrar H.Khan, and Mitsuru Nakagawa*
Geological Setting of PGE-bearing Ultramafics in Northern Pakistan

(2) *Ibrar H.Khan, Mitsuru Nakagawa, and Said Rahim Khan*
Mineral Chemistry of the PGM

(3) *Mitsuru Nakagawa, Ibrar H.Khan, and Said Rahim Khan*
Significance of Finding and Discussion for Further Research

2. Post-field Report of the Survey in Chilas Area

(1) *Allah B.Kausar*
The Kohistan Batholith: field, petrological, and geochemical aspects.

(2) *Masumi Ujiie*
Correlation of Kohistan Batholith with Granitic Rocks in Japan.

(3) *Teruo Shirahase*
Future Plans and Conclusion.

3. *Iffat Jabeen, Arshad Ali, Abdul Aziz, and Masumi Ujiie*
Application of the Compton Scattering Method in XRF Analysis.

***

The 29th Geoscience Colloquium
May 18, 1994 (Wednesday)

1. *Muhammad Naseem*
ICP training in Japan

2. *Iftikhar Mustafa Khadim*
Rock Magnetic Study of Mesozoic igneous rocks in Hokkaido, Japan

3. *Tahir Karim, Ibrar H.Khan, and Iftikhar M.Khadim*
Can we develop our "Data Processing Room" from a word processing room to *real* data processing room?

4. *Yoshiki Fujiwara*
Future Data Processing System in the Geoscience Laboratory:
A Recommendation

The 30th Geoscience Colloquium
June 9, 1994 (Thursday)

Feasibility Study of Fused Magnesian Phosphate in Pakistan

1. Outline of Works
   Tahir Karim and Jiro Hirayama

2. What is Fused Magnesian Phosphate
   Jiro Hirayama

3. Phosphorite Deposit
   Masao Satoh and Takahito Naka

4. Manufacturing
   Susumu Hata and Jiro Hirayama

5. Marketing and Concluding Remarks
   Naoki Okamura and Jiro Hirayama

***

The 31st Geoscience Colloquium
August 16, 1994 (Tuesday)

1. *Muhammad Yousaf*
   Field Study of the Khaltoro Pegmatites

2. *Rehan-ul-Haq Siddiqui*
   A Brief Study of Petrochemical Evolution of Chagai Island Arc, Balochistan, Pakistan

3. *Iffat Jabeen, Arshad Ali, and Abdul Aziz*
   Off-line Analysis by XRF Using FP Method.

***

The 32nd Geoscience Colloquium
October 12, 1994 (Wednesday)

1. *Shehzad Hassan and Takahito Naka*
   A Review of Permian-Triassic Boundary Problems and Preliminary Field Report in Salt Range.

2. *Yuhei Takahashi*
Modes of plagioclase twining in the Chilas Complex and Kohistan Batholith.

***

The 33rd Geoscience Colloquium
November 17, 1994 (Thursday)

1. *Kazuyá Kubo*
Magmatism of Chilas Complex - Special Reference to the Ultramafic-Mafic Association.

2. *Allah B.Kausar, Tehseenullah Khan, Yuhei Takahashi, Yutaka Takahashi, and Teruo Shirahase*
Comments

The programs of colloquia before the 26th Geoscience Colloquium were reported in previous volumes of the Proceedings. *Editors*

Instructions for Submitting a Manuscript
(November, 1994)

Manuscripts are photographed exactly as they are received, with an 84% reduction in size for printing in the Proceedings of Geoscience Colloquium You are recommended to use a ***12-point font size ('Times' or 'Times New Roman')***, and printed on an ***A4 paper (21cm x 29.7cm) with 1.5 spacing*** The format of page setup is as follows

(1) Do not exceed the following margins on an A4 paper (Top margin 2 5cm, Bottom margin 3 0cm, Left Margin 3 0cm, Right Margin 3 0cm) Below the top margin two blank lines should be left, and start the title

(2) The title of the paper should be in Bold type and in centering format Only for the title 14pt font size is required All words of four or more letters should be typed in caps and lowercase Leave one line blank after the title

(3) The author's full name and affiliation should be in centering format Italic-style characters are recommended Leave two blank lines after the author(s)-affiliation block, and start the text of main body

(4) Headings should be centered, typed in caps and not underlined A several ranks of subdivision can be done by the following sideheads 1 , 1-1 , (1)

(5) Indent the first line of each paragraph

(6) Mount figures and/or photographs with clear glue or rubber cement Arrangement of these figures and/or photographs in the text should be done by author

(7) References should be given in the text by quoting the author's name and the year of publication, i e , Gauhar(1992) Full references should be listed in alphabetical order at the end of paper, and should appear as follows

Abbas,S G ,1974, Brief report on geology of chromite deposits near Bucha Valley, Mohmand Agency, Malakand Division, Pakistan *Geol.Surv.Inf.Release*,87,7p

Ahmad,Z ,1978, Chromite from Sakhakot-Qila area, Malakand Agency, Pakistan *Mn.Mag.*, v 42,155-157.

Tahirkheli,R A.K ,Mattauer,M ,Proust,F , and Tapponnier,P , 1979, The India-Eurasia suture zone in Northern Pakistan synthesis and interpretation of recent data at plate scale in Farah and DeJong(eds) "*Geodynamics of Pakistan*", 1-4,Geol Surv.Pakistan,Quetta, 361p

Gansser A ,1964, Geology of the Himalayas Wiley-Interscience,London,289p

Kazmi,A H and Rana,R A ,1982, *Tectonic Map of Pakistan (Scale 1·2,000,000)*. Geol Surv Pakistan,Quetta

(8) Text-file documents saved on a 720KB or 1 44MB 3.5" floppy disk by NEC98-, IBMPC-, or Machintosh- format are acceptable In particular, files processed by a software 'Microsoft Word for Windows' are most welcome

(9) Submission of two typescripts (original and its photocopy) is requested

(10) A sample manuscript is displayed on next page

Manuscript and correspondence should be addressed to:

Editorial Board
Proceedings of Geoscience Colloquium
Geoscience Laboratory, Geological Survey of Pakistan, P O Box1461, Islamabad, PAKISTAN
Tel +92-51-240423 Fax +92-51-240223

Printed in Pakistan / PanGraphics (Pvt) Ltd , Islamabad

<Sample>

1.5 spacing Times New Roman font (Times) 2.5 cm

2 lines blank (only for the 1st page)

Mineral Deposits in Chak Shahzad Area, Islamabad: A Progress Report* — 14pt·bold

Tahir Karim, Muhammad Naseem*, Shiro Itoh**, Teruo Shirahase** and Mitsuo Yoshida*** — 12pt·Italics

** Geoscience Laboratory, Geological Survey of Pakistan, Islamabad* — 12pt·Italics
***JICA expert, Geoscience Laboratory Project, Islamabad*

2 lines blank

Abstract — 12pt

□□□ — 10pt

INTRODUCTION — 12pt·Cap

□□ — 12pt
□□□
□□□□□□□□□□□□□□□□□

ORE DEPOSITS

1 Metallic Ore Deposits — 12pt·bold

□□ — 12pt
□□□

1-1. Gold — 12pt

3 cm ↔ □□□ ↔ 3 cm
□□□

(1) Distribution — 12pt

□□□
□□□

(2) Mineralogy

□□□
□□□
□□□

Table 1 □□□□□□□□□□□□□□□□□□□□□□□□□□□□□□ — 10pt

□□□□□□□□□□□□□□□□□□□□□□□
□□□□□□□□□□□□□□□□□□□□□□□□□□
□□□□□□□□□□□□□□□□□□□□□□□□□□
□□□□□□□□□□□□□□□□□□□□□□□□□□

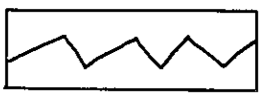

Figure 1. □□□□□□□□□□□□□ — 10pt

Acknowledgments — 12pt

□□ — 12pt
□□□

References — 12pt

□□□ — 12pt
□□□

3 cm

A4 paper (21×29.7cm)

Proceedings of Geoscience Colloquium
Geoscience Laboratory, Geological Survey of Pakistan, Islamabad
Volume 9

Geoscience Laboratory Project
November, 1994